UDK 621.3:(53+54+621+66)(05)(497.1)=00 ISSN 0352-9045

INFORMACIJE MIDEM

Strokovno društvo za mikroelektroniko elektronske sestavne dele in materiale

3°2009

Strokovna revija za mikroelektroniko, elektronske sestavne dele in materiale
Journal of Microelectronics, Electronic Components and Materials

INFORMACIJE MIDEM, LETNIK 39, ŠT. 3(131), LJUBLJANA, september 2009

UDK 621.3:(53+54+621+66)(05)(497.1)=00 ISSN 0352-9045

INFORMACIJE MIDEM 3 ○ 2009

INFORMACIJE MIDEM LETNIK 39, ŠT. 3(131), LJUBLJANA, SEPTEMBER 2009
INFORMACIJE MIDEM VOLUME 39, NO. 3(131), LJUBLJANA, SEPTEMBER 2009

Revija izhaja trimesečno (marec, junij, september, december). Izdaja strokovno društvo za mikroelektroniko, elektronske sestavne dele in materiale - MIDEM.
Published quarterly (march, june, september, december) by Society for Microelectronics, Electronic Components and Materials - MIDEM.

Naslov uredništva
Headquarters
Uredništvo Informacije MIDEM
MIDEM pri MIKROIKS
Stegne 11, 1521 Ljubljana, Slovenija
tel.: + 386 (0)1 51 33 768
faks: + 386 (0)1 51 33 771
e-pošta: Iztok.Sorli@guest.arnes.si
http://www.midem-drustvo.si/

Letna naročnina je 100 EUR, cena posamezne številke pa 25 EUR. Člani in sponzorji MIDEM prejemajo Informacije MIDEM brezplačno.
Annual subscription rate is EUR 100, separate issue is EUR 25. MIDEM members and Society sponsors receive Informacije MIDEM for free.

Znanstveni svet za tehnične vede je podal pozitivno mnenje o reviji kot znanstveno-strokovni reviji za mikroelektroniko, elektronske sestavne dele in materiale. Izdajo revije sofinancirajo JAKRS in sponzorji društva.
Scientific Council for Technical Sciences of Slovene Research Agency has recognized Informacije MIDEM as scientific Journal for microelectronics, electronic components and materials.
Publishing of the Journal is financed by Slovenian Book Agency and by Society sponsors.

Znanstveno-strokovne prispevke objavljene v Informacijah MIDEM zajemamo v podatkovne baze COBISS in INSPEC.

Prispevke iz revije zajema ISI® v naslednje svoje produkte: Sci Search®, Research Alert® in Materials Science Citation Index™

Scientific and professional papers published in Informacije MIDEM are assessed into COBISS and INSPEC databases.

The Journal is indexed by ISI® for Sci Search®, Research Alert® and Material Science Citation Index™

Po mnenju Ministrstva za informiranje št.23/300-92 šteje glasilo Informacije MIDEM med proizvode informativnega značaja.

Grafična priprava in tisk
Printed by
BIRO M, Ljubljana

Naklada
Circulation
1000 izvodov
1000 issues

Poštnina plačana pri pošti 1102 Ljubljana
Slovenia Taxe Percue

UDK621.3:(53+54+621+66), ISSN0352-9045 Informacije MIDEM 39(2009)3, Ljubljana

Obnovitev članstva v strokovnem društvu MIDEM in iz tega izhajajoče ugodnosti in obveznosti

Spoštovani,

V svojem več desetletij dolgem obstoju in delovanju smo si prizadevali narediti društvo privlačno in koristno vsem članom.Z delovanjem društva ste se srečali tudi vi in se odločili, da se v društvo včlanite. Življenske poti, zaposlitev in strokovno zanimanje pa se z leti spreminjajo, najrazličnejši dogodki, izzivi in odločitve so vas morda usmerili v povsem druga področja in vaš interes za delovanje ali članstvo v društvu se je z leti močno spremenil, morda izginil. Morda pa vas aktivnosti društva kljub temu še vedno zanimajo, če ne drugače, kot spomin na prijetne čase, ki smo jih skupaj preživeli. Spremenili so se tudi naslovi in način komuniciranja.

Ker je seznam članstva postal dolg, očitno pa je, da mnogi nekdanji člani nimajo več interesa za sodelovanje v društvu, se je Izvršilni odbor društva odločil, da stanje članstva uredi in **vas zato prosi, da izpolnite in nam pošljete obrazec priložen na koncu revije.**

Naj vas ponovno spomnimo na ugodnosti, ki izhajajo iz vašega članstva. Kot član strokovnega društva prejemate revijo »Informacije MIDEM«, povabljeni ste na strokovne konference, kjer lahko predstavite svoje raziskovalne in razvojne dosežke ali srečate stare znance in nove, povabljene predavatelje s področja, ki vas zanima. O svojih dosežkih in problemih lahko poročate v strokovni reviji, ki ima ugleden IMPACT faktor.S svojimi predlogi lahko usmerjate delovanje društva.

Vaša obveza je plačilo članarine 25 EUR na leto. Članarino lahko plačate na transakcijski račun društva pri A-banki : 051008010631192. Pri nakazilu ne pozabite navesti svojega imena!

Upamo, da vas delovanje društva še vedno zanima in da boste članstvo obnovili. Žal pa bomo morali dosedanje člane, ki članstva ne boste obnovili do konca leta 2009, brisati iz seznama članstva.

Prijavnice pošljite na naslov:

MIDEM pri MIKROIKS

Stegne 11

1521 Ljubljana

Ljubljana, september 2009

Izvršilni odbor društva

MERILNIK TEMPERATURE NA OSNOVI FLUORESCENCE OKSIDNIH SINTENTIČNIH MONOKRISTALOV

J. Križan[1], I. Bajsić[2] in J. Možina[2]

[1]AMI d. o. o., Ptuj, Slovenija

[2]Univerza v Ljubljani, Fakulteta za strojništvo, Ljubljana, Slovenija

Kjučne besede: optična temperaturna zaznavala, fluorescenca, sintetični oksidni monokristali,

Izvleček: V prispevku so prikazani rezultati razvoja nove generacije temperaturnih merilnih zaznaval, ki delujejo na osnovi fluorescence sintetičnih oksidnih monokristalov. Raziskane so nekatere termo-optične lastnosti sintetičnih oksidnih monokristalov na osnovi Al_2O_3, kakor so $Cr^{3+}MgAl_2O_4$ (Cr:špinel) in $Cr^{3+}Y_3Al_5O_{12}$ (Cr:YAG) in več inačic kristalov z dodatki oksidov redkih zemelj. V prispevku je opisan eksperimentalni sistem za merjenje temperature na osnovi razmerja vrhov fluorescenčnega spektra. V ta namen je bila razvita tudi programska oprema za obdelavo merilnih signalov. Prvi od predstavljenih prototipov merilnega sistema temelji na prenosu merilnega signala po optičnem vlaknu, pri drugem pa se določa temperatura na površini merjenca brezdotikalno. Nakazane so tudi nekatere možnosti praktične uporabe tovrstnega merjenja temperature.

Thermometer Based on Syntetic Oxide Monocrystals Fluorescence

Key words: optical temperature sensors, fluorescence, synthetic oxide monocrystals.

Abstract: The article presents some of the results of the development of new generation temperature sensors working on the basis of fluorescent synthetic oxide monocrystals. Research involved some termo-optical characteristics of synthetic oxide monocrystals with an Al_2O_3 basis such as: $Cr^{3+}MgAl_2O_4$ (Cr:Spinel), $Cr^{3+}Y_3Al_5O_{12}$ (Cr:YAG) and some other variations of crystals doped with rare earth oxides. The experimental system for temperature measurement on the basis of fluorescence spectrum peaks ratios is examined. Computer hardware and software for processing measured signals is catalogued. The first of the represented measurement systems prototypes is based on the transfer of the measuring signal via the optical fibre, the second uses non-contact measuring of the object surface temperature. Some possible applications of the discussed temperature measurement are also indicated.

1. Uvod

Merjenje temperature z optičnimi brezdotikalnimi merilniki ima v nekaterih praktičnih primerih prednost pred dotikalnimi temperaturnimi merilniki ali pa je to celo edina možna rešitev za določanje temperaturnega stanja merjenca. V merilni praksi obstaja vrsta različnih termometrov na osnovi fluorescence oksidnih monokristalov /1 - 4/.

Obstajata dve temeljni metodi merjenja temperaturnega odziva termografskega materiala. Pri prvi metodi je uporabljen bliskovni svetlobni vir. Po vsakem svetlobnem blisku poteka eksponencialno ugašanje svetlobe, ki jo oddaja kristal. Časovna konstanta eksponencialnega ugašanja je temperaturno odvisna. Višja ko je temperatura, hitreje kristal ugaša. Časi ugašanja pri povišani temperaturi so tipično pod 1 ms.

Druga metoda temelji na temperaturni odvisnosti razmerja dveh spektralnih vrhov fluorescenčnega spektra in smo jo v tem prispevku preizkusili na kristalu špinela $MgAl_2O_4$ in kristalu $Y_3Al_5O_{12}$ oba dopirana s kromom /11 - 14/.

Brezdotikalna metoda je občutljiva na stransko svetlobo v spektralnem območju od 600 do 700 nm in jo je zato treba pred izračunom razmerja izločiti. Uporaba fosforjev z modro svetlobo zmanjša občutljivost na stransko svetlobo /5/. Merilno načelo, ki temelji na razmerju emisije dveh spektralnih črt, znatno zmanjša negotovost meritve.

2. Eksperimentalni sistem

2.1 Sinteza fluorescentnih monokristalov

V raziskavah uporabljeni kristali so bili izdelani po Verneuilevem postopku. V ta namen je bila zgrajena posodobljena verzija laboratorijske peči za rast monokristalov, ki je posebno primerna predvsem za safirje, rubine in špinele /6/.

Posodobljena verzija Verneuileve peči za rast monokristalov, ki je prikazana na sliki 1, zagotavlja široke možnosti izdelave sintetičnih monokristalov /7/. Na sliki je prikazan tudi potek rasti kristala safirja pri 2050 °C od začetnega kristala do končnega premera, tako kakor se vidi skozi kontrolno odprtino. Sintetizirali smo različne kristale, ki so primerni za temperaturne meritve. Izdelali smo tudi kristale YAG in YAP dopirane z redkimi zemljami in več aluminatnih kristalov /13,15, 16, 17/. Med njimi so - poleg v prispevku prikazanih - še: Cr^{3+}:$YAlO_3$ - Cr:YAP, Tb^{3+}:$Y_3Al_5O_{12}$ - Tb:YAG, Pr^{3+}:$Y_3Al_5O_{12}$ - Pr:YAG, Tb^{3+}:$YAlO_3$ - Tb:YAP, Yb^{3+}: $Y_3Al_5O_{12}$ - Yb:YAG, Eu^{3+}: $Y_3Al_5O_{12}$ - Eu:YAG, Dy^{3+}:$Y_3Al_5O_{12}$ - Dy:YAG, $SrAl_2O_4$: Eu^{2+}: Dy^{3+}, $CaAl_2O_4$: Eu^{2+}: Nd^{3+}.

Za meritve temperature je mogoče uporabiti tudi kristale v praškasti obliki. V nekaterih primerih je praškasti material potreben zaradi nanosa na merjeni objekt.

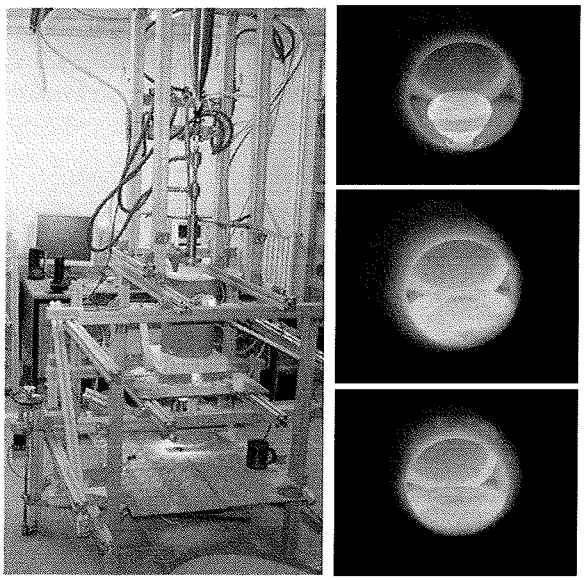

Slika 1: Laboratorijska peč in potek rasti kristala

2.2 Merilna oprema

Osnovni instrument je bil spektrometer OceanOptics USB4000, ki omogoča priključitev na prenosni računalnik brez dodatnega napajanja. Uporabili smo različne svetlobne vire, kakor so cenene LED diode različnih valovnih dolžin za osvetljevanje prek optičnega vlakna in diodni laser valovnih dolžin 405 nm in 532 nm za osvetljevanje pri brezdotikalnem merjenju. Za določanje značilnic kristalov na osnovi fosforjev /8/ smo izdelali grelni blok s primerjalno temperaturno meritvijo z uporovnim temperaturnim zaznavalom Pt100. Vključili smo tudi optične komponente različnih izdelovalcev in profesionalni optični sistem firme Hamamatsu A10043 z zrcalom 455 nm. Za snemanje poteka temperaturnih značilnic je bila oprema podprta z National Instruments LabView platformo in z DAQ merilno opremo NI-USB-6221. Za merjenje teh sprememb potrebujemo detektorje s hitrim frekvenčnim odzivom in fotopomnoževalko za šibke vire svetlobe /8/. Pri drugem dvobarvnem merilnem načelu imamo stalno ali bliskovno osvetljevanje. Merimo odziv v obliki temperaturno odvisnega razmerja vrhov dveh spektralnih črt, ki ju oddaja osvetljeni kristal /9/.

V tem prispevku je opisan sistem za merjenje temperature s Cr dopiranimi kristali in USB spektrometrom. Isto merilno načelo je mogoče uporabiti tudi na drugih termografskih materialih, ki imajo lastnost, da je več spektralnih črt bolj ali manj temperaturno občutljivih. Idealno bi bilo, če bi bila ena spektralna črta neobčutljiva na temperaturo. Fluorescenčni materiali s temi lastnostmi lahko delujejo kot dvobarvni premazi. Pomembno je, da osvetljujemo z enim virom svetlobe in da je možno preprosto ločiti svetlobo dveh emitiranih črt /10/.

2.3 Programska oprema

Eksperimentalni sistem upravlja prenosni računalnik, ki je s spektrometrom povezan prek Omni gonilnika. Razvili smo lastno programsko opremo v okolju SpectraSuite za komunikacijo merilnega sistema s spektrometrom in linearizacijo, za vrednotenje spektra in za prikaz temperature pa v programskem okolju Visual Basic. Merilni sistem je univerzalen in omogoča obdelavo in vpis kalibracijske krivulje za različne tipe kristalov.

Programska oprema je tudi podlaga za izvedbo samostojnega merilnega sistema. Iz priloženih vezalnih shem je razvidna končna verzija temperaturne merilne sonde na načelu fluorescence. Večina merilnih funkcij poteka neposredno v spektrometru, vključno z obdelavo merilnih signalov. Prilagajanje poteka prek izračuna parametrov, ki je del aplikacijske programske opreme. Gonilnik spektrometra omogoča uporabo teh funkcij iz različnih programskih okolij, zato smo lahko preizkusili tudi okolje LabView in programsko okolje Visual Basic. V aplikacijski programski opremi sta izdelana tudi grafični vmesnik in linearizacija izmerjenih vrednosti z uporabo polinomske funkcije, katere parametri so potrebni za izvedbo kalibracijskega postopka.

3. Rezultati

3.1 Fluorescenčni spekter izdelanih monokristalov

Na slikah 2 in 3 sta prikazana fluorescenčna spektra dveh od večjega števila izdelanih monokristalov pri 25 şC. Kot vzbujevalni vir pri brezdotikalnem merjenju smo uporabili lasersko diodo, ki oddaja stalno modro svetlobo moči 5 mW in z valovno dolžino 405 nm, pri merilnem sistemu z optičnim vlaknom pa je uporabljena šibkejša 400 nm LED dioda. Oba kristala imata 4 izrazite vrhove, ki so različno občutljivi na temperaturo.

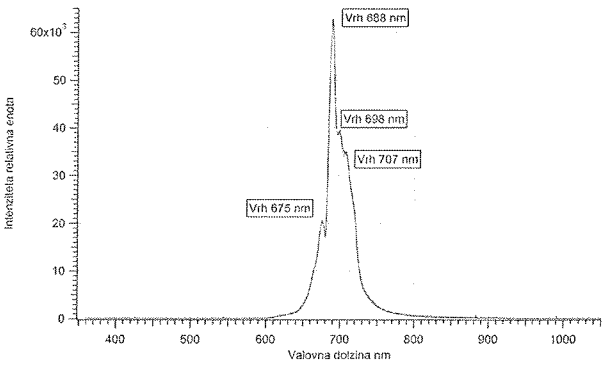

Slika 2: Spekter Cr:špinel (Cr:$MgAl_2O_4$), vzbujen s 400 nm LED pri 25 °C

3.2 Temperaturna odvisnost

Iz izmerjenega fluorescenčnega spektra je razvidno, da ima špinel štiri spektralne vrhove (slika 2). Vsi intenzitetni vrhovi so odvisni od temperature. Da se izognemo merjenju in računanju z absolutnimi vrednostmi, je smotrno uporabiti razmerja vršnih intenzitet za različne kombinacije vrhov. Za naš merilni sistem smo uporabili razmerje intenzitetnih vrhov pri valovnih dolžinah 675 nm in 688 nm, ki je se je pokaza-

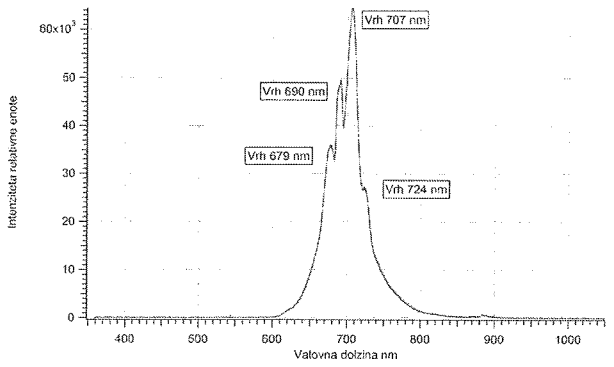

Slika 3: Spekter Cr:YAG (Cr^{3+} $Y_3Al_5O_{12}$), vzbujen s 400 nm LED pri 25 °C

lo kot najbolj občutljivo na temperaturne spremembe. Z LabView razvojnim sistemom smo posneli zvezo med temperaturo kristala in razmerjem intenzivnosti, ki je prikazana v obliki točk na diagramu na sliki 4. Odvisnost razmerja fluorescence od temperature je aproksimirana s polinomom tretje stopnje, kakor je prikazano na sliki 4 z modro krivuljo, ki se zelo dobro prilega izmerjenim točkam. Vzbujanje kristala špinela je prav tako kakor pri rubinu možno z zeleno svetlobo ali UV svetlobo. Povezavo odvisnosti razmerja intenzitete fluorescence od temperature predstavlja splošna polinomska funkcija,

$$T\,°C = K_0 + K_1 \cdot x + K_2 \cdot x^2 + K_3\, x^3 \qquad (1)$$

K_0 do K_3 so koeficienti polinoma, x je razmerje intenzitet izbranega para spektralnih vrhov.

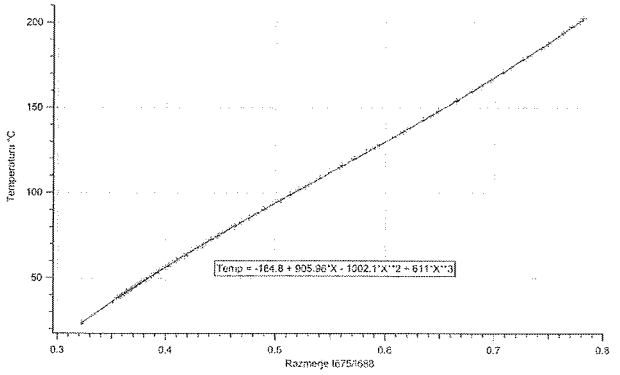

Slika 4: Zveza med temperaturo in razmerjem fluorescenčnih vrhov za špinel

Za vsak tip kristala smo posneli odvisnost razmerja vrhov od temperature in jo po metodi najmanjših kvadratov aproksimirali s polinomsko funkcijo, katere aproksimacijske koeficiente smo vnesli kot parametre v aplikacijsko programsko opremo.

Za kristal špinela, ki je dopiran z 0,5 wt % Cr_2O_3, in za razmerje vrhov pri 675 nm in 688 nm smo dobili naslednjo polinomsko povezavo:

$$T\,°C = -184{,}8 + (905{,}96)\cdot x + (-1002{,}1)\cdot x^2 + (611)\, x^3 \qquad (2)$$

Kristal špinela je primeren za uporabo v meritvi temperature po dvobarvnem merilnem načelu. Pri njem je primerno vzbujanje s svetlobo valovne dolžine blizu 400 nm ali s cenejšim virom svetlobe 530 nm.

Tudi kristal YAG dopiran z 0,5 wt % Cr_2O_3 ima štiri spektralne vrhove (slika 3).

V tem primeru smo za razmerje vrhov pri 724 nm in 707 nm dobili naslednji polinom:

$$T\,°C = -250{,}2 + (941{,}7)\, x + (-1020{,}4)\, x^2 + (840{,}76)\, x^3 \qquad (3)$$

Povezava med razmerjem fluorescenčnih vrhov in temperaturo je prikazana na sliki 5. in je bila posneta na enak način kot pri špinelu.

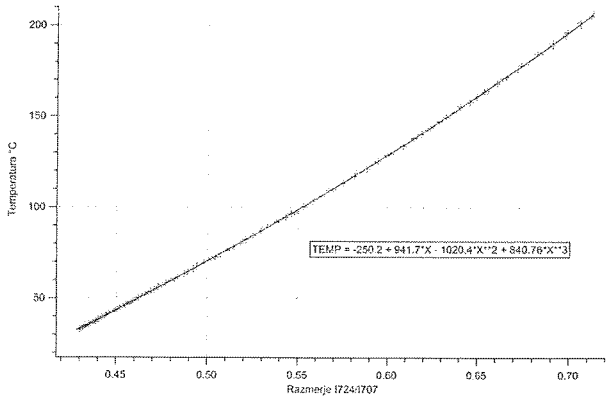

Slika 5: Zveza med temperaturo in razmerjem fluorescenčnih vrhov za YAG

S kromom dopirani YAG kristal je primeren za uporabo v meritvi temperature po dvobarvnem merilnem načelu. Pri njem je primerno vzbujanje s svetlobo valovne dolžine blizu 400 nm. Sprememba razmerja intenzitete fluorescence je dovolj velika, da omogoča občutljivost meritve 0,1 K na območju od 20 °C do 200 °C.

3.3 Prototipa merilnega sistema

Izdelana sta dva prototipa merilnega sistema, ki imata zelo podobno merilno opremo (sliki 6 in 7). Pri prvi merilni verigi je vzbujevalni žarek usmerjen prek kolimatorske leče v optično vlakno. Na drugem koncu vlakna je merilni kristal v obliki merilnega zaznavala /4/. Med kristalom in optičnim vlaknom mora biti optična in mehanska povezava, to pa je mogoče zagotoviti z lepljenjem kristala ali dopiranjem konice vlakna. Ker so optična vlakna navadno iz silicijevega oksida SiO_2, je dopiranje mogoče le pri silikatnem kristalu. Lepljenje je mogoče le s transparentnimi lepili, ki so tudi temperaturno in UV obstojna. Zaradi različnih termičnih raztezkov SiO_2 vlakna in keramičnega kristala so takšni spoji težko izvedljivi in zahtevajo posebna lepila. Tedaj je svetlobni vir lahko tudi LED dioda, saj zadošča manjša jakost svetlobe. Vsako merilno zaznavalo je treba umeriti. Koeficienti polinoma in fluorescenčni vrhovi karakterizirajo merilni kristal. Valovna dolžina osvetljevanja je odvisna od tipa kristala in od njegovega področja največje absorpcije vz-

bujalne svetlobe. Optična povezava med kristalom in vlaknom /4/ je bila izvedena s povezavo kristala in enega optičnega vlakna, po katerem se prenaša vzbujanje in istočasno odziv.

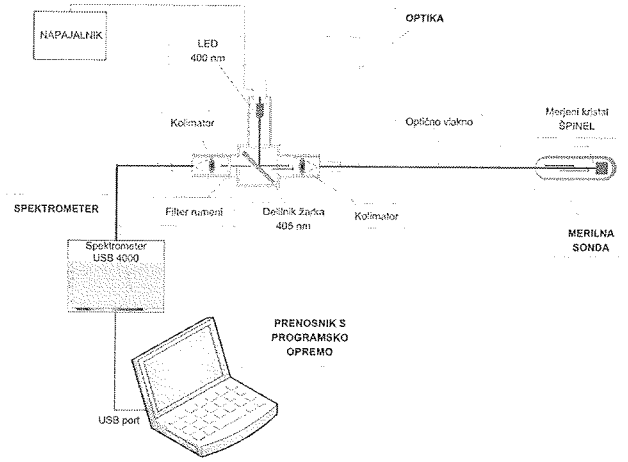

Slika 6: Merilni sistem z optičnim vlaknom

V drugi merilni verigi za brezdotikalno meritev je kontinuirni laserski vir, ki omogoča vzbujanje iz razdalje nekaj metrov. Svetloba, ki jo fluorescira kristal, se zbira s sistemom leč in usmerja prek kolimatorja v optično vlakno spektrometra. S to merilno opremo je mogoče brezdotikalno meriti temperaturo in je kot takšna uporabna za meritve fluorescenčnih ognjevarnih premazov, pri katerih se skušamo izogniti direktnemu kontaktu ali pa ta sploh ni mogoč. Pri izbiri filtrov je treba upoštevati spektralni profil ozadja v različnih merilnih situacijah. Vsekakor je ugodneje, če je spekter emisije kristala pomaknjen proti modremu področju, kjer infrardeči spekter ozadja lahko preprosto izločimo. V našem primeru so spektralne črte v rdečem področju, to pa je bilo dovolj dobro za razvoj merilne metode. Kristali, kakor je BAM $BaMgAl_{10}O_{17}$:Eu ali YAG:Dy (ima emisijo pri 455 nm in 497 nm), so zelo primerni tudi s tega stališča /5/. Programska oprema omogoča preprosto prilagoditev na različne fluorescenčne materiale. Parametri so valovne dolžine vrhov fluorescence, katerih razmerje se izračunava, in polinomski koeficienti ter nekateri parametri, povezani z delovanjem in občutljivostjo spektrometra. Programska oprema omogoča tudi hkratno zapisovanje merjenih vrednosti v spremenljivem rastru v datoteko, ki jo je možno obdelovati s klasično programsko opremo ali prikazati v grafikonu.

Na sliki 8 je prikazan merilni sistem za brezdotikalno merjenje temperature. Vidni so optični blok z diodnim laserskim modulom na stojalu pred električno pečjo, spektrometer in prenosni računalnik z grafičnim vmesnikom. Spektrometer ima dovolj veliko optično občutljivost, tako da smo v večini primerov lahko izvajali meritve s časom vzorčenja 100 ms in krajše. Merilni sistem s pečjo je pripravljen za brezdotikalno merjenje v temperaturnem območju do 1400 °C - z njim bomo v nadaljnjih raziskavah testirali uporabo tudi drugih kristalov. Zato je konstrukcija peči prilagojena potrebam testnega merilnega sistema. Tako je

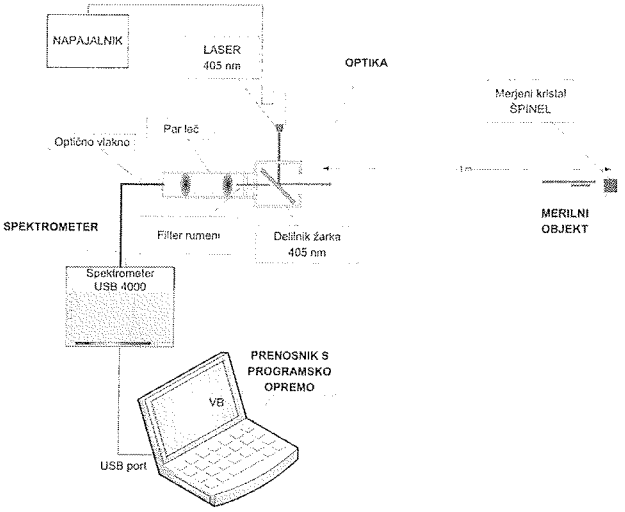

Slika 7: Brezdotikalna meritev temperature

vgrajen primerjalni termopar PtRh-Pt, ki se dotika merilnega kristala, zalitega v keramičnem nosilcu, in programska oprema za snemanje in prikaz merilnih podatkov in za njihovo analizo. Pri meritvah do 400 °C pa je predvidena primerjalna meritev s Pt100 uporovnim zaznavalom in s pripadajočim merilnim pretvornikom.

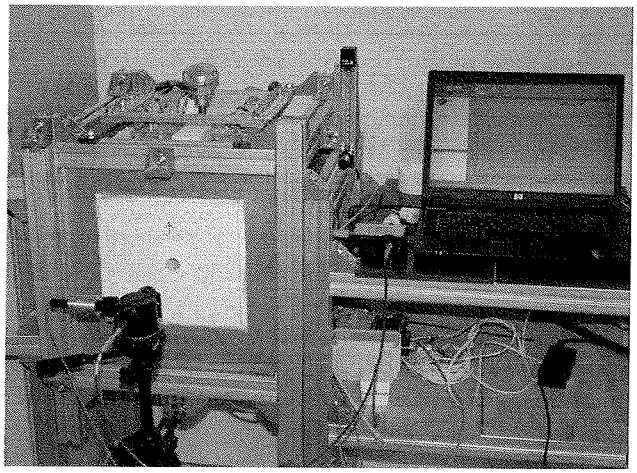

Slika 8: Sistem za brezdotikalno merjenje temperature

V območju do 400 °C je mogoče uporabljati s kromom dopirane kristale. Na sliki 9 so prikazani različni kristali, zaliti v keramičnem nosilcu in pripravljeni za testiranje.

V temperaturnem razponu od 25 °C do 200 °C je točnost merilnega sistema boljša od ± 0,4 °C. Pri tem je največji del izmerjenega odstopanja zaradi zakasnitve pri primerjalni meritvi temperature oksidnega kristala s Pt100 zaznavalom, ki ima tudi svojo termično vztrajnost. Za višje temperature so primerni kristali, dopirani z redkimi zemljami, na primer z Dy dopirani YAG. Do nedavnega je bil disprozij edini poznani aktivator iz družine redkih zemelj, ki kaže odziv v obliki razmerja intenzivnosti fluorescence pri visokih temperaturah /10/. Merilni sistem omogoča uporabo različnih merilnih oksidnih kristalov - z lastnostjo temperaturno odvis-

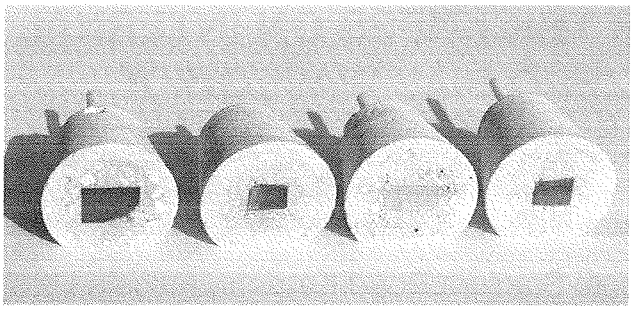

Slika 9: Različni kristali v keramičnem nosilcu

nega razmerja vrhov fluorescence - za različna temperaturna območja. Nadaljnji koraki začetih raziskav bodo usmerjeni v razvoj nanofluorescenčnih materialov, ki se potencialno lahko uporabljajo kot temperaturni fluorescenčni premazi ali kot inteligentni ognjevarni premazi /10/, /18/ in pri razvoju merilne opreme za določanje temperaturnega stanja v različnih industrijskih aplikacijah .

4. Sklepi

Rezultati opravljenih raziskav so pomembni za nadaljnji razvoj merilne opreme za merjenje temperature na temelju fluorescence oksidnih monokristalov. Načrtovana in izdelana je univerzalna cenovno ugodna prenosna merilna oprema, ki omogoča preprosto prilagoditev na različne tipe dvobarvnih merilnih fosforjev. S tem lahko optimalno prilagodimo merilni sistem na zahtevano aplikacijo in merilno področje temperatur od kriogenskega do visokih temperatur. Pri iskanju primernih fluorescenčnih materialov je bil obdelan širok spekter dosegljive novejše strokovne literature s področja lastnosti oksidnih kristalov in spremljajoče patentne dokumentacije. Izdelani so bili eksperimentalni oksidni monokristali na lastni tehnološki opremi, in to po Verneuilevem postopku. Pri izdelavi merilne opreme je potekalo razvojno delo načrtno od izbire najbolj temeljnih sestavnih elementov do konfiguriranja končnega merilnega sistema, ki omogoča snemanje temperaturnih karakteristik oksidnega monokristala, določanje korekcijskih funkcij ter shranjevanje in obdelavo izmerjenih signalov. Merilna oprema je primerna tudi za uporabo na fluorescenčnih temperaturnih premazih, na primer v nanotermometriji /19/.

5. Literatura

/1/ K. T. V. Grattan in Z. Y. Zhang: Fiber Optic Fluorescence Thermometry, Chapman and Hall, London, 1995

/2/ V. C. Fernicola, T. Sun, Z. Y. Zhang in K. T. V. Grattan: Investigations on exponential lifetime measurements for fluorescence thermometry. *Review of Scientific Instruments*, zv. 71, št. 7, julij 2000

/3/ De Huang in Hui Hu: Molecular tagging thermometry for transient temperature mapping within a water droplet. *Optics Letters*, zv. 32, št. 24/15. december 2007

/4/ Babnik, A., Kobe, A., Kuzman, D., Bajsić, I., Možina, J.: Improved probe geometry for fluorescence-based fibre-optic temperature sensor. *Sensors and Actuators, A. Physical*, zv. A 57, pp. 203-207, 1996

/5/ Gustaf Sarner, Mattias Richter in Marcus Alden: Investigations of blue emitting phosphors for thermometry. *Meas. Sci. Technol.* 19, 125304 (10pp), 2008

/6/ Verneuil, Auguste Victor Luise, *Process for producing sinthetic sapphires,* Patent US 988, 230, 28. mar. 1911

/7/ Križan, Janez: Sinteza in fluorescenca oksidnih monokristalov : 1. podiplomski seminar. Fakulteta za strojništvo, Ljubljana, 2008

/8/ A. L. Heyes, S. Seefeldt, J. P. Feist: Two-colour phosphor thermometry for surface temperature measurement, *Optics & Laser Technology*, 38 pp. 257-265, 2006

/9/ Maria Cristina Vergara: Window Glass Temperature With a Fluorescence Intensity Ratio Optical Fibre Sensor, A thesis for degree of Master of Science, Optical Technology Research Laboratory/School of Electrical Engineering, Victoria University, 2003

/10/ Ashiq Hussain Khalid in Konstantinos Kontis: Thermographic Phosphors for High Temperature Measurements: Principles, Current State of the Art and Recent Applications. *Sensors 8*, 5673-5744, 2008

/11/ J. Someya, C. Nojiri, H. Aizawa, T. Katsumata, S. Komuro in T. Morikawa: Fluorescence Thermometer Application of Cr Doped Spinel Crystals, SICE-ICASE International Joint Conference 2006, 18.-21. okt. 2006, in Bexco, Busan, Korea

/12/ M. Kaneda, K. Orihara, H. Aizawa, T. Katsumata, S. Komuro in T. Morikawa: Thermo-Sensor Based on Peak Intensity Ratio of Photoluminescence from Cr Doped YAG Crystals, SICE-ICASE International Joint Conference 2006, 18.-21. okt. 2006, in Bexco, Busan, Korea

/13/ J. Someya, C. Nojiri, H. Aizawa, T. Katsumata, S. Komuro in T. Morikawa: Fluorescence Thermo-Sensor Sheet Using Cr Doped YA103 Crystals, SICE-ICASE International Joint Conference 2006, 18.-21. okt. 2006, in Bexco, Busan, Korea

/14/ T. L. Phan in S. C. Yu, M. H. Phan, T. P. J. Han.: Photoluminescence Properties of Cr3+-Doped MgAl2O4 Natural Spinal. *Journal of the Korean Physical Society*, zv. 45, št. 1, julij 2004, pp. 63-66

/15/ Kokta, M., Stone - Sundberg, Jennifer: Spinel Articles and Methods for Forming Same. WO 2005/031048 A1, Patent

/16/ Falcenberg, R.: Verneuil Apparatus for Growing Spinel-Type Oxide, United States Patent US 3,876.382, 8. apr. 1975

/17/ William M. Yen, Shigeo Shionoya, Hajime Yamamoto: Phosphor Handbook, Second Edition, CRC Press is an imprint of the Taylor & Francis Group, 2006

/18/ S. W. Allison, D. L. Beshears, M. R. Cates, M. Paranthaman: LED-induced fluorescence diagnostics for turbine and combustion engine thermometry, http://www.ornl.gov/phosphors

/19/ Jaebeom Lee and Nicholas A. Kotov: Thermometer design at the nanoscale. *Nanotoday,* zv. 2, št. 1, pp. 48-51, 2007

J. Križan,
AMI d. o. o., Trstenjakova 5, SI-2250 Ptuj

I. Bajsić; J. Možina
Univerza v Ljubljani, Fakulteta za strojništvo,
Aškerčeva 6, SI-1000 Ljubljana

Prispelo (Arrived): 02.09.2009 *Sprejeto (Accepted): 09.09.2009*

EFFECT OF ABSORPTION LAYER THICKNESS ON INTERNAL QUANTUM EFFICIENCY OF ZERO-BIAS WAVEGUIDE PHOTODETECTORS

Abid Karim

Bahria University (Karachi Campus), National Stadium Road Karachi, Pakistan

Key words: Waveguide photodetector, internal quantum efficiency, photodetection, *pn*-junction photodiodes

Abstract: Side illuminated waveguide photodetectors (WGPDs) are suitable choice for monolithic optoelectronic integrated circuits (OEICs) since the structure of a WGPD is similar to that of laser structure. However, the main disadvantage of a WGPD is the poor coupling efficiency which leads to a low value of external quantum efficiency. The simple way to increase the coupling efficiency is to increase the thickness of the absorption or active layer of a WGPD. In this paper, the effect of active layer thickness on quantum efficiencies (i.e. external and internal quantum efficiencies) of WGPDs is examined experimentally.

Vpliv debeline absorpcijske plasti na kvantno učinkovitost fotodetektorja z valovodom

Kjučne besede: valovodni fotodetektor, kvantna učinkovitost, fotodetekcija, fotodioda s pn-spojem

Izvleček: Valovodni fotodetektorji s stransko osvetlitvijo (WGPDs) so primerni za uporabo v optoelektronskih integriranih vezjih (OEICs), ker je njihova struktura podobna laserski strukturi. Glavna slabost WGPD je slaba sklopitvena učinkovitost, kar vodi do nizke vrednosti zunanje kvantne učinkovitosti. Najlažja pot do povečanja sklopitvene učinkovitosti je povečati debelino absorbcijske ali aktivne plasti WGPD. V tem članku eksperimentalno ugotavljamo vpliv debeline aktivne plasti na kvantno učinkovitost WGPD.

1. Introduction

Through monolithic integration, OEICs are expected to bring higher complexity and new functionality in addition to other advantages usually associated with monolithic integration. It is also expected that the largest application of OEICs would be in the fields of telecommunication and signal processing. Optical detector is an essential component of an OEIC as it ultimately limits the overall system performance. Major trends in photodetectors development are the achievement of higher efficiencies and larger bandwidths /1/. A waveguide photodetector is very attractive device for achieving these goals. Furthermore, these devices have advantage of packaging technology, since waveguide structure, which is similar to laser structure, is suitable for monolithic OEICs. However, as mentioned earlier, efficient optical coupling between the input optical field and the optical field at the input facet of WGPD is a technological challenge because the diameter of an input optical beam falling on the input facet of a WGPD, even focused with a sophisticated lens system, is much higher than the thickness of the active layer of a WGPD. The poor coupling efficiency leads to low value of measured or external quantum efficiency (η_{ext}) in a WGPD and the low value of η_{ext} is often taken as actual conversion efficiency of a WGPD. However, as a matter of fact, η_{ext} is the external conversion efficiency and it does not represent the internal conversion efficiency of the device.

2. internal quantum effieciency of WGPD

A semiconductor laser diode under reverse bias or zero bias conditions can act as a WGPD and the active layer can work as depletion or absorption region. Photocurrent of a WGPD can be obtained as:

$$I_{ph} = S_{in} P_{in} \tag{1}$$

where S_{in} is the internal sensitivity of WGPD and P_{in} is the input power coupled into the active layer of a WGPD. In the case of a waveguide photodetector, the actual sensitivity (i.e. the internal sensitivity) can be given as /2/:

$$S_{in} = \frac{S_{ext}}{\zeta(1-R)} \tag{2}$$

where S_{ext} is the external sensitivity of the detector, z is the coupling efficiency of optical radiation and R is the facet reflectivity. S_{ext} can be defined as:

$$S_{ext} = \frac{\eta_{ext} e\lambda}{hc} \tag{3}$$

and the coupling efficiency can be calculated as /3/:

$$\zeta = \frac{\eta_{ext}}{(1-R)(1-e^{-\Gamma\alpha_{ib}L})} \tag{4}$$

where c is the speed of light in vacuum, h is the Plank's constant, λ is the wavelength of the incident radiation, e is the charge on an electron, η_{ext} is the external differential quantum efficiency, α_{ib} is the interband absorption, Γ is

the confinement factor and L is the length of the device. The internal quantum efficiency, η_{in} is given as /4/:

$$\eta_{in} = \frac{S_{in} hc}{e\lambda}\left(1 - \frac{\alpha_o}{\alpha}\right) \quad (5)$$

here α_o represents the residual waveguide losses absorption and α represent the total absorption inside the active layer of a WGPD. α can be calculated as:

$$\alpha = \alpha_o + \Gamma\alpha_{ib} \quad (6)$$

3. Experimental procedure

In order to demonstrate the validity of the proposed technique, three different stripe geometry A. R. coated laser like devices were investigated while a 5 um wide stripe laser was used as the source laser throughout the work reported in this paper. Structural parameters of the various devices used during the work reported in this paper are listed in table-1. Device-1, 2 and 4 were essentially made from the same GaAs/AlGaAs material and for these devices, α_o was measured as 24/cm using the conventional cutback loss measurement technique /5/. Whereas device-3 had an active layer thickness of 0.5 μm and α_o was expected to be the approximately same since α_o depends upon length of the device. The length of all devices was 250 um. This length was quite sufficient for complete absorption of optical radiation coming from the source.

Table -1. Structural parameter of different devices used during the work reported in this paper.

DEVICE NUMBER	STRIPE WIDTH, W (μm)	ACTIVE LAYER THICKNESS (μm)	R_1 (%)	R_2 (%)
1	2.5	0.15	4	4
2	5	0.15	4	4
3	5	0.5	4	4
4 (Source laser)	5	0.15	30	30

All the devices were mounted on separate copper heat sink blocks. Temperatures of the device being tested and of the source laser were controlled independently using thermoelectric Peltier devices and a multi-channel temperature controller. Throughout the work reported in this paper, the test devices were subjected to pulsed input from the source laser which was operated under pulse conditions using a HP8082A pulse generator to avoid overheating in order to achieve more reliable results. The width of current pulses was kept constant at 200ns with a repetition frequency of 10 KHz. This proportion between the pulse width and pulse repetition frequency was sufficient to isolate the transient temperature effects caused by one pulse from other pulses. Along with an optical lens system, a pre-calibrated large area Si detector (LAD) and WGPD (being investigated) were used to measure light output. An infrared camera was used to for alignment of LD and WGPD in place of WGPD and LAD as and when required. The source laser and WGPD were aligned using a free-space alignment technique /6/.

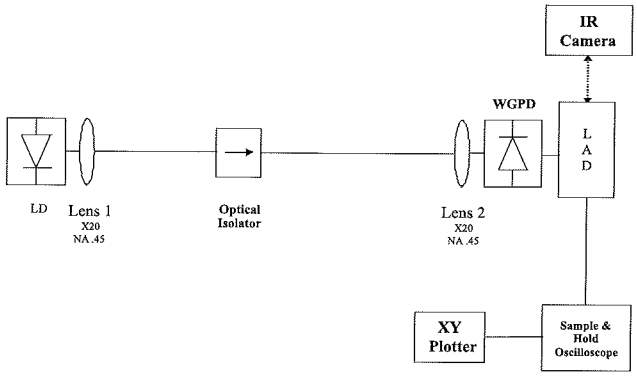

Fig. 1. Schematic representation of experimental set-up used.

Results were plotted using a Tektronix sample & hold oscilloscope and an X-Y plotter. Figure 1 shows the schematic of experimental set-up used during the work reported here.

4. Results and discussion

4.1. Response of WGPD

After achieving the maximum alignment between the source laser and WGPD, the response of WGPD was analyzed by measuring I-L characteristic of the source laser using the device-1 as a WGPD. Also I-L characteristic of the source laser was measured by placing a LAD just after lens-2 (in place of WGPD). Results of both measurements are given in fig. 2. It can be seen from fig. 2 that the response of a pre-calibrated Si LAD and the GaAs WGPD are similar to each other except the sensitivity. This indicates that there was a perfect alignment between the source laser and WGPD.

The same experimental procedure was repeated using a 5μm wide stripe device (device-2) instead of device-1 as an WGPD. The response of both WGPDs (i.e. device 1 & 2) as a function of stripe width is plotted in fig. 3. It can be seen from fig. 3 that the change in the stripe width does not have much effect on the response of GaAs WGPD. This was expected because the minimum achievable spot size achieved by lens-2 was around 1.165μm at λ=860nm and was smaller than the stripe width of 2.5μm. From fig.

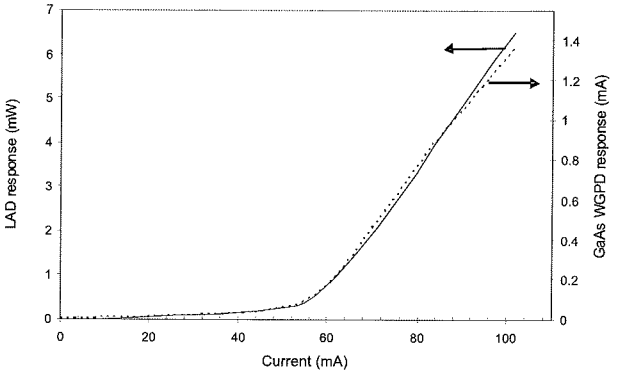

Fig. 2. I-L characteristics of the source laser measured using LAD and GaAs WGPD.

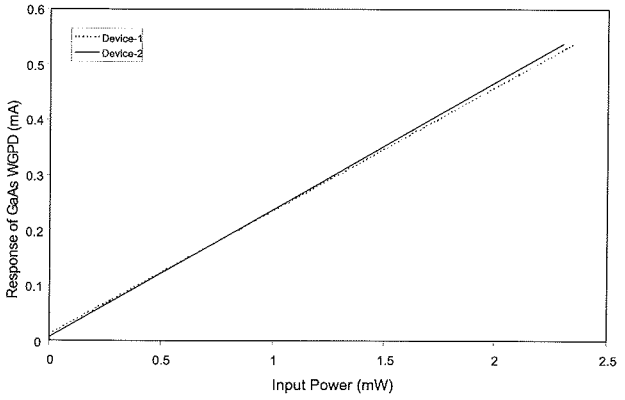

Fig. 3. Response of WGPDs with active layer thickness of 0.15 μm as a function of stripe width.

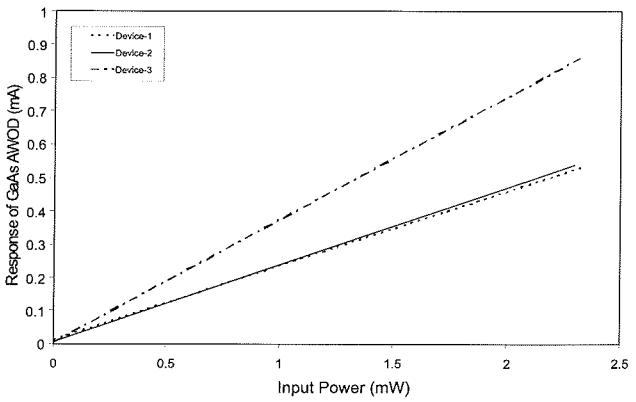

Fig. 4. Response of WGPDs as a function active layer thickness.

3, the external sensitivity, S_{ext} of GaAs WGPD was calculated as around 0.22A/W. This value does satisfy the reported values of refs. 3 and 7. Using eq. (3), the external quantum efficiency was estimated as 31. 8%. For the typical values of η_{ext} = 31.8%, $R_1 = R_2$ = 4%, L = 250 μm and Γ = 46%, α_{ib}= 200/cm /2/, ζ was calculated as 35.26% and S_{in} was calculated as 0.63 A/W. Finally, η_{in} for the devices being investigated was estimated as around 72% by substituting all required values in eq. (5).

4.2. Effect of active layer thickness on the response of WGPD

Generally, the coupling efficiency and hence η_{ext} of a detector can be improved by increasing the thickness of the intrinsic layer. In order to look at the effect of intrinsic layer thickness on the response of the GaAs WGPD, the device-3 was used as an WGPD. This device had a 0.5 μm thick active layer. Figure 4 shows the response of device-1, 2 and 3 as a function of the active layer thickness. Increase in external sensitivity of the GaAs WGPD with an increase in the active layer thickness is in agreement with theoretical and experimental predictions. Figure 4 gives an external sensitivity value of 0.33 A/W for device-3 which corresponds to an external quantum efficiency of 48%. For the typical values of η_{ext} = 48%, $R_1 = R_2$ = 4%, L = 250μm and Γ = 90%, α_{ib}= 200/cm /2/, ζ was calculated as 50.6% and S_{int} was calculated as 0.64 A/W. Finally, η_{in} for the devices being investigated was estimated as 74%. Estimated value of S_{int} and η_{in} are nearly the same in the case of device-1, 2 and 3 because S_{int} η_{in} are independent of active layer thickness.

Conclusion

In conclusion we can say that a WGPD with thick absorption or active layer has higher η_{ext}. However, η_{ext} is the external conversion efficiency and it does not represent the internal conversion efficiency of the device. Hence increase in active layer thickness does not affect the internal quantum efficiency. η_{in} of WGPDs made from the same material with different active layer thickness would be more or less same provided incoming light is fully decayed in waveguide.

References

/1./ D. Lasaosa, J.W. Shi, D. Pasquariello, K.G. Gan, Ming-Chun M.C. Tien H.H. Chang S.W. Chu, C.K. Sun Y.J. Chiu, J.E. Bowers, "Traveling-wave photodetectors with high power-bandwidth and gain-bandwidth product performance" IEEE J. of **Selected Topics in Quantum Electron, 10**, 728-741, (2004).

/2./ D. Moss, D. Landheer, D. Conn, D. Halliday, S. Charbonneau, G. Aers, R. Barber and F. Chatenoud, "High-speed photodetection in a reverse biased GaAs/AlGaAs GRINSCH SQW laser structure", IEEE Photonics Tech. Lett., **4**, 609-611 (1992).

/3./ J. Alping, "Waveguide *pin* photodetectors: Theoretical analysis and design criteria", IEE Proc. **136-J**, 177-182 (1989).

/4./ A. Larsson, P.A. Andrekson, S.T. Eng, and A. Yariv, "Tuneable superlattice p-i-n photodetectors: Characteristics, theory and applications", IEEE J. Quantum Electron., **QE-24**, 787-801 (1988).

/5./ E. Pinkas, B.I. Miller, I. Hayashi, and P.W. Foy, "Additional data on the effect of doping on the lasing characteristics of GaAs-AlxGa1-xAs double heterostructure lasers", IEEE J. of Quantum Electron., **QE-9**, 281-282 (1973).

/6./ A. Karim, "A free-space alignment technique for active optical waveguide components", Semiconductor Physics, Quantum Electronics & Optoelectronics, **5**, 319-321 (2002).

/7./ A. Sasaki, M. Nishiuma, and Y. Takeda, "Energy band structure and lattice chart of III-V mixed semiconductors and AlGaSb/AlGaAsSb semiconductor lasers on GaSb substrate", Jap. J. of Applied Phys., **9**, 1695-1702 (1980).

Abid Karim
Bahria University (Karachi Campus),
National Stadium Road Karachi, Pakistan
Tel. (92 21) 9240002 (5 lines), Fax. (92 21) 9240351)
Email: abid@bimcs.edu.pk, akarimpk@yahoo.com

Prispelo (Arrived): 23.02.2009 Sprejeto (Accepted): 09.09.2009

DOLOČANJE RADIJSKE VIDLJIVOSTI UPORABNIKOV AIR STORITEV S POMOČJO SIMULACIJSKEGA ORODJA OPNET MODELER IN MODULA 3DNV

Saša Klampfer, Jože Mohorko, Peter Planinšič, Žarko Čučej

Univerza v Mariboru, Fakulteta za elektrotehniko, računalništvo in informatiko, Maribor, Slovenija

Kjučne besede: OPNET Modeler, radijska vidljivost, model širjenja radijskih valov, TIREM4, karakteristika slabljenja, brezžične storitve, 3DNV, višinska kartografija, virtualni teren.

Izvleček: Ideja za strokovni prispevek je nastala na podlagi vse večje razširjenosti brezžičnih AIR storitev, katere delujejo na izredno visokih frekvenčnih pasovih, le ti pa pogojujejo direktno radijsko vidljivost uporabniške opreme na posamezen oddajnik. Članek opisuje enega izmed možnih načinov preverjanja radijske vidljivosti uporabnikov AIR storitev z uporabo simulacijskega orodja OPNET in virtualne višinske kartografije DTED za področje Maribora z okolico. Pri tem smo se omejili na gradnike, ki jih AIR sistem vsebuje. V prvem delu članka smo se omejili predvsem na posamezne gradnike, ki se morajo skladati z gradniki realnega sistema, tukaj imamo v mislih predvsem oddajno moč in ostale karakteristike oddajnika, občutljivost sprejemnih enot, modulacije, model širjenja radijskih valov, ki se mora tembolj prilegati realnemu razširjanju radijskega valovanja v odprtem prostoru, natančnost virtualnega terena v simulaciji itd. Opisali smo tri različne principe s pomočjo katerih lahko ugotavljamo ustreznost radijske vidljivosti, kamor spada analiza statistik oddanega in sprejetega prometa (oddajnik pošilja poizvedovalne pakete (ping)), analiza slabljenja oddane moči v odvisnosti od reliefa terena, prevodnosti prenosnega medija in v odvisnosti od oddaljenosti, ter direktna analiza posameznih radijskih povezav na virtualnem 3D terenu, z grafičnim prikazom radijske vidljivosti. Da bi bili rezultati simulacij čimbolj verodostojni podajamo v nadaljevanju še rezultate simulacij pri katerih je upoštevana prevodnost prenosnega kanala po zraku, ki vključuje različne vremenske motnje (dež, sneg,...). Vremenske vplive smo upoštevali v modelu širjenja radijskih valov, kamor smo vnašali poznane vrednosti prevodnosti zraka, kjer se le te spreminjajo od količine vlažnosti v zraku, večjih delcev v zraku itd.

Defining Radio Visibility of AIR Users with OPNET Modeler Simulation Tool and 3DNV Module

Key words: OPNET Modeler, radio visibility, radio propagation model, TIREM4, line attenuation characteristic, wireless services, 3DNV, DTED maps, virtual terrain.

Abstract: The main idea is concerned with today well spread wireless AIR services which work on high frequencies and frequency bandwidths, and this is the main reason, why users need direct radio visibility that their AIR equipment can be connected on radio transmitter. In this paper is described one of the many possible radio visibility check approaches where also belongs OPNET Modeler simulation tool with virtual DTED maps of Maribor with neighborhood. At the beginning of this paper we introduce main parts of AIR system which plays important part when defining radio visibility between user equipment and radio transmitter. Those main parts must have similar as possible characteristics as real elements have in real systems. Here we are concentrated on transmitting power, modulations, receiver station density, free space radio propagation model, virtual terrain preciseness etc. During this introduction we give detail description of three possible methods which could give us some conclusions about radio visibility. These three approaches are; received traffic (ping) statistic analysis on the receiver side, line attenuation characteristic analysis considering cross terrain intersection and air interface conductivity, and direct radio visibility analyze on virtual 3D terrain with graphical path loss illustration. To obtain precise as possible results is important to consider weather conditions especially air conductivity (rain, snow, storms...), because such communication occurs on high frequencies (5 GHz upstream and 12 GHz downstream). Such weather conditions are included as appoint parameters in radio propagation model TIREM4.

1. Uvod

Sodobni načini telekomunikacijskih infrastruktur, ki smo jih do sedaj poznali samo v tujini, prodirajo z veliko hitrostjo tudi na naše tržišče. Glede na pestro razgibanost reliefnega terena Republike Slovenije se je pojavila ideja o postavitvi brezžičnih sistemov, s katerimi bi lahko zagotavljali sodobne storitve, tako imenovane trojčke (internet, televizija, telefonija), ki jih uporabniki na optičnih povezavah in lokacijah blizu lokalnih central že dlje časa poznajo. Ideja se je tako uresničila, za to pa je zaslužno podjetje GlobTel, ki je razvilo ustrezno opremo za zagotavljanje sodobnih brezžičnih storitev. Zaradi narave delovanja sistema na visokih frekvencah je s tem pogojena tudi direktna radijska vidljivost na glavni oddajnik v kolikor uporabniki želijo spremljati AIR storitve. To sicer zoži nabor potencialnih uporabnikov, pa vendarle še venomer ostaja veliko takšnih, ki do sedaj iz različnih razlogov niso imeli dostopa do sodobnih internetnih storitev. Pogoj radijske vidljivosti pa je takoj ponudil idejo o analizi le-te s pomočjo simulacijskih orodij s katerimi razpolagamo. Iz tega razloga smo opravili študijo analize radijske vidljivosti s pomočjo simulacijskega orodja OPNET Modeler in modula 3DNV. Orodje vključuje kvaliteten model širjenja radijskih valov, imenovan TIREM4, kateremu je možno spreminjati številne parametre, ki opisujejo vremenske pogoje (prevodnost zraka ipd.). Model TIREM4 uporablja prav tako ameriška vojska za modeliranje svojih komunikacijskih radijskih povezav na virtualnem terenu. V orodju lahko modeliramo oddajnike (oddajna moč, višina antene, polarizacija antene, modulacija, frekvenčno področje itd.) kakor tudi sprejemnike (uporabniška oprema). Tekom opravljene študije smo uspešnost radijske

vidljivosti s pomočjo orodja OPNET lahko preverili na tri različne načine, le te pa bomo podrobneje predstavili v nadaljevanju. Študija je namenjena potencialnim ponudnikom AIR storitev, kateri še nimajo dorečenih modelov preverjanja vidljivosti, in jim je lahko naš pristop v veliko pomoč pri preverjanju dostopnosti na njihovo brezžično omrežje.

V drugem poglavju predstavljamo osrednjo problematiko, iz katere se je razvila naša ideja o preverjanju radijske vidljivosti s pomočjo simulacije. V okviru istega poglavja bomo na kratko podali še kratek pregled nad AIR sistemom, ki je postavljen na Pohorju. V tretjem poglavju opisujemo glavne gradnike, ki smo jih modelirali v simulaciji in kateri so potrebni pri analizi radijske vidljivosti. V četrtem poglavju smo predstavili uporabljen model širjenja radijskih valov TIREM4, ter njegove lastnosti, medtem ko v petem poglavju podajamo kratko predstavitev simulacijskega orodja OPNET Modeler. Šesto poglavje prikazuje testni simulacijski scenarij z uporabljeno DTED višinsko kartografijo, katerega smo uporabljali za določanje radijske vidljivosti. V sedmem poglavju so predstavljeni rezultati in vsi trije možni načini opazovanja radijske vidljivosti med oddajnikom in posamezno uporabniško enoto. Članek zaključujemo s sklepnim osmim poglavjem.

2. Osnovna problematika in ideja

S pojavom in uspešno implementacijo brezžične tehnologije AIR storitev na mariborskem Pohorju, se nam je takoj porodila ideja o preučevanju radijske vidljivosti glede na frekvenčno naravo delovanja samega sistema. Ker gre za frekvenčno področje nad 5GHz, je vidljivost uporabnika na oddajnik ključnega pomena. V razpoložljivem simulacijskem orodju, s katerim razpolagamo, smo uvideli, da lahko radijsko vidljivost ocenimo na tri različne načine, ter hkrati simulacijski sistem modeliramo v potankosti, da se le-ta čimbolj sklada z realnim sistemom. Kot bomo spoznali v nadaljevanju, lahko v orodju modeliramo polarizacijo oddajnika, sevalni kot oddajnika, višino, frekvenčni pas, modulacijo..., ter na uporabnikovi strani občutljivost uporabniške opreme, frekvenčni pas, v katerem naj sprejemnik deluje, način modulacije itd. Vsi omenjeni parametri vplivajo na natančnost modeliranja, le-to pa bo pogojeno tudi z natančnostjo višinske kartografije, ko jo vključimo v simulacijsko orodje. Čimbolj natančna je kartografija, tembolj natančen bo simulacijski model. Ideja kako opazovati vidljivost v simulacijskem okolju je sila preprosta; če upoštevamo, da smo vse gradnike modelirali dovolj natančno, imamo na voljo za preverjanje, ali vidljivost obstaja ali ne, sledeče možnosti: preverimo karakteristiko slabljenja signala med oddajnikom in sprejemnikom v odvisnosti od vpliva terena, pri čemer oddajamo nek simbolni promet (npr. ping). Če le-ta na določeni oddaljenosti (pozicija) pade pod določeno mejo, je to za nas znak, da se uporabniška enota in oddajnik med seboj ne vidita oziroma v nasprotnem primeru karakteristika slabljenja signala ostane v celotnem obsegu nad pred-definirano mejo (ang. threshold). V drugem primeru lahko opazujem statistiko oddanega in sprejetega prometa. V kolikor med postajama ne obstaja direktna vidljivost, bo oddajnik promet oddajal, sprejemnik pa le tega ne bo sprejemal. Zadnja možnost pa se navezuje na interaktivno spremljanje dogajanja v 3DNV paketu, kjer dogajanje prikazujemo na virtualnem 3D terenu (Slika 1). Ob vsaki enoti se izpisujejo parametri o stanju povezave do oddajnika, iz katerih lahko sklepamo o radijski vidljivosti. Ta način tudi uporabnika obvešča o sami vidljivosti z barvo označenih povezav. Če je povezava do oddajnika označena z rdečo, to simbolizira, da le-ta ne more eksistirati. Vse do sedaj naštete možnosti preučevanja radijske vidljivosti bomo predstavili v obliki rezultatov v sedmem poglavju. Tekom študije smo prišli do zaključka, da lahko z našim predlaganim sistemom preverjanja radijske vidljivosti v simulaciji operater preveri, več različnih scenarijev, na katero geografsko pozicijo se mu bolj izplača postaviti oddajnik, da bo pokril čim večji geografski del, na katerem se nahajajo morebitni potencialni uporabniki njegovih storitev.

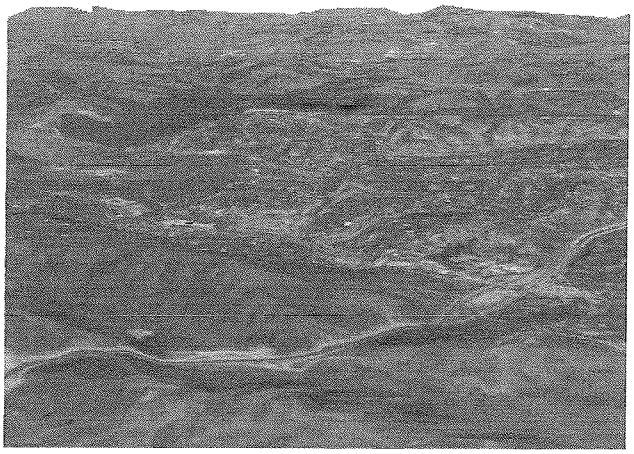

Slika 1: Višinska karta v 3D prikazu (3DNV)

3. Osnovni gradniki, kot osnovni sestavni del za preverjanje radijske vidljivosti v simulaciji

Med osnovne gradnike, od katerih zavisi natančnost rezultata simulacije spadajo oddajnik, višina antene, frekvenčni pas oddajanja, modulacija, oddajna moč, geografska pozicija, natančnost virtualne višinske kartografije in občutljivost ter višina antene sprejemne enote /2/.

Oddajnik: Večtočkovni oddajnik sprejme signale iz osnovne postaje. Signal se nato pretvori v visoke oddajne frekvence, ki se najprej filtrirajo in ojačijo. Pasovna širina je ekvivalentna tisti, ki jo oddajnik prejme od osnovne enote (ang. main station). Signal se nato distribuira čez omni sektorizirane antene s tipičnim ojačenjem 10dB. Da bo simulacijski model čim bolj precizen, najprej oddajni anteni definiramo njeno višino, ki se sklada z višino, na kateri je nameščena realna antena in tudi sama geografska pozicija v simulacijski strukturi se mora ujemati z geografsko pozicijo realnega oddajnika. Le-to določimo v simulaciji z vnosom koordinat. Tako zadovoljimo kriterij ujemanja. Ključen pomen pri kvaliteti prenosa ima modulacija. Le-ta

se izbira glede na potrebe robustnosti, v največji meri pa se uporablja kvadraturna amplitudna modulacija QAM-16 /4/. Iz tega razloga podajamo v nadaljevanju še kratek opis omenjene modulacije, ki predstavlja pomemben gradnik prenosa radijskega valovanja.

QAM modulacija: Kvadraturna amplitudna modulacija je osnovni predstavnik digitalnih modulacij, kjer se hkrati spreminjata amplituda in faza nosilnega signala. Za lažjo predstavo prikazujemo na sliki 2 blokovno shemo modulatorja na strani oddajnika.

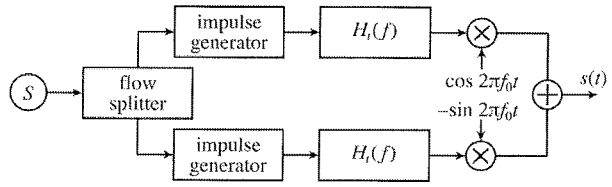

Slika 2: Blokovna shema modulatorja na strani oddajnika

V prvi fazi se bitni tok, ki se prenaša, porazdeli v dva ekvivalentna dela, kar zagotavlja dva neodvisna signala, ki se prenašata. Oba signala se nato individualno kodirata. Po postopku kodiranja se en kanal (tisti, ki je v fazi) pomnoži s kosinusno funkcijo, medtem ko je preostali kanal (preostali pravokoten, ang. quadrature) pomnožen s sinusno funkcijo. V takšnem primeru je med obema kanaloma 90° faznega zamika. Oba signala se nato združita in pošljeta preko prenosnega medija. Na prejemnikovi strani se skupen signal demodulira po principu, ki je prikazan na sliki 3.

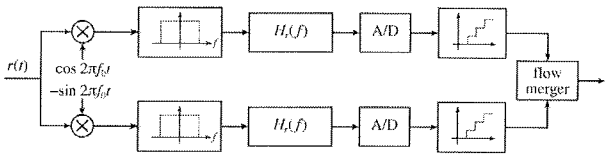

Slika 3: Blokovna shema demodulatorja na strani sprejemnika

Na strani sprejemnika ob pogoju poznanih nosilcev naprava najprej skupen sprejeti signal razdruži na 90° fazno zamaknjena signala, ki smo ju spoznali pri modulaciji, nato se izvede A/D pretvorba, bitna kvantizacija, kjer šele nato, po bitni kvantizaciji, ob združitvi obeh bitnih tokov, dobimo skupen bitni tok podatkov, ki jih prenašamo. Demodulacija predstavlja inverzni postopek modulaciji. Ker je QAM način modulacije najpogosteje uporabljen v AIR sistemu (odvisno od zahtev) in ker ima le ta ključno vlogo pri natančnosti modeliranja, smo na kratko podali njen opis /4/.

Frekvenčni pas /2/: Kot smo že v uvodu omenili, deluje AIR sistem na precej visokih frekvencah (nekaj GHz). Iz tega razloga je tudi natančnost modela odvisna od natančno definiranega frekvenčnega pasu. Le ta pa se v Sloveniji za različne regije razlikuje (glej APEK) /6/. To pomeni, da moramo v simulaciji izbrati takšno opremo, ki omogoča nastavitve frekvenčnega pasu, modulacije, oddajne moči itd. Omenjene parametre vključujejo tako MANET, kot tudi Wireless modeli v simulacijskem okolju. Iz tega razloga lahko s pravilno izbiro simulacijskih elementov zadostimo številnim kriterijem, ki smo si jih pred modeliranjem sistema postavili. Kriterije, ki morajo biti izpolnjeni, pa smo v predhodnem poglavju že spoznali.

Geografska pozicija in natančnost višinske kartografije: Z poznavanjem geografskih koordinat na katerih se nahaja realna oprema, lahko identične koordinate vnesemo v simulacijsko strukturo. S tem zagotovimo usklajenost pozicij enot na virtualnem terenu s pozicijami enot na realnem terenu. Za določanje realnih koordinat si lahko pomagamo z GPS sistemom. Na ta način lahko določamo geografske pozicije uporabniške opreme (sprejemne antene), kakor tudi pozicije obstoječih oddajnikov. Usklajenost pozicij enot na virtualnem in realnem terenu ima prav tako ključen vpliv na natančnost simulacijskega modela.

Oddajna moč, višina antene in občutljivost: Do tovrstnih parametrov lahko pridemo bodisi z meritvami (mišljeni vsi našteti parametri) ali s prebiranjem podatkovnih listov proizvajalcev posameznih komponent (oddajna moč in občutljivost). Ker smo že na začetku zadostili pogoju, ki se navezuje na izbiro takšne simulacijske enote, katera omogoča vnos vseh ključnih parametrov, nam preostane zgolj še vnos pridobljenih parametrov v simulacijske postaje.

4. Model širjenja radijskih valov TIREM4

TIREM je kratica izpeljana iz angleške besede *Terrain Integrated Rough Earth Model*, kar v prevodu pomeni integriran razgiban teren zemlje. TIREM vključuje dva modela TIREM3 in TIREM4, ki se v največji meri uporabljata pri modeliranju brezžičnih povezav. TIREM3 izhaja iz oddelka za obrambo Združenih držav Amerike, le tega pa je v zadnjih letih nadomestil izboljšani in natančnejši model razširjanja radijskih valov, ki ponuja hitrejši izračun izgube poti (ang. path loss), še posebej v primerih ko gre za v detajle dodelan 3D teren. TIREM je sposoben predvideti izgubo razširjanja radijskega valovanja (RF) za frekvenčna področja od 1MHz pa vse do 40 GHz, tako za področja kopnega kot tudi za področja na morju. V modelu lahko določimo parametre prevodnosti tal (ang. ground conductivity), relativno permeabilnost (ang. relative permittivity), vlažnost (ang. humidity), lomljenje valov na površini (ang. surface refractivity) in resolucijo, t.j. razdaljo med izohipsami na višinski karti /7/, /8/, /9/.

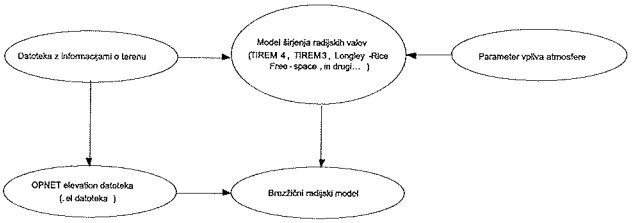

Slika 4: Povezava kartografije in modela razširjanja radijskih valov z brezžičnim omrežjem

5. Simulacijsko orodje OPNET Modeler

OPNET Modeler je vodilno simulacijsko okolje v komunikacijski industriji. Omogoča konstruiranje in študije telekomunikacijskih infrastruktur, posameznih naprav, protokolov, aplikacij ipd. Orodje stremi k objektno orientiranemu modeliranju. Ustvarjeni modeli predstavljajo zrcalo strukture dejanskih omrežij in omrežnih komponent. Prisotna je podpora za vse tipe komunikacijskih mrež z naprednimi tehnologijami kot so fast ethernet, WiFi, UMTS, GSM, itd. Simulacijski jezik bazira na seriji hierarhičnih urejevalnikov, ki vzporedno ponazorijo strukturo protokolov, opreme, mreže. Omogočena je tudi animacija dogajanja v omrežjih, kar še dodatno poenostavi razumevanje delovanja posameznega elementa. Nudi možnost ustvarjanja povsem novih enot oziroma preurejanja že obstoječih. Preureditev že obstoječe enote je možna celo na kodnem nivoju, ki je izveden s C/C++ programskim jezikom. Orodje omogoča tudi simulacije na virtualnem terenu z uporabo višinskih DTED kart, ki jih lahko prikažemo v 3D obliki z modulom 3DNV. Z natančnostjo višinske kartografije je pogojen realističen prikaz na 3D virtualnem terenu. Da bi 3D relief čimbolj ustrezal realnemu, kjer imamo v mislih predvsem ceste in ključne objekte, lahko le te v obliki ustreznih slik po plasteh uvozimo na želeno kartografijo. V zadnjem času se v OPNET orodju zelo uveljavlja modul SITL, ki omogoča povezavo simuliranih omrežij, elementov, naprav, z zunanjimi realnimi omrežji, elementi oziroma napravami. To pomeni, da nam v simulaciji ni več potrebno modelirati prometa, temveč lahko le tega zajamemo iz realnega omrežja, elementa, naprave, in ga pretočimo čez simulirano omrežje, nato pa ga vrnemo nazaj v realno omrežje. Na ta način nam orodje omogoča opazovanje stanja v omrežju, če nanj na primer »virtualno« v simulaciji priključimo dodatne uporabnike itd. Zadnja različica simulacijskega orodja vsebuje še zelo natančen model razširjanja radijskih valov imenovan TIREM4, ki velja za enega izmen najbolj natančnih modelov in ga v simulacijah uporablja celo ameriška vojska. Omenjen model smo pri analizi radijske vidljivosti s pridom izkoristili tudi mi /1/, /3/, /5/.

6. Simulacijska struktura preverjanja radijske vidljivosti

V simulacijsko strukturo smo vključili vse do sedaj omenjene ključne elemente, ki vplivajo na potek komunikacije med oddajnikom in sprejemnikom (slika 5).

V prvem scenariju smo na virtualni teren naključno postavili sprejemne enote, le-te pa se nahajajo na različnih geografskih pozicijah (hribi, doline...) in na različnih oddaljenostih. Namen tega scenarija je pokazati končnemu uporabniku, kako lahko predvidi področje pokritosti s signalom. Testni promet, ki smo ga pretakali čez omrežje zagotavlja *http* strežnik, ki v kratkih časovnih intervalih pošilja testni promet do končnih uporabnikov, seveda tistih, ki so v dosegu oddajnika in imajo direktno radijsko vidljivost. Z

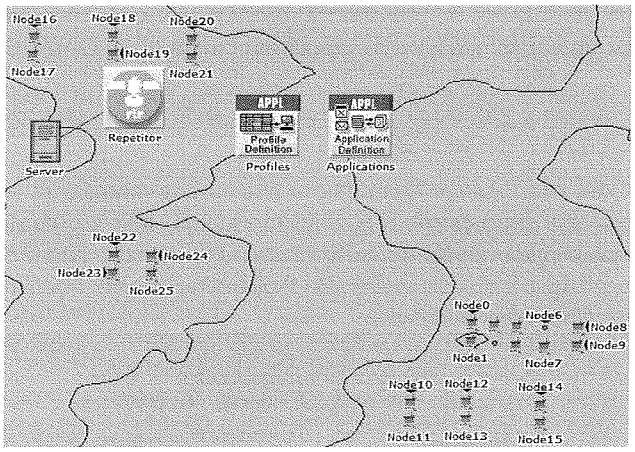

Slika 5: Scenarij postavitve enot na virtualnem terenu z višinsko DTED kartografijo z enim oddajnikom

blokom *'Applications'* definiramo aplikacije za katere želimo, da so prisotne v simuliranem omrežju (za naš primer samo *http*), medtem ko z blokom *'Profiles'* določimo uporabniške profile, ki jih nato priredimo uporabnikom. Strežnik in oddajnik sta med seboj povezana z 100BaseT ožičeno povezavo. Rezultati simulacij, ki jih bomo spoznali v sedmem poglavju bodo nazorno prikazali pomanjkljivosti takšnega scenarija, saj bo večina enot izven radijske vidljivosti. Iz tega razloga smo ustvarili še drugi scenarij, v katerem smo dodali še en dodaten oddajnik, ki pokriva JV sektor (slika 6), s čimer pokrijemo še dodatna področja, katera prej niso imela direktne radijske vidljivosti. Kljub temu, pa tudi na ta način ne moremo zagotoviti vidljivosti vsem uporabnikom, saj je narava razgibanosti terena v Sloveniji preveč pestra.

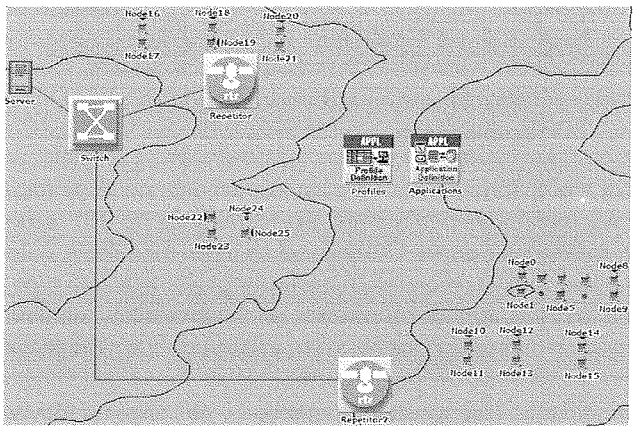

Slika 6: Scenarij postavitve enot na virtualnem terenu z višinsko DTED kartografijo z dvema oddajnikoma

V drugem scenariju povezavo razdelimo na dva dela s pomočjo omrežnega stikala, kjer vsako izmed obeh povezav priključimo na posamezen oddajnik. Drugi scenarij je prav tako pripravljen na tako imenovane 'roaming' eksperimente, ki bi prišli v poštev v primeru uporabe mobilnih postaj z definiranimi trajektorijami na terenu. Za oba scenarija so

enote, ki predstavljajo uporabniško opremo fiksne. Predstavljeni rezultati drugega scenarija v sedmem poglavju bodo nazorno pokazali, da smo z JV oddajnikom pokrili dodatne postaje.

7. Simulacijski rezultati in možni načini preverjanja vidljivosti

Simulacijsko orodje omogoča več možnih načinov preverjanja radijske vidljivosti. Prvi in tudi najenostavnejši način se navezuje na analizo karakteristike slabljenja oddanega signala v odvisnosti od razdalje in v odvisnosti od oblike terena. Pri vseh načinih analiz je bil v simulaciji uporabljen TIREM4 model razširjanja radijskih valov, ki je opisan v četrtem poglavju. Analiza slabljenja oddanega signala v odvisnosti od terena je prikazana na sliki 7. Gre za analitično orodje, ki v prečnem prerezu predstavi obliko terena med oddajnikom in sprejemnikom (vrhovi, doline, ovire) in v navezi z reliefom izračuna model slabljenja signala. Tako imamo na sliki 7 prikazan prečni prerez terena, ki se nahaja med oddajnikom ('Repetitor' na sliki 5) in sprejemnikom ('Node15' na sliki 5). Iz prečnega prereza lahko direktno opazimo, da komunicirajoči enoti nimata med seboj radijske vidljivosti, saj se med njima nahajajo vmesne ovire. S številnimi empiričnimi poizkusi smo tudi določili mejno območje slabljenja, kjer komunikacija pade. To mejno območje znaša -95dB. Zgornji graf na sliki 6 prikazuje karakteristiko slabljenja oddanega signala v odvisnosti od terena za dve različni frekvenčni področji. Zgornja krivulja prikazuje slabljenje za frekvenco 1MHz in pasovno širino 100kHz, medtem ko spodnja krivulja ponazarja frekvenco 12GHz in pasovno širino 296MHz. Iz prvega rezultata je lepo opazna večja občutljivost visokofrekvenčnega signala v odvisnosti od terena v primerjavi z manjšo občutljivostjo nižje frekvenčnega signala. Za obe frekvenčni področji pa v tem scenariju ne moremo zagotoviti radijske vidljivosti, saj se med komunicirajočima enotama nahajajo vmesne ovire. Iz karakteristike slabljenja vidimo, da je slabljenje med -100 in -200dB, kar avtomatsko pomeni, da je takšna vrednost pod mejo -95dB, to pa pomeni, da komunikacija pri takšnem slabljenju ne more eksistirati. Z navpično črtkano črto je označen položaj enote na terenu, ki hkrati določa še vrednost slabljenja za to pozicijo. Vmesnik nam ponudi še številne druge prametre, ki jih lahko spreminjamo, sem pa spadajo lega oddajnika in sprejemnika po zemljepisni dolžini in zemljepisni širini, višina oddajne antene, višina sprejemne antene, nastavitev centralne frekvence, nastavitev pasovne širine in izbira modela širjenja radijskih valov (Longley-Rice, TIREM3, TIREM4...). V modelu smo nastavili višino oddajne antene na 10 metrov, sprejemne pa 1 meter.

Za vse vnesene podatke se izvrši izračun karakteristike slabljenja. V kolikor želimo prestaviti sprejemno enoto na drugo geografsko pozicijo, vnesemo nove vrednosti zemljepisne dolžine in širine ter poženemo analizo, ki nam nakaže, ali ima nova pozicija radijsko vidljivost ali ne, pri čemer se tudi avtomatično osveži prerez terena. Podobno

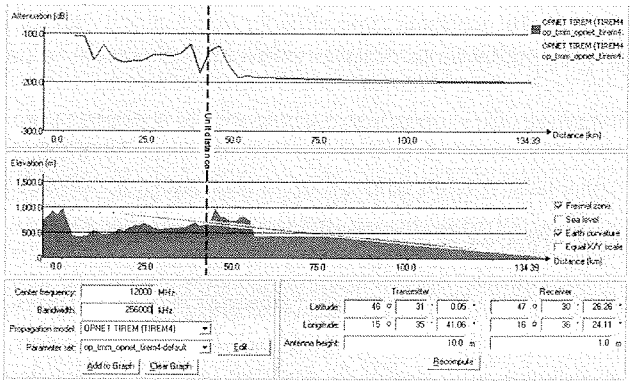

Slika 7: Karakteristika slabljenja signala v odvisnosti od terena in oddaljenosti za scenarij na sliki 5.

lahko spremljamo karakteristiko slabljenja za vsak posamezen parameter, ki ga spremenimo. Ob spremembi parametra in opravljeni analizi se nova karakteristika slabljenja doda na isti graf, s čimer imamo omogočeno spremljanje morebitnih izboljšav/poslabšanj glede na predhodne nastavitve.

Podobno analizo smo izvedli še za drugi scenarij na sliki 6, kjer smo zagotovili dodatno pokritost s signalom z dodatnim oddajnikom. S takšnim scenarijem smo pokrili večji del JV sektorja (glej sliko 6) in s tem tudi enoto 'Node15', ki v prvem scenariju ni imela radijske vidljivosti. S takšno postavitvijo oddajnika imajo enote v JV sektorju, vključno z 'Node15' direktno radijsko vidljivost na ta oddajnik, kar je tudi razvidno iz prečnega prereza terena na sliki 8.

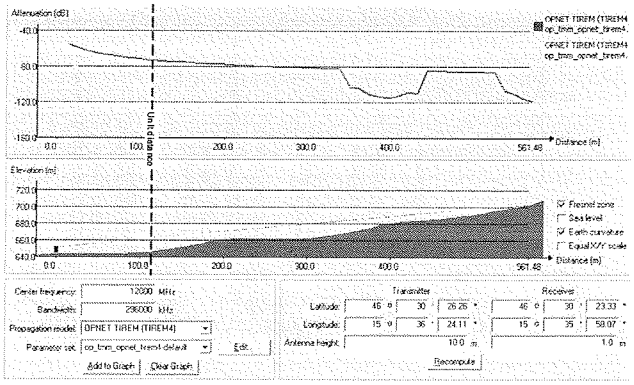

Slika 8: Karakteristika slabljenja signala v odvisnosti od terena med oddajnikom in enoto 'Node15' za scenarij na sliki 6.

V tem primeru je iz karakteristike slabljenja razvidno, da ima uporabnikova enota za obe frekvenčni področji na točki kjer se nahaja (navpična črtkana črta) zadovoljiv signal, saj slabljenje ne pade pod mejo -95dB.

Na enak način lahko preverimo vidljivost za vse ostale enote. Geografsko pozicijo lahko spreminjamo kar v vmesniku, ali pa dejansko prestavimo enoto na virtualni kartografiji na drugo pozicijo.

Kot smo že uvodoma omenili je to eden izmed številnih načinov ugotavljanja radijske vidljivosti v simulaciji ni pa edini, zato bomo v nadaljevanju predstavili še dva načina. Prvi izmed njiju je opazovanje karakteristike sprejetega prometa. To pomeni, da iz strežnika na oddajnik pošiljamo testni minimalni promet (ang. ping), ki služi zgolj za indikacijo dosega/nedosega uporabniških postaj, pri tem pa minimalno vpliva na zasedenost prenosnih kanalov. Na osnovi analize statistike sprejetega prometa lahko sklepamo, katera postaja je v vidnem dosegu oddajnika in katera ne. Da bi se prepričali v verodostojnost analize rezultata sprejetega prometa, smo vpeljali še dodaten ukrep analize bitnih napak, t.i. BER (ang. Bit Error Rate). Znano je dejstvo, da v primeru odpovedi sprejemne enote, ali da le-ta ni v radijskem dosegu, se karakteristika bitne napake strmo povzpne, saj sprejemnik ne sprejema ACK potrjevalnih okvirjev, okvirji, ki pa so poslani pa ne prispejo na cilj, kar je povod, da se zavržejo, nekateri popačijo, BER pa začne strmo naraščati.

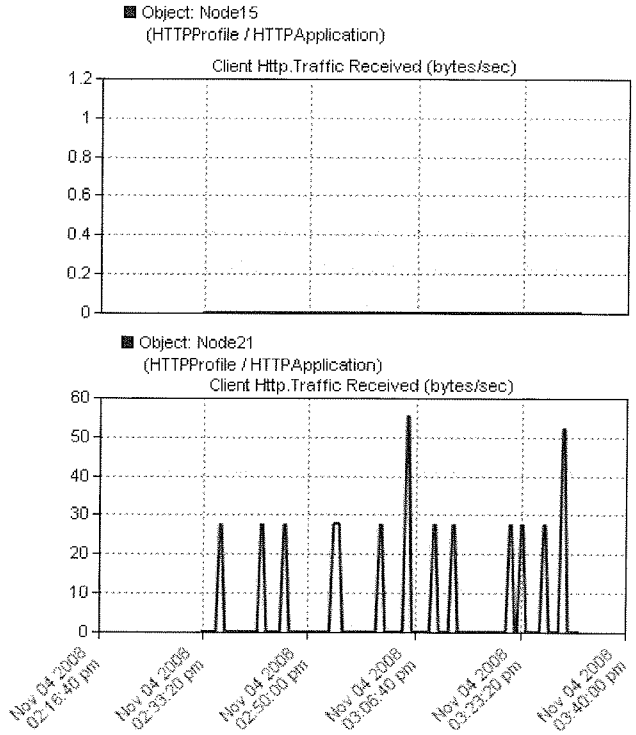

Slika 9: Analiza karakteristik sprejetega prometa enot 'Node15' in 'Node21' za prvi scenarij na sliki 5

V prvi fazi predstavljamo zgolj analizo sprejetega prometa prvega scenarija z enim oddajnikom, kjer opazujemo enoti 'Node21' in 'Node15' v dveh različnih sektorjih (glej sliko 5). Kot smo že iz prve metode ugotovili 'Node15' ni v vidnem polju oddajnika zato prometa ne more sprejemati (slika 9, gornji graf) in je iz tega razloga tudi karakteristika sprejetega prometa venomer na vrednosti 0. Obratno je z enoto 'Node21', katera se nahaja v vidnem polju oddajnika in skladno s tem tudi lahko sprejema promet (slika 9, spodnji graf). V prvem scenariju je ostal celoten JV sektor brez direktne vidljivosti. Da bi lahko pokazali še primer pokritosti področij z več oddajniki, smo v drugi scenarij vključi dodatno oddajno enoto (slika 6). Z dodatnim oddajnikom smo dosegli še dodatno območje pokritosti, vendar se je potrebno zavedati, da tudi z več deset oddajniki, ne moremo zagotoviti 100% pokritosti. Iz grafov na sliki 11 za 'Node15' in 'Node21' se lepo vidi, da je tokrat tudi 'Node15' v obsegu vidljivosti drugega oddajnika, in lahko promet sprejema, za razliko od prvega scenarija. Pri uporabi dveh oddajnikov smo uporabili sektorske antene, saj smo s tem zagotovili sevalne kote, ki se med seboj ne pokrivajo, ob tem pa se izognemo raznim interferencam in drugim pojavom, ki lahko vplivajo na kakovost komunikacije. Orodje omogoča celo modeliranje anten in antenskih sistemov, ki jih lahko nato uporabimo na že obstoječih elementih namenjenih brezžični komunikaciji ipd. Na ta način smo modelirali anteno z 270° kotom pokritosti. Sevalni diagram se lahko v 3D prikazu spremlja že med samo fazo načrtovanja, kar je načrtovalcu v veliko pomoč. Kot pokritosti in karakteristika sevanja sta še dodatno prikazani v posebnem grafu, ki je prikazan na sliki 10.

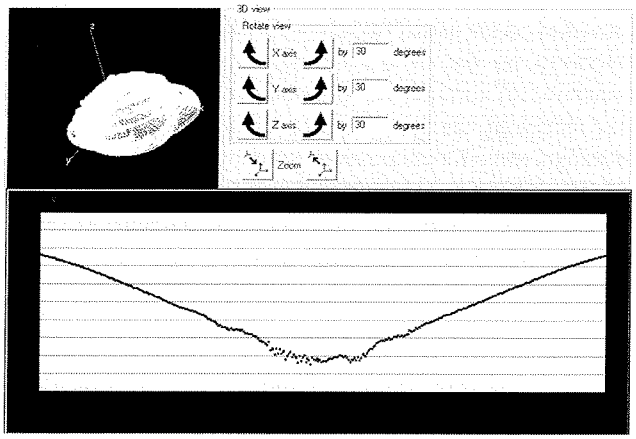

Slika 10:Modeliranje antene in prikaz sevalnega diagrama v 2D in 3D pogledu

V drugem scenariju smo tekom testiranj preizkusili tudi mobilne enote z definiranimi trajektorijami. Ker gre za dva oddajnika (dve bazni postaji), smo v simulacijo vpeljali tako imenovani 'roaming' ali gostovanje. S tem pristopom omogočimo prehajanje enot iz sektorja ene bazne postaje v sektor druge bazne postaje. Pristop nakazuje, da lahko preizkušamo tudi variante mobilnosti, določamo trajektorije poti oziroma odseke, kjer ima uporabniška oprema vidno polje na oddajnik itd., prav tako smo preizkusili scenarij, kjer je lahko posamezna uporabniška postaja z direktno vidljivostjo zastopana kot dostopna točka, preko katere se okoliške enote v njeni vidljivosti preko nje povezujejo na glavni oddajnik, vendar je to že obstranska tematika, ki se ne navezuje na ta članek.

Da bi bila informacija o nezadostni radijski vidljivosti tem bolj točna smo k vzporedni analizi vključili še analizo parametra BER. Z dodatno informacijo BER bomo lahko z veliko gotovostjo potrdili sklep iz predhodne metode. Rezultati vzporedne analize karakteristike sprejetega prometa in karakteristike BER za enoti 'Node15' in 'Node21' prvega scenarija so prikazani na sliki 12.

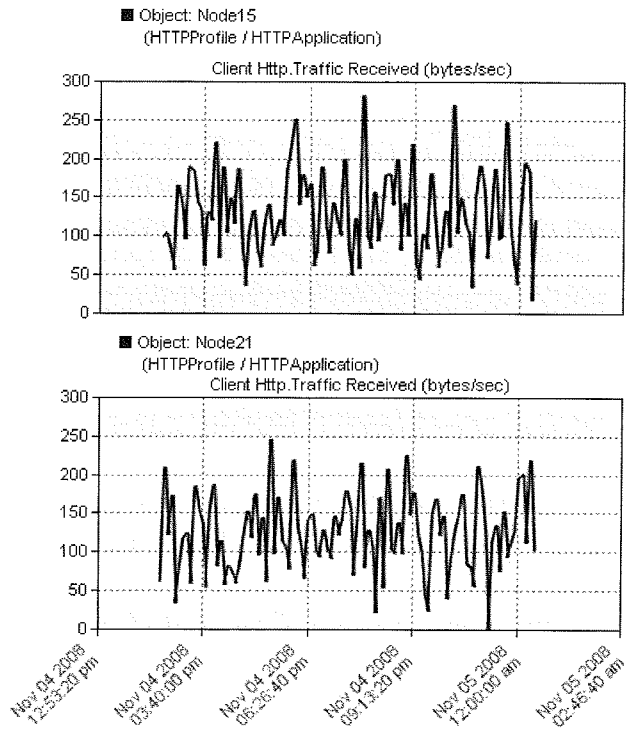

Slika 11: Analiza karakteristik sprejetega prometa enot 'Node15' in 'Node21' za drugi scenarij na sliki 6.

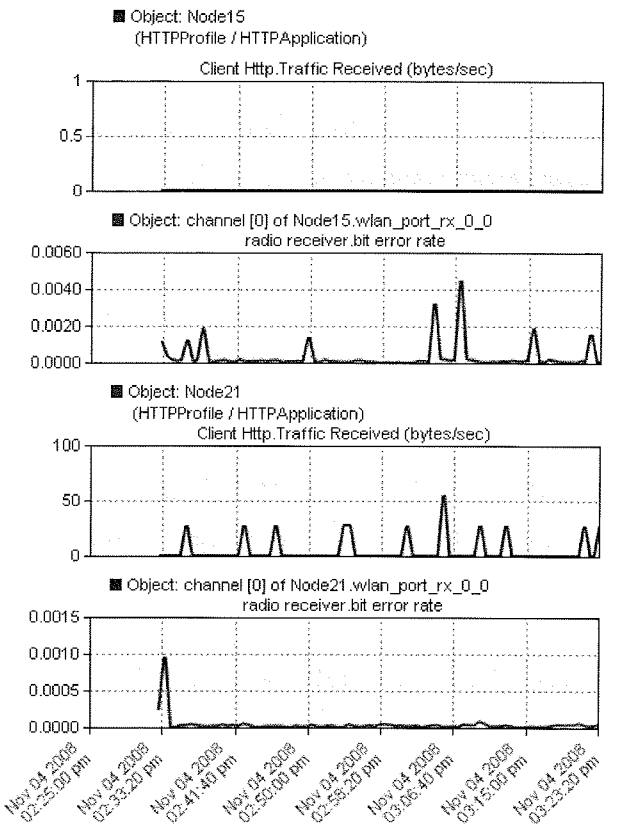

Slika 12: Prikaz vzporedne analize karakteristik BER in sprejetega prometa za enoti 'Node15' in 'Node21' prvega scenarija.

Prvi in drugi graf na sliki 12 (od zgoraj navzdol) prikazujeta sprejeti promet in BER na enoti 'Node15', medtem ko preostala dva (tretji in četrti) prikazujeta identični karakteristiki za enoto 'Node21'. Kot smo že v uvodu tega poglavja za prvi scenarij spoznali, 'Node15' nima vidnosti na oddajnik zato ne more sprejemati nobene prometa. Tej enoti je oddajnik namenil v določenem simulacijskem intervalu, določeno število paketov. Ker enota ne vidi oddajnika teh paketov ne more sprejeti, in ker jih ne more sprejeti tudi ne more odgovoriti z ACK potrditvenimi okvirji. Ko se obdobje obstoja paketa izteče TTL (ang. Time-To-Live), se le ta zavrže in zabeleži kot izgubljen, v veliko primerih pa se deformira zaradi česar, ga več ni moč prepoznati, kar se smatra kot bitna napaka. Iz drugega grafa na sliki 12 opazimo, da se v določenih primerih BER sunkovito poveča (konice), kar ob pogoju nič sprejetih podatkov iz prvega grafa na sliki 12 jasno nakazuje na problematičnost direktne vidljivosti na oddajnik. Kot smo že zgoraj omenili, enota 'Node21' sprejema promet, kar iz prvega pogoja nakazuje na direktno vidljivost. Da je takšen sklep tem bolj popoln se v to prepričamo še z analizo četrtega grafa na sliki 12, ki prikazuje tekom celotne simulacije praktično ničelno vrednost bitne napake. Na osnovi vzporedne analize lahko z veliko verjetnostjo potrdimo, da se opazovani postaji med seboj vidita. S tem smo opisali drugo metodo analize kjer smo z vzporedno analizo povečali verjetnost veljavnosti izraza, da se določeni komunicirajoči postaji vidita med seboj. Obe do sedaj predstavljeni metodi z opisanimi rezultati sta dokaj hitri in enostavni za uporabo.

Tretja možnost analize s pomočjo modula 3DNV in prikaza vidljivosti na 3D virtualnem terenu je nekoliko zahtevnejša kar se tiče priprave, rezultati pa so prikazani vizualno s pomočjo barvnih povezav in njim pripadajočih parametrov. Za simboliziranje povezave se uporablja pet osnovnih barv (črna, modra, rdeča, zelena in rumena). Za nas je pomembna predvsem rdeča barva povezave, ki simbolizira, da je s komunikacijo nekaj narobe. Metoda ima številne prednosti, saj si lahko v 3D načinu iz različni perspektiv ogledamo položaj posameznih enot, reliefno pozicijo, okolico enote itd. Eden izmed možnih prikazov perspektive opazovanja enote je prikazan na sliki 13.

V tem načinu, lahko za vsako enoto pogledamo njene parametre, kot so višinska pozicija, koordinate, ime enote in nenazadnje, če gre za mobilno enoto še njeno hitrost premikanja po terenu. Na sliki 14 imamo prikazane vse možne poti komuniciranja, tudi med uporabniškimi enotami direktno med seboj, pri upoštevanju parametrov oddajne moči, sprejemne moči, občutljivosti, modulacije itd., ki smo jih za vsako enoto posebej nastavili v simulaciji. Z rdečo povezavo so prikazane vse relacije med katerimi komunikacija ne more obstajati, bodisi zaradi oddaljenosti, bodisi zaradi vmesnih ovir na terenu. Z modro, črno in zeleno so prikazani zadovoljivi komunikacijski pogoji, medtem ko rumena barva ponazarja mejno-kritične povezave. V primeru tako imenovanega 'online' opazovanja dogajanja na virtualnem 3D terenu med samo simulacijo, se na vsaki barvni označeni povezavi izpišejo še karakteristike same povezave, ki jih

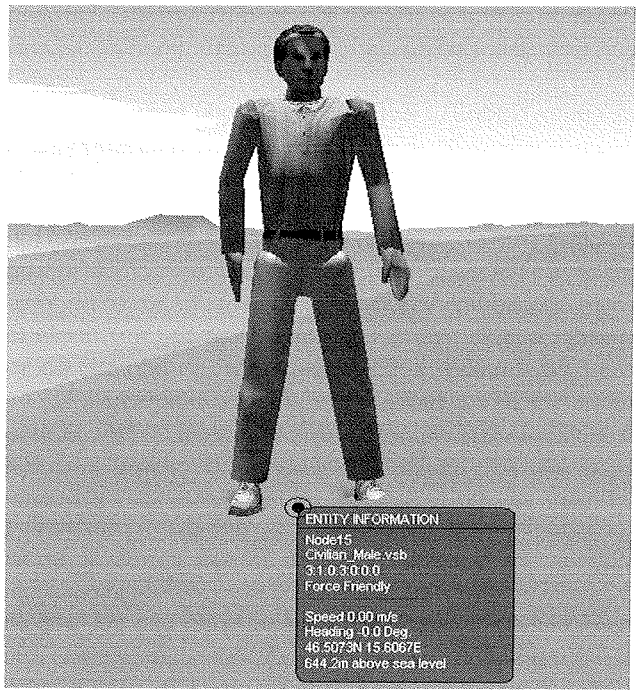

Slika 13:Prikaz položaja enote 'Node15' na virtualni 3D višinski kartografiji

lahko spremljamo tako, da se prestavimo v detajlni pogled posamezne enote, t.j. v perspektivo kot je prikazana na sliki 13.

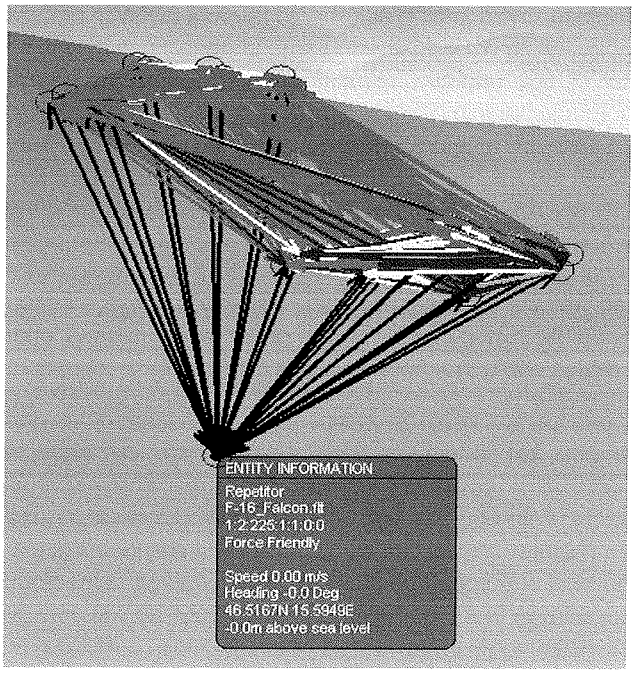

Slika 14:Prikaz vseh možnih povezav ki lahko ali pa ne morejo eksistirati za vse možne kombinacije med postajami

Zaradi lažje preglednosti smo priložili sliko 15, na kateri so vizualizirane komunikacijske poti do oddajnika in med obema opazovanima enotama 'Node15' in 'Node21', s pogledom iz ptičje perspektive. V osnovi gre za enak prikaz kot na sliki 14, vendar samo s tremi opazovanimi enotami.

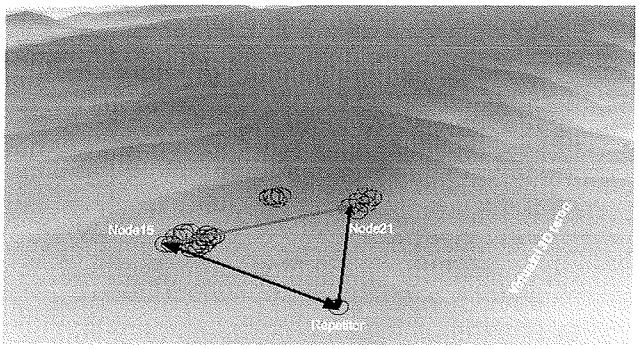

Slika 15:Prikaz enot 'Repetitor', 'Node15' in 'Node21' prvega scenarija na virtualnem 3D terenu

Tudi na virtualnem terenu z opazovanjem stanja povezav pridemo do enakih zaključkov, kot smo prišli z obema predhodnima metodama. Ker se slika 15 navezuje na prvi scenarij, je iz slike lepo opazno, da se enota 'Node15' ne vidi z oddajnikom, komunikacija torej ne eksistira, prav tako pa ne more eksistirati komunikacija med enotama 'Node15' in 'Node21'. Obe komunikacijski povezavi sta na sliki 14 označeni z rdečo barvo. Komunikacijska pot, ki pa lahko obstaja, in je bila tudi potrjena z obema predhodno predstavljenima metodama, pa je pot med oddajnikom in enoto 'Node21'. V kolikor bi se s perspektivo prestavili v položaj enote, kot je prikazan na sliki 13, bi se ob vsaki enoti prikazali povezavi, kot jih vidimo na sliki 15, od katerih bi vsaka imela izpisane svoje parametre slabljenja linije, ki smo jih spoznali že pri prvi metodi.

8. Sklep

Tekom članka smo predstavili študijo analize radijske vidljivosti s pomočjo simulacijskega okolja OPNET Modeler, modula 3DNV in višinske kartografije DTED. S takšnim pristopom lahko dovolj natančno ocenimo parameter radijske vidljivosti do posamezne uporabniške enote, brez, da bi se fizično podajali na teren in opravljali meritve vidljivosti. Natančnost modela vsekakor zavisi od natančnosti modeliranja gradnikov, ki smo jih spoznali v predhodnih poglavjih, vendarle, pa je modeliranje ob pogoju poznanih parametrov enostavno in hitro. Da je vizualizacija na 3D terenu bolj pristna se lahko v orodje uvozijo še številne kartografije s cestami in objekti. Uvažanje poteka v več plasteh, kjer lahko eno izmed plasti predstavljajo ceste, drugo plast npr. objekti itd. Rezultati, ki smo jih prejeli so zadovoljivi, in pridobljeni na hiter ter predvsem enostaven način.

9. Literatura

/1/ Mohorko Jože, Matjaž Fras, Žarko Čučej, Modeling of IRIS Replication Mechanism in Tactical Communication Network with OPNET

/2/ http://www.air-tv.net/

/3/ J. Mohorko, M. Fras, Ž. Čučej, Modeling methods in OPNET simulations of Tactical Command and Control Information Systems

/4/ http://en.wikipedia.org/wiki/Quadrature_amplitude_modulation

/5/ Saša Klampfer, Jože Mohorko, Žarko Čučej, Simulation tools in telecommunications education process

/6/ http://www.apek.si/en/operators_register?imetnik=272&storitev=-1

/7/ M. Fras, J. Mohorko, Ž. Čučej, A new approach to the modeling of network traffic in simulations, Informacije MIDEM 2008 (Junij)

/8/ M. Fras, J. Mohorko, Simulacija komunikacijskih sistemov v realnem času z realno komunikacijsko opremo v simulacijski zanki, Informacije MIDEM 2008 (Junij)

/9/ Opnet Documentation

Saša Klampfer, Jože Mohorko,
Peter Planinšič, Žarko Čučej

Univerza v Mariboru, Fakulteta za elektrotehniko, računalništvo in informatiko
Smetanova 17, Maribor, 2000, Slovenija
Epošta: sasa.klampfer@uni-mb.si

Prispelo (Arrived): 23.02.2009 *Sprejeto (Accepted): 09.09.2009*

NADGRADNJA TELEVIZIJSKEGA KANALNEGA PRETVORNIKA IN MOŽNOSTI UPORABE V DIGITALNEM TELEVIZIJSKEM OMREŽJU

Andrej Kosi, Mitja Solar

Univerza v Mariboru, Fakulteta za elektrotehniko, računalništvo in informatiko, Maribor, Slovenija

Kjučne besede: televizijski kanalni pretvornik, analogna prizemeljska televizija, digitalna prizemeljska televizija, propagacijski modeli, zaznava televizijskega signala.

Izvleček: Prehod oddajanja analognega prizemeljskega televizijskega signala v oddajanje digitalnega televizijskega signala poteka v večini evropskih držav in tudi v državah izven evropske unije. V prvi fazi izgradnje oddajniškega omrežja se običajno postavijo oddajniki z večjo oddajno močjo, ki pokrijejo s televizijskim signalom večji del prebivalstva. V naslednji fazi sledi pokrivanje s signalom na območjih, ki zaradi oddaljenosti, naravnih ali umetnih ovir še niso zadovoljivo pokrita s signalom. Pri analognih televizijskih omrežjih se v takšnih primerih običajno uporabljajo kanalni pretvorniki. Analogna televizijska omrežja so v osnovi večfrekvenčna. To pomeni, da so oddajniki in kanalni pretvorniki na različnih frekvenčnih kanalih. Digitalna televizijska omrežja so lahko večfrekvenčna, enofrekvenčna ali kombinacija obeh. Oddajanje sosednjih oddajnikov na enaki frekvenci omogoča tehnologija ortogonalnega frekvenčnega multipleksiranja (OFDM - Orthogonal Frequency-Division Multiplexing). Zaradi uporabe OFDM so tehnične zahteve za kanalni pretvornik za digitalno televizijsko omrežje drugačne kot za analogno. Spremembe so na lokalnem oscilatorju, detekcijskih vezjih, frekvenčnem pretvorniku navzdol, frekvenčnem pretvorniku navzgor in ostalih sklopih.

V prispevku je predstavljen nadgrajeni televizijski kanalni pretvornik z možnostjo delovanja v analognem in digitalnem načinu delovanja. Uporaba takšnega kanalnega pretvornika je zato še posebej zanimiva na območjih, kjer se bo analogna televizija uporabljala še dlje časa. V primeru prehoda na digitalno oddajanje bo kanalni pretvornik prešel avtomatsko v digitalni način delovanja. Nov način prenosa televizijskega signala OFDM prinaša tudi nove možnosti in izvedbe televizijskih kanalnih pretvornikov. Glede na način uporabe lahko ločimo kanalne pretvornike za večkanalno omrežje (MFN – multi frequency network) ali enokanalno omrežje (SFN – single frequency network). V MFN omrežju lahko uporabimo regenerativne in klasične kanalne pretvornike. V SFN omrežju pa se uporabljajo enostavni ojačevalniki signala, klasični kanalni pretvornik z enako sprejemno in oddajno frekvenco in enokanalni pretvorniki z izničevanjem odbojev. Izbira je odvisna od več faktorjev in glede na posamezne zahteve in omejitve za vsak primer izberemo najbolj primerno rešitev. Če naštejemo le nekaj faktorjev, kot so nivo in kvaliteta sprejetega signala, velikost območja pokrivanja, konfiguracije terena, razpoložljivosti frekvenčnega spektra, ciljna cene in ostale specifične pogoje. S pomočjo propagacijskih modelov in ostalih izračunov za pokrivanje terena s signalom bomo na praktičnih primerih predstavili omejitve in prednosti kanalnega pretvornika.

Upgrade of Television Channel Translator and Possibility of Usage in Digital Television Network

Key words: television channel translator, analog terrestrial television, digital terrestrial television, propagation models, television signal detection

Abstract: Transition from analog terrestrial television to digital television signal transmission is in progress in many countries. Usually in first phase of transition transmitting points with higher RF (radio frequency) output power are set. In this way most of the population and area is covered with digital signal quickly and efficient. Covering areas to far away from main transmitting point or covered with obstacles (natural or artificial) is done in next phase. For covering such areas in analog television translators are used. Analog television network are multi frequency networks (MFN). This means that neighbor transmitting cells are using different frequencies. Digital terrestrial television (DVB-T/H Digital Video Broadcasting – Terrestrial/Handheld) are single frequency networks (SFN), multi frequency network (MFN) or combination of both. Usage of OFDM (Orthogonal Frequency-Division Multiplexing) is allowing transmission of digital television signal for two or more neighbor transmitters on same frequency. Demands for translator used in digital terrestrial television signal are stricter as for analog television. For this reason most current analog translators are not usable for digital television, especially older ones. Changes are depending on current analog translator performance, but in most cases local oscillator, frequency up and down converter, detection circuits and other must be improved.

In article upgrade of television translator and advantages of such solution over other concepts is presented. Presented translator is capable operating in analog or digital television broadcasting network. Depending on monitored input signal, working mode is automatically changed. Because of that usage of presented translator is also very attractive in areas where analog television is still used. When main analog transmitters are replaced with digital transmitters presented translator will work forward in digital transmission mode. Digital transmission brings some new possibilities to fill uncovered areas or holes in coverage. In case of MFN network usually traditional translator concept or regenerative translator is used. In case of SFN network traditional translator concept (with same input and output frequency), on channel repeater (echo canceller) or simple amplifier (limited to very small area, usually buildings) is used. Choice depends on many factors. For example input signal level, quality of received input signal, wanted coverage area, available frequencies, price and other specific demands. Advantages and possible limits of presented channel translator are shown with usage of propagation models and calculations for coverage. There are many advantages of proposed translator as lower cost against other solutions, usage in analog or digital television network (MFN and SFN), automatic change of working mode, reliability and robustness.

1 Uvod

Prehod oddajanja analognega televizijskega signala na tako imenovani digitalni televizijski signal prinaša nove zahteve za televizijske kanalne pretvornike. Nov način prenosa televizijskega signala ortogonalno frekvenčno multipleksiranje (OFDM - Orthogonal Frequency-Division Multiplexing) prinaša tudi nove možnosti in izvedbe televizijskih kanalnih pretvornikov, ki pri analognih kanalnih pretvornikih niso bili možni. Novost so tako imenovana enofrekvenčna omrežja (single frequency network). Tako se glede na tip uporabljenega omrežja najbolj pogosto uporabljajo naslednji modeli kanalnih pretvornikov /1, 2, 3/.

MFN omrežje:

- klasični kanalni pretvornik (uporaba medfrekvence)
- regenerativni pretvornik

SFN omrežje:

- ojačevalnik signala (samo vhodni filter in ojačevalnik)
- klasični kanalni pretvornik z enako sprejemno in oddajno frekvenco (enokanalni pretvornik)
- enokanalni pretvornik z izločevanjem odbojev (echo canceller)

V MFN omrežju je možno uporabiti klasični pristop pretvorbe vhodnega signala na medfrekvenco, filtriranje in oddajanje na drugi izhodni frekvenci oziroma kanalu. Ker pri pretvorbi pride do manjše degradacija koristnega signala je zaporedno veriženje več pretvornikov številčno omejeno. Enak koncept je možno uporabiti tudi v primeru SFN omrežja. Vendar je pri SFN omrežju potrebno upoštevati omejitev, ki jo predstavlja izolacija med sprejemno in oddajno anteno, saj oddajamo signal na enaki frekvenci kot ga sprejemamo. S tem pogojem je omejena tudi največja oddajna moč kanalnega pretvornika.

Drugi pristop je regenerativni pretvornik, kjer vhodni signal najprej demoduliramo in ga potem ponovno moduliramo. V tem primeru ni degradacije kvalitete koristnega signala in veriženje pretvornikov ni omejeno. Zaradi časa procesiranja pristop ni uporaben v SFN omrežju, saj je čas procesiranja daljši od zaščitnega intervala znotraj katerega mora biti simbol ponovno oddan v eter.

Prva rešitev ki je omejena samo na SFN omrežje je uporaba ojačevalnikov signala. Prednost take rešitve je cenovna ugodnost in enostavna uporaba. Praktično pa je rešitev omejena s kvaliteto oddajnega signala in izolacijo med antenama na pokrivanje manjših področij, kot so na primer stavbe (sprejemna antena zunaj stavbe, oddajna znotraj stavbe). Druga rešitev, ki je prav tako omejena na uporabo v SFN omrežju je pristop s pomočjo izničevanja odbojev. Ta pristop omogoča višjo oddajno moč oziroma omogoča manjšo izolacijo med sprejemno in oddajno anteno v primerjavi s klasičnim kanalnim pretvornikom.

Odvisno od tehničnih pogojev, fizičnih omejitev in cene se izbere najbolj primerna metoda za posamezen primer. Ker imamo v podjetju že razvite produkte regenerativnega pretvornika in pretvornika z izničevanjem odbojev je bil naslednji korak dopolnitev ponudbe s klasičnim kanalnim pretvornikom /4/. Klasični kanalni pretvornik je zelo zanimiv predvsem zaradi ugodne cene, zanesljivosti, robustnosti in možnosti uporabe v različnih situacijah. Tako ga je možno uporabiti v vseh kombinacijah (v analognem in v obeh konceptih digitalnega omrežja).

2 Možnosti uporabe nadgrajenega kanalnega pretvornika

2.1 SFN omrežje

Na sliki 1 je prikazan primer uporabe kanalnega pretvornika v SFN omrežju. Če je kanalni pretvornik uporabljen v SFN omrežju, kot enokanalni pretvornik je treba upoštevati, da je največja izhodna moč pretvornika omejena z izolacijo med sprejemno in oddajno anteno /5/. Minimalno razliko, ki jo moramo zagotoviti imenujemo varnostna rezerva ojačanja (gain margin). Na sliki 2 je vidna povezava med varnostno rezervo ojačanja in nihanjem v izhodnem OFDM spektru.

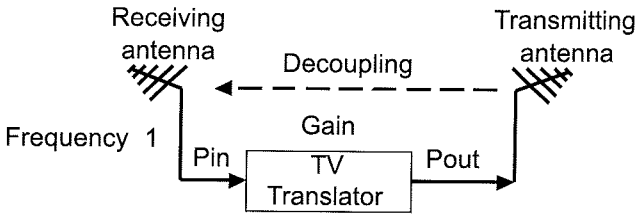

Slika 1: Uporaba kanalnega pretvornika v SFN omrežju.

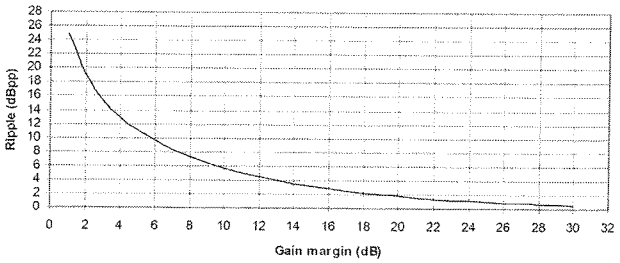

Slika 2: Povezava med varnostno rezervo ojačenja in nihanjem v izhodnem spektru.

Na naslednjem primeru si bomo ogledali relacije med vhodnim signalom, izolacijo med antenami in največjo dovoljeno izhodno močjo. Za hipotetičen antenski sistem imamo podane naslednje vrednosti:

Izolacija med antenami (isolation between antennas): 80 dB

Varnostna rezerva ojačenja (gain margin): 10 dB

Izgube zaradi kablov na oddajni anteni (antenna cable loss): 2 dB

Ojačenje antenskega sistema (transmitting antenna gain): 12 dB

Nivo vhodnega signala (input signal level): -40 dBm

Največje ojačenje kanalnega pretvornika: (80-10) dB = 70 dB

Največja oddajna moč kanalnega pretvornika: -40 dBm + 70 dB = 30 dBm (1 W)

ERP (Effective Radiated Power): 30 dBm -2 dB+12 dB= **40 dBm** (10 W)

Varnostna rezerva ojačenja zagotavlja stabilno delovanje kanalnega pretvornika. Dokler je razlika (izolacija med antenama - ojačenje kanalnega pretvornika) večja od varnostne rezerve, je nihanje (ang. ripple) v izhodnem OFDM spektru še sprejemljivo. V primeru, da ta pogoj ni izpolnjen in je razlika manjša ali negativna, se to odraža na izhodnem OFDM spektru kot preveliko nihanje. Kar lahko privede do nestabilnega delovanje oziroma oscilacij. Za dani primer vidimo, da je zgornja vrednost oddajne moči kanalnega pretvornika omejena na 30 dBm. Največja oddajna moč je neposredno odvisna od izolacije med antenama. Če želimo povečati oddajno moč je potrebno povečati izolacijo med antenama. V praksi je možno v nekaterih primerih doseči izolacije tudi do 100 dB (običajno pa se vrednosti gibljejo med 75 do 85 dB). Če izolacije ni možno povečati in kljub temu rabimo večjo oddajno moč lahko kanalni pretvornik uporabimo, kot kanalni pretvornik z različno izhodno frekvenco (MFN). Druga možnost pa je uporaba enofrekvenčnega pretvornika z izločevanjem odbojev, kjer imamo lahko od 10 do 15 dB večjo izhodno moč kot pri pristopu s klasičnem kanalnim pretvornikom.

2.2 Teoretični izračuni pokritosti s signalom

Za lažjo predstavo, kakšno področje lahko pokrijemo z določeno oddajno močjo, si bomo pogledali še teoretični izračun za pokrivanje s signalom. Sam izračun je odvisen od mnogo parametrov, zato bomo izbrali parametre, ki se uporabljajo v Sloveniji oziroma v sosednjih državah. Najprej določimo potrebno razmerje med močjo nosilca signala in šumom (C/N carrier to noise ratio) za zadovoljiv sprejem signala. Zadovoljiv sprejem predstavlja pojavljanje bitne napake (Bit Error Rate - BER) z vrednostjo manjšo od $2x10^{-4}$. Za različne oddajne parametre lahko podatke razberemo iz slike 3 oziroma iz tabel zapisanih v ETSI standardih /6/. Za parametre oddajanja, ki jih uporabljamo v Sloveniji (kanal 8 MHz, modulacija 64QAM, kodno razmerje 2/3) za digitalno oddajanje in ob predpostavki Ricean kanala je vrednost C/N enaka 17,1. Podatke za Ricean kanal uporabimo v primeru strešne antene, kjer je sprejem signala možen neposredno od oddajnika (pretvornika) in

		Required C/N for BER = 2×10^{-4} after Viterbi QEF after Reed-Solomon			Bitrate (Mbit/s)			
Modulation	Code rate	Gaussian channel	Ricean channel (F_1)	Rayleigh channel (P_1)	Δ/T_U = 1/4	Δ/T_U = 1/8	Δ/T_U = 1/16	Δ/T_U = 1/32
QPSK	1/2	3,1	3,6	5,4	4,98	5,53	5,85	6,03
QPSK	2/3	4,9	5,7	8,4	6,64	7,37	7,81	8,04
QPSK	3/4	5,9	6,8	10,7	7,46	8,29	8,78	9,05
QPSK	5/6	6,9	8,0	13,1	8,29	9,22	9,76	10,05
QPSK	7/8	7,7	8,7	16,3	8,71	9,68	10,25	10,56
16-QAM	1/2	8,8	9,6	11,2	9,95	11,06	11,71	12,06
16-QAM	2/3	11,1	11,6	14,2	13,27	14,75	15,61	16,09
16-QAM	3/4	12,5	13,0	16,7	14,93	16,59	17,56	18,10
16-QAM	5/6	13,5	14,4	19,3	16,59	18,43	19,52	20,11
16-QAM	7/8	13,9	15,0	22,8	17,42	19,35	20,49	21,11
64-QAM	1/2	14,4	14,7	16,0	14,93	16,59	17,56	18,10
64-QAM	2/3	16,5	17,1	19,3	19,91	22,12	23,42	24,13
64-QAM	3/4	18,0	18,6	21,7	22,39	24,88	26,35	27,14
64-QAM	5/6	19,3	20,0	25,3	24,86	27,65	29,27	30,16
64-QAM	7/8	20,1	21,0	27,9	26,13	29,03	30,74	31,67

Slika 3: Razmerje C/N podano za različne oddajne parametre.

posredno preko odbojev signala. Iz slike 4 oziroma ETSI tehničnega poročila lahko razberemo, da je za takšno razmerje C/N in 70% lokacijsko verjetnost (location probability) pokrivanja potrebna poljska jakost E_{med} = 48 dBμV/m (za 95% lokacijsko verjetnost pa 54 dBμV/m) /7/. Če vzamemo za primerjavo sosednjo Avstrijo (modulacija 16QAM in kodno razmerje 3/4) je potrebno razmerje C/N=13,0 (oziroma E_{med} = 44 dBμV/m).

Frequency	f (MHz)	800				
Minimum C/N required by system	(dB)	2	8	14	20	26
Min. receiver signal input power	$P_{s\,min}$ (dBW)	-126,2	-120,2	-114,2	-108,2	-102,2
Min. equivalent receiver input voltage, 75 Ω	$U_{s\,min}$ (dBμV)	13	19	25	31	37
Feeder loss	L_f (dB)	5				
Antenna gain relative to half wave dipole	G_a (dB)	12				
Effective antenna aperture	A_e (dBm²)	-5,4				
Min power flux density at receiving place	ϕ_{min} (dBW/m²)	-115,9	-109,9	-103,9	-97,9	-91,9
Min equivalent field strength at receiving place	E_{min} (dBμV/m)	30	36	42	48	54
Allowance for man made noise	P_{rmmn} (dB)	0				
Location probability: 70 %						
Location correction factor	C_l (dB)	2,9				
Minimum median power flux density at 10 m a.g.l. 50 % of time and 50 % of locations	ϕ_{med} (dBW/m²)	-113	-107	-101	-95	-89
Minimum median equivalent field strength at 10 m a.g.l. 50 % of time and 50 % of locations	E_{med} (dBμV/m)	33	39	45	51	57
Location probability: 95 %						
Location correction factor	C_l (dB)	9				
Minimum median power flux density at 10 m a.g.l. 50 % of time and 50 % of locations	ϕ_{med} (dBW/m²)	-106,9	-100,9	-94,9	-88,9	-82,9
Minimum median equivalent field strength at 10 m a.g.l. 50 % of time and 50 % of locations	E_{med} (dBμV/m)	39	45	51	57	63

Slika 4: Poljska jakost E_{med} glede na zahtevano razmerje C/N.

Sedaj, ko poznamo minimalno poljsko jakost za zadovoljivo pokrivanje s signalom lahko izračunamo oddajna moč potrebno za pokrivanje določenega terena. Iz naslednjih enačb bomo dobili povezavo med poljsko jakostjo, oddajno močjo in propagacijskimi izgubami /8/

$$P_r = \left(\frac{\lambda}{4\pi}\right)^2 \frac{E^2}{30} = \left(\frac{c}{4\pi * f_{Hz}}\right)^2 \frac{E^2}{30} \qquad \text{(v W EIRP)}.$$

Enačba v logaritemski obliki in s frekvenco podano v MHz je sledeča

$$P_r = E - 20\log f + 12{,}782 \qquad \text{(v dBW EIRP)}.$$

Sprejeto moč P_r lahko izrazimo, kot oddano moč P_t zmanjšano za izgube razširjanja L_p

$$P_r = P_t - L_p$$

Ob upoštevanju zgornjih enačb dobimo naslednjo enačbo.

$$E(dBV/m) = P_t + 20\log f - 12{,}782 - L_p$$

$$E(dB\mu V/m) = P_t + 20\log f + 107{,}218 - L_p$$

Ker za naš hipotetični sistem že poznamo vrednost za poljsko jakost in največjo oddajno moč pretvornika lahko izračunamo področje pokrivanja s signalom, če upoštevamo izgube razširjanja valov. Pri oddajni moči je potrebno upoštevati, da je moč v formuli podana za izotropni vir EIRP (effective isotropically radiated power). Pri izračunu oddajne moči pretvornika pa imamo vrednost podano v ERP. Vrednosti EIRP, zato prištejemo 2,2 dB. Za obe vrednosti poljske jakosti izračunamo kolikšna je dovoljena izguba razširjanja za zagotavljanje želene poljske jakosti.

$$L_p(\text{za } 48\,\text{dB}\mu\text{V/m}) = 10 + 2{,}2 + 20\log 800 + 107{,}218 -$$

$$-E = 177{,}48 - E = 177{,}48 - 48 = 129{,}48\,dB$$

$$L_p(\text{za } 54\,\text{dB}\mu\text{V/m}) = 177{,}48 - E = 177{,}48 - 54 = 123{,}48\,dB$$

Sedaj nas zanima kakšno področje lahko pokrijemo s signalom. Pri izračunu pokrivanja s signalom je potrebno upoštevati več parametrov, kot so na primer: višina oddajnega stolpa, višina sprejemne antene, oddajne frekvence in seveda same konfiguracije terena. Trenutno poznamo veliko različnih modelov in pristopov za določanje pokrivanja oziroma določitev razširjanja signala. Razdelimo jih lahko v tri skupine empirične, deterministične in semi- deterministične. Empirični bazirajo na predhodnih meritvah in statističnih zakonitostih. Deterministični modeli rabijo mnogo vhodnih geometrijskih podatkov in se izračunavajo za vsak primer posebej. Semi-deterministični modeli pa bazirajo na kombiniranju empiričnih in deterministične modelov /9/. Med empiričnimi modeli je pogosto uporabljen Okumura-Hata model /10/. Model oziroma izračuni temeljijo na meritvah pridobljenih v mestu in v okolici Tokia na Japonskem. Izračun propagacijskih izgub in korekcijski faktorji za različna okolja so naslednji:

$L_{dB}(Urban) = A + B\log_{10} R - E$ (za mestna območja)

$L_{dB}(Suburban) = L_{dB}(Urban) - C$ (za primestna območja)

$L_{dB}(Open) = L_{dB}(Urban) - D$ (za odprta območja)

$A = 69{,}55 + 26{,}16\log_{10} f_c - 13{,}82\log_{10} h_b$

$B = 49{,}9 - 6{,}55\log_{10} h_b$

$C = 2(\log_{10}(f_c/28))^2 + 5{,}4$

$D = 4{,}78(\log_{10} f_c)^2 - 18{,}33\log_{10} f_c + 40{,}94$

$E = 3{,}2(\log_{10}(11{,}7554h_m))^2 - 4{,}97$ za velika mesta

$E = (1{,}1\log_{10} f_c - 0{,}7)h_m - (1{,}56\log_{10} f_c - 0{,}8)$ za srednje velika mesta

Kjer posamezne oznake predstavljajo naslednje podatke:
R (1-20 km)* - razdaljo med oddajnikom in sprejemno anteno (v kilometrih)
f_c (150-1500 MHz)* - frekvenca oddajanja (v MHz)
H_b (30-200 m)* - višina oddajnika oziroma oddajne antene (v metrih)
h_m (1-10 m)* - predstavlja višino sprejemne antene (v metrih)
* omejitve posameznih parametrov

Na primeru praktičnega izračuna si oglejmo rezultate za vrednosti, ki smo jih doslej izračunali. Za frekvenco bomo izbrali 800 MHz (za to frekvenco imamo podatek o potrebnem razmerju C/N). Višina oddajne antene naj bo 70 m in sprejemne 8 m (primer strešne antene). Za prvi primer $L_p(48dB\mu V/m) = 129{,}48dB$ in mestno okolje dobimo, da je velikost pokrivanja zadovoljiva znotraj območja 6 km, oziroma za primestno okolje znotraj 12 km. Za drugi primer $L_p(54dB\mu V/m) = 123{,}48dB$ in mestno okolje dobimo, da je velikost pokrivanja zadovoljiva znotraj območja 4 km, oziroma za primestno okolje znotraj 8 km.

2.3 MFN omrežje

Na sliki 5 je prikazan primer uporabe kanalnega pretvornika v MFN omrežju. Signal iz glavnega oddajnika kanalni pretvornik sprejme in odda na drugi frekvenci. Pri pretvorbi iz ene na drugo frekvenco pride do degradacije koristnega signala. Ena izmed prednosti uporabe kanalnega pretvornika v MFN omrežju je uporaba obstoječe infrastrukture uporabljene pri oddajanja analognega televizijskega signala. V primeru, da uporabljamo kanalni pretvornik, ki lahko deluje v obeh načinih delovanja (analognem in digitalnem), ni potrebno investirati v novo opremo ob prehodu na digitalno oddajanje.

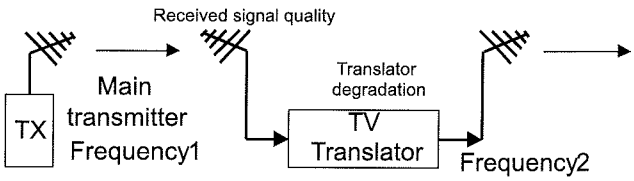

Slika 5: Uporaba kanalnega pretvornika v MFN omrežju.

2.4 Sekundarno SFN omrežje

S pomočjo kanalnih pretvornikov lahko izgradimo tudi sekundarno SFN omrežje (slika 6). V sekundarnem SFN omrežju imamo običajno glavni oddajnik z veliko oddajno močjo in kanalne pretvornike za pokrivanje območij, ki niso pokrita z glavnim oddajnikom. Prednosti take rešitve so v manjših stroških, saj za sekundarno SFN omrežje ne rabimo infrastrukture za distribucijo oddajnega signala do oddajnika kot pri običajnem SFN omrežja. Uporabimo kar sprejeti signal iz glavnega oddajnika. Odpade tudi omejitev oddajne moči, ki smo ji bili priča pri uporabi enokanalnih pretvornikov.

Drugi primer smiselnosti izgradnje sekundarnega SFN omrežja je zagotovitev sprejema signala v stavbah brez zunanje antene (indoor reception). Za sprejem v stavbah brez zunanje antene rabimo večjo poljsko jakost signala, kar lahko zagotovimo s kanalnimi pretvorniki.

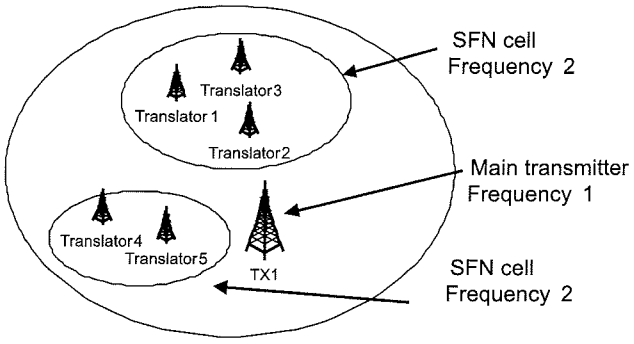

Slika 6: Uporaba kanalnega pretvornika v sekundarnem SFN omrežju.

3 Blokovna shema nadgrajenega kanalnega pretvornika

Na sliki 7 je prikazana blokovna shema nadgrajenega kanalnega pretvornika. Nadgrajen kanalni pretvornik se po blokovni shemi bistveno ne razlikuje od doslej uporabljenega. Razlika je pri izvedbi posameznih sklopov in zahtevanih lastnostih posameznih sklopov. Zaradi strožjih zahtev je bilo

potrebno izboljšati lastnosti starih in dodati nove sestavne sklope pretvornika. Največje spremembe so izvedene na lokalnem oscilatorju, kjer je izboljšana frekvenčna ločljivost in karakteristika faznega šuma /11/. Novost pri izvedbi je med drugim tudi detekcijsko vezje in logika za avtomatski preklop delovanja pretvornika.

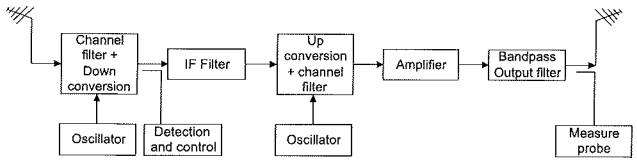

Slika 7: Blokovna shema kanalnega pretvornika za MFN omrežje.

Glede na nove možnosti, ki jih ponuja digitalno oddajanje, je možno nadgrajeni kanalni pretvornik uporabiti tudi za enofrekvenčno omrežje. Uporabiti je možno enak kanalni pretvornik kot v MFN omrežju. Za uporabo samo v SFN omrežju lahko kanalni pretvornik še optimiziramo. Na sliki 8 je prikazana blokovna shema kanalnega pretvornika za primer SFN omrežja. V tem primeru ni potreben avtomatski preklop in zadošča en lokalni oscilator, kar dodatno zmanjša kompleksnost in ceno samega izdelka. Glede na način delovanja SFN omrežja moramo poskrbeti za frekvenčno sinhronizacijo oziroma točnost oddajne frekvence. Običajno uporabimo v ta namen posebne GPS (Global Positioning System) sprejemnike, ki zagotavljajo sinhronizacijo frekvenčne normale (10MHz). Ker ima lokalni oscilator v kanalnem pretvorniku možnost priklopa zunanje referenčne ure s frekvenco 10MHz je na ta način zagotovljena točnost in stabilnost oddajne frekvence.

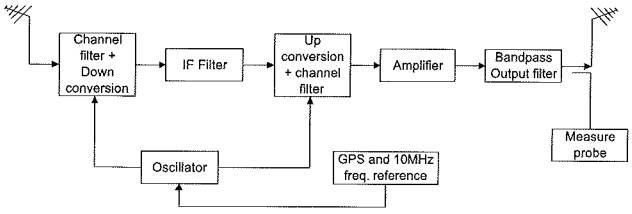

Slika 8: Blokovna shema kanalnega pretvornika za uporabo omejeno na SFN omrežje.

3.1 Avtomatski preklop delovanja

Kanalni pretvornik omogoča avtomatski preklop delovanja na podlagi zaznavanja vhodnega RF signala. Za zaznavanje analognega televizijskega signala je ena izmed možnosti spremljanje sinhronizacijskih signalov v video signalu. V analognem signalu imamo signale za horizontalno in vertikalno sinhronizacijo. S horizontalno sinhronizacijo je označen konec posamezne vrstice, ki se izrisuje na televizijskem sprejemniku. Vertikalna sihronizacija pa označuje trenutek, ko se žarek za izris slike vrne nazaj na vrh ekrana. Na sliki 9 je prikazana meritev analognega signala s sinhronizacijskimi signali. S pomočjo vezja, ki zaznava omenjene impulze in dodatno logiko lahko uspešno ugotovimo ali je vhodni signal analogni televizijski signal /12/.

V primeru, da analogni signal ni zaznan lahko izvedemo preklop v digitalni način delovanja.

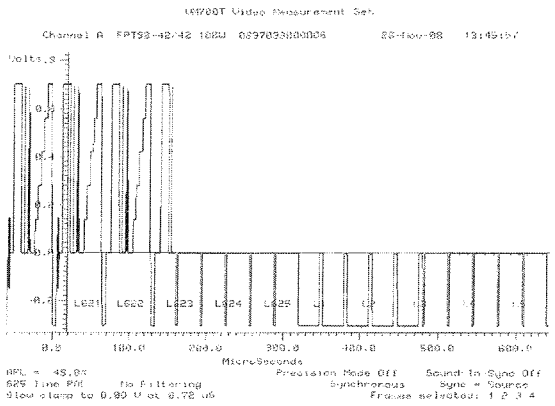

Slika 9: Analogni televizijski signal.

4 Zaključek

Digitalna televizija prinaša številne spremembe pri nastajanju, produkciji in oddajanju vsebin za prizemeljsko in mobilno televizijo. V prispevku smo se osredotočili na kanalne pretvornike in možnosti uporabe le-teh. Zaradi uporabe drugačne modulacije in zahtev, ki iz tega izhajajo so kanalni pretvorniki za analogno televizijo neustrezni za oddajanje digitalnega televizijskega signala. Z nadgradnjo sklopov kanalnega pretvornika smo uporabo pretvornika razširili tudi na digitalno televizijo. Dodatno smo funkcionalnost razširili na delovanje v obeh režimih in avtomatizirali delovanje.

Na nekaj primerih smo za izbrane podatke prikazali in navedli prednosti in omejitve uporabe kanalnih pretvornikov. Glavne prednosti nadgrajenega kanalnega pretvornika glede na druge rešitve so: cenovna ugodnost, robustnost, zanesljivost in uporabnost rešitve za analogno ali digitalno televizijo. Pri digitalni televiziji imamo, za razliko od drugih rešitev, pri katerih je uporaba omejena, dodatno možnost uporabe kanalnih pretvornikov v različnih konceptih postavljanja televizijskih omrežij (MFN, SFN ali kombinacija obeh). Na primeru smo izračunali največjo oddajno moč in področje pokrivanja s signalom in na ta način prikazali možnosti in omejitve uporabe kanalnega pretvornika v SFN omrežju za dan primer. Na enak način lahko ocenimo možnosti uporabe kanalnega pretvornika, če imamo drugačne parametre in razmere na oddajni lokaciji.

5 Literatura

/1/ PI B. Kenington, K. Hayler, PI N. Moss, D. J. Edwards, A. PI Jenkins and M. Johnstone, Transposer systems for digital terrestrial television, ELECTRONICS & COMMUNICATION ENGINEERING JOURNAL, February 2001.

/2/ Copot Daniel, Koncepti radiofrekvenčnih pretvornikov za gradnjo enokanalnih omrežij za zemeljsko in mobilno digitalno televizijo: magistrska naloga, 2005.

/3/ C. Trolet, SPOT: FILLING GAPS IN DVB-T NETWORKS WITH DIGITAL REPEATERS, Harris Broadcast Europe, France, July

2002, http://www.broadcastpapers.com/whitepapers/SPOT-Filling-Gaps-In-DVB-T-Networks-With-Digital-Repeaters.cfm?objid=32&pid=245&fromCategory=53

/4/ Products for digital TV transmitters and repeaters, Elti d.o.o., 2008, http://www.elti.com/products/digital_tv_transmitters_and_repeaters.

/5/ ETSI TR 102 377 V1.2.1, Technical report, Digital Video Broadcasting (DVB); DVB-H Implementation Guidelines, Chapter 9.4: Considerations on the use of repeaters in DVB-H networks, November 2005. http://www.dvb-h.org/PDF/Implementation%20Guidelines%20TR102377.V1.2.1.pdf

/6/ European Standard, ETSI EN 300 744 V1.5.1, Digital Video Broadcasting (DVB); Framing structure, channel coding and modulation for digital terrestrial television, Annex A: Simulated system performance for 8 MHz channels, November 2004.

/7/ ETSI TR 101 190 V1.2.1, Technical report, Digital Video Broadcasting (DVB); Implementation guidelines for DVB terrestrial services; Transmission aspects, Chapter 9.2: Minimum field strength considerations, November 2004.

/8/ Spectrum Planning Report, Investigation of Modified Hata Propagation Models, Attachment: Converting propagation loss to field strength at the receiver, Australian Communications Authority, Document: SP 2/01 April 2001.

/9/ Oktay Akcakaya, Eda Kocaman, Osman Kaldirim, Terrestrial and satellite based radio systems for TV and multimedia, Propagation models, http://130.83.66.8/fileadmin/lehre/Radio_Systems/material-ien/PROPAGATION%20MODELS.pdf

/10/ Masaharu Hata, Empirical Formula for Propafation Loss in Land Mobile Radio Services, IEEE Transactions on Vehicular Technology, VOL. VT-29, NO.3, August 1980.

/11/ A. Kosi, M. Solar, Hybrid Oscillator for analog and Digital Terrestrial Television Transmission, Informacije Midem, March 2007.

/12/ Monolithic Video Sync Separators, Datasheet, Gennum Corporation, July 2004.

mag. Andrej Kosi univ. dipl. inž. je zaposlen v podjetju ELTI d.o.o Gornja Radgona,

docent dr. Mitja Solar je predavatelj na Fakulteti za elektrotehniko, računalništvo in informatiko v Mariboru. Fakulteta za elektrotehniko, računalništvo in informatiko v Mariboru, Smetanova 17, 2000 Maribor

Prispelo (Arrived): 23.11.2008 Sprejeto (Accepted): 09.09.2009

DEVELOPMENT OF MAXIMUM POWER POINT TRACKING PLATFORM FOR PHOTOVOLTAIC SYSTEM

Tine Andrejašič, Marko Jankovec, Marko Topič

University of Ljubljana, Faculty of Electrical Engineering, Ljubljana, Slovenia

Key words: Maximum Power Point Tracking, high efficiency non-inverting buck-boost DC-DC Converter, photovoltaic system output maximization

Abstract: This paper describes a development of a prototype of Maximum Power Point Tracking platform for Photovoltaic Systems which is used for testing maximum power point tracking algorithms for different electric loads and to analyze the behavior of photovoltaic (PV) generator at different load regime during monitoring. The platform is composed of a power transfer circuit and periphery with microcontroller, signal acquisition and communication. The main part of the power circuit is designed as a high efficiency non-inverting buck-boost direct current-to-direct current (DC-DC) converter that enables power transfer of up to 400 W. Separate buck DC-DC converter is integrated to power all employed integrated circuits. Both current and voltage are measured at the input and output of the platform. FLASH program memory based microcontroller is used to apply integrated maximum power point algorithms and to control and harmonize the entire periphery. For simple communication between a computer and the platform's microcontroller a RS-485 based protocol was used with user interface developed in a graphical programming language LabVIEW.

Razvoj platforme za sledenje točke največje moči pri fotonapetostnih sistemih

Kjučne besede: sledenje točke največje moči, DC-DC pretvornik z visoko učinkovitostjo pretvorbe, maksimiranje izhodne moči fotonapetostnega sistema

Izvleček: Članek opisuje razvoj prototipa platforme za sledenje točke največje moči fotonapetostnega generatorja, ki služi testiranju učinkovitosti algoritmov in preučevanju delovanja fotonapetostnih modulov pri različnih obremenitvah. Sistem je sestavljen iz glavnega DC-DC stikalnega pretvornika, ki skrbi za prenos energije iz fotonapetostnega generatorja na breme in periferije, ki jo sestavlja mikrokrmilnik, vezje za zajemanje in merjenje signalov in komunikacijsko vezje. Glavni DC-DC stikalni pretvornik deluje v vezavi neinvertirajočega pretvornika navzgor-navzdol (izhodna napetost je lahko nižja ali višja od vhodne napetosti) z visoko stopnjo učinkovitosti pretvorbe za moči do 400 W. Sekundarni DC-DC stikalni pretvornik skrbi za napajanje vseh potrebnih integriranih vezij, ki delujejo na nizkem napetostnem nivoju. Platforma omogoča meritve toka in napetosti tako na vhodu kot tudi na izhodu sistema. Mikrokrmilnik skrbi za izvajanje implementiranih algoritmov iskanja in sledenja točke največje moči ter usklajuje delovanje ostale periferije. Za enostavno komunikacijo platforme z osebnim računalnikom smo izdelali tudi uporabniški vmesnik v programskem jeziku LabVIEW, ki deluje na podlagi protokola RS-485.

1. Introduction

Sustainable energy sources like PV solar systems are becoming important as eco-friendly alternatives to fossil fuels. Research and development efforts together with economy of scale in the photovoltaics lead to decreasing costs and strengthen implementation of different solar powered systems. Photovoltaic solar powered industrial applications include among others water pumping, air conditioning, electric vehicles and ventilation systems (predominantly acting as dynamic loads).

PV generator has a specific output characteristic. Output current-voltage (*I-V*) and power-voltage (*P-V*) characteristics of Phaesun 25 Wp poly-Si PV module under different solar irradiances in the plain of array (G_{poa}) and cell temperatures are shown in Fig. 1 and Fig. 2.

In *P-V* characteristics P_{MPP} designates the power at the maximum power point (MPP).

As seen in Fig. 1, short circuit current (I_{sc}) and open circuit voltage (V_{oc}) are irradiance and temperature dependent. I_{sc} is linearly proportional to the solar irradiance, while the V_{oc} shows logarithmic dependence to irradiance. Since PV generators are still the most expensive part of the PV system, they must be loaded optimally to maximize conversion efficiency and decrease costs, size and weight. System should always operate in the P_{MPP} regardless instantaneous circumstances and temporal changes, such as solar irradiance, ambient temperature or any other ambient parameter. To achieve operation of the PV generator near the vicinity of the P_{MPP} with its specific value of voltage and

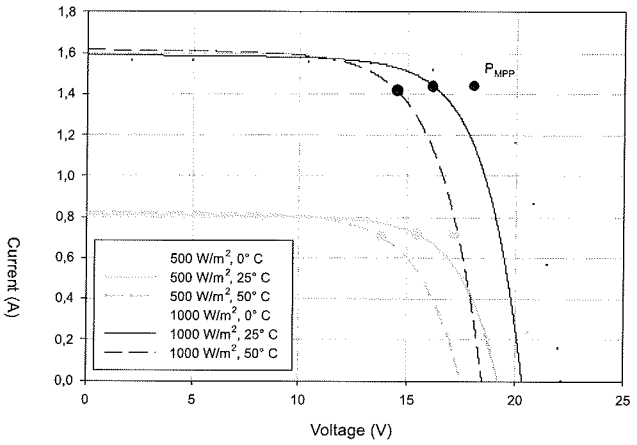

Fig. 1: Measured I-V photovoltaic panel characteristics for different solar irradiances in plane of array and cell temperatures.

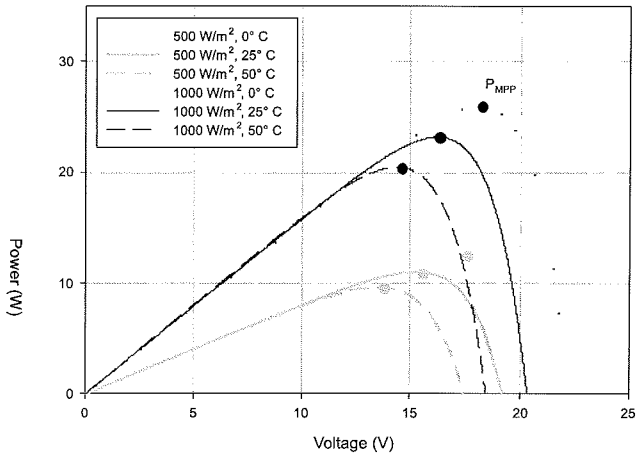

Fig. 2: Measured P-V photovoltaic characteristics for different solar irradiances in plane of array and cell temperatures.

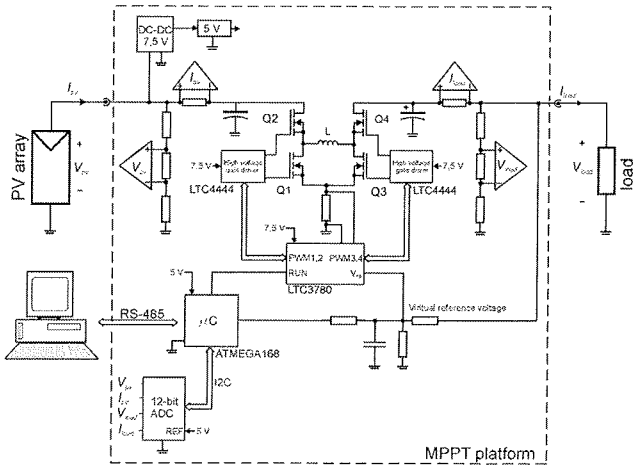

Fig. 3: Block diagram of maximum power point tracking platform.

current, switching mode pulse-width modulation (PWM) DC-DC converter /1/ must be inserted between the PV generator and electric load. The converter's primary task is to continuously adapt to the load and to track the instantaneous maximum power point of the PV generator.

Many MPP tracking algorithms for the DC-DC converters have been developed in the last decades. Recently, reviews of direct/indirect methods were presented in /2/ and /3/. Five of several direct methods have been implemented in our system.

2. Development of MPPT platform

High-efficiency maximum power point tracking (MPPT) system that could be connected to majority of PV modules available on the market and would act as a testing platform for maximum power point tracking algorithms was impossible to buy, so we had to develop it ourselves. Different MPPT algorithms are to be implemented and their performance compared while optimally regulating the power transferred to the load for different scenarios. Output voltage and current range should be high enough for battery powered system loads of voltages 48 V and below.

On the basis of those requirements we designed and built a microcontroller based maximum power point tracking platform that is comprised of a main DC-DC switching converter in buck/boost configuration, a low output voltage buck DC-DC converter, a voltage and current sensing circuit, a microcontroller and a communication circuit (Fig. 3).

The main converter continuously adapts the load impedance to track the instantaneous maximum power point of the PV generator or regulates constant output voltage in its regime. Input and output voltage range is from 0 to 60 V and maximum input and output currents are 8 A. The buck DC-DC converter is used to convert the applied voltage down to 7,5 V to power the main DC-DC converter regulator, high voltage gate drivers and voltage sensing amplifiers. Linear regulator is added with an output voltage of 5 V to power the microcontroller, the AD converter and the communication circuit.

Output voltage, input voltage and current are filtered and scaled down for the input range of the analog-to-digital (AD) converter. ATMEGA168 microcontroller /4/ is used to communicate with the user interface and to harmonize the platform operation. It communicates with AD converter via I2C protocol to receive digitalized measurements that are required to execute maximum power point tracking algorithms. Microcontroller is able to set/reset the main regulator, set its feedback voltage and switch between continuous, discontinuous and burst mode of operation. For communication between the computer and microcontroller a RS-485 based protocol was used with user interface developed in a graphical programming language LabVIEW. It allows a user to choose between maximum power point algorithms and their parameters, set constant output voltage and track all measurable quantities.

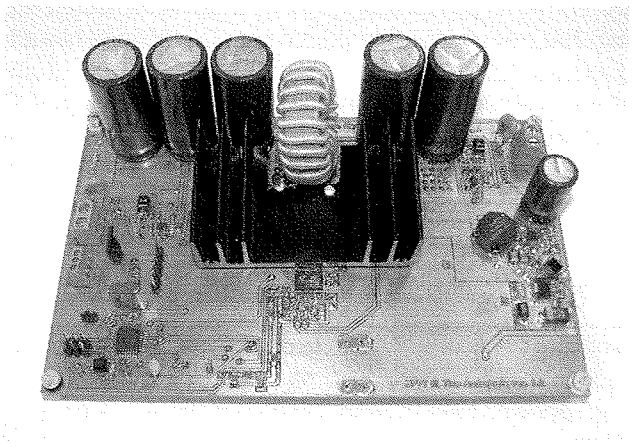

Fig. 4: Prototype of maximum power point tracking platform.

2.1 Buck/boost converter

Main DC-DC switching converter's task is to deliver as much power as possible from the connected PV generator to the load applied. Buck and boost topology were joined together in this converter regulated by LTC3780 /5/ current mode controller that provides an output voltage above, equal to or below the input voltage. It consists of four MOSFET switches in bridge configuration, inductor, input and output capacitors. If the input voltage is lower than output voltage the system works as a boost converter. MOSFET tranzistor Q2 stays on, while transistor Q1 stays off. Output is determined by pulse width modulation (PWM) signal applied to transistors Q3 and Q4. Every ten cycles Q1 and Q2 invert for 300 ns to charge Q2's bootstrap capacitor. When input voltage is near the output voltage, PWM signal is applied to all four switches. Converter operates in buck mode when the output voltage is lower than the input voltage. PWM signal is applied to transistors Q1 and Q2, transistor Q4 stays open and transistor Q3 is closed except for Q4's bootstrap capacitor recharging period every ten cycles. Output voltage is determined with feedback voltage by voltage divider circuit. To actively control the output voltage by microcontroller additional current is forced via RC circuit to the feedback voltage. Virtual feedback voltage sets the output voltage to its maximum (60 V), if no current is forced from microcontroller, and to 0 V when maximum current is forced.

Maximum input/output voltage rating for LTC3780 to safely operate is 36 V. To increase this voltage up to 60 V we inserted high voltage gate drivers LTC4444 /6/ on both output and input side of the converter.

2.2 Signal measurement

All direct maximum power point algorithms operate based on measured information from input or output power quantities. Implemented algorithms require both input and output signal measurements.

Main switching DC-DC converter and low voltage level DC-DC converter produce high level of noise in measured signal. The main converter operates at 200 kHz and has additional glitches every ten cycles at 20 kHz when bootstrap capacitors are charged. Low voltage level DC-DC converter works at 60 to 150 kHz according to the output current. Due to the noise and glitches in measured signals a lot of effort was invested to optimize signal measurement.

Input and output current measurement is implemented as measurement of voltage drop across high tolerance resistor. For this purpose high voltage high side operational amplifier LTC6101 /7/ was used to avoid common mode problems. To maintain high efficiency, resistors with low resistance and Kelvin connection were chosen. A low-pass filter was inserted between the AD converter and output of the amplifier.

Input and output voltage is measured on voltage divider (see Fig. 5).

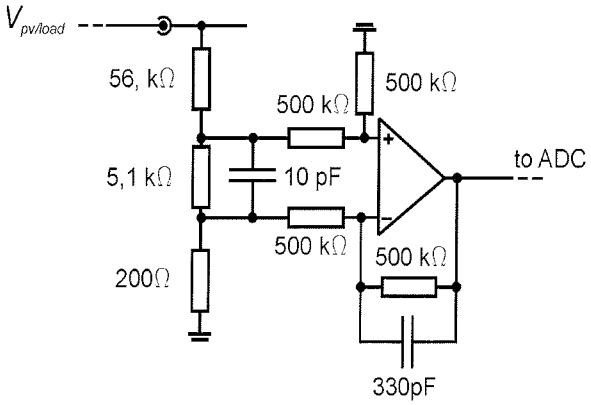

Fig. 5: Voltage measurement circuit.

Operation amplifier subtracts voltage across 5,1 kΩ resistor and adds a low-pas filter with cut-off frequency of 1 kHz. This kind of configuration eliminates majority of glitches and AC component in the signal. To filter the entire AC component in the signal lower cut-off frequency should be chosen, but this would affect regulation frequency of applied algorithms. That is the reason to implement additional weighted average digital filtering with a microcontroller.

MOSFET temperature is also monitored to ensure power-down when the heat dissipation is too high or at malfunction.

2. Conversion efficiency

Conversion efficiency as an important steady-state performance parameter was measured at input voltage of typical PV modules maximum power point voltage (V_{MPP}) of 16,1 V (12 V system), 28,5 V (24 V system) and representative of grid - tied module with V_{MPP} of 43,1 V. Output voltage was set to typical battery powered system voltages of 12, 24, 36 and 48 V. As we can observe from Fig. 6 to 9, the conversion efficiency drops at increasing ratio between input and output voltage and at increasing load currents.

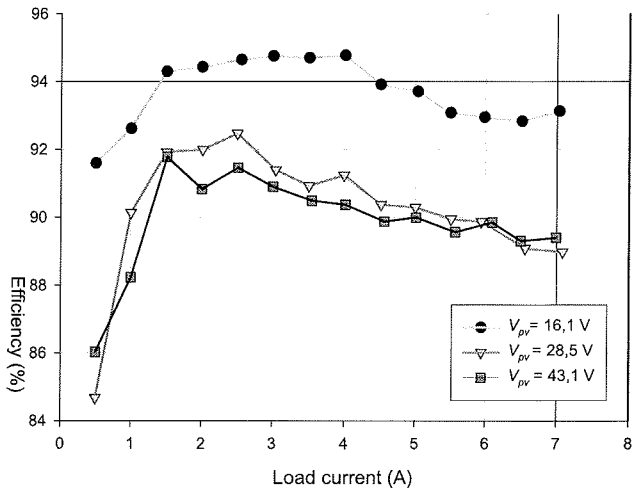

Fig. 6: Conversion efficiency at V_{load} = 12 V.

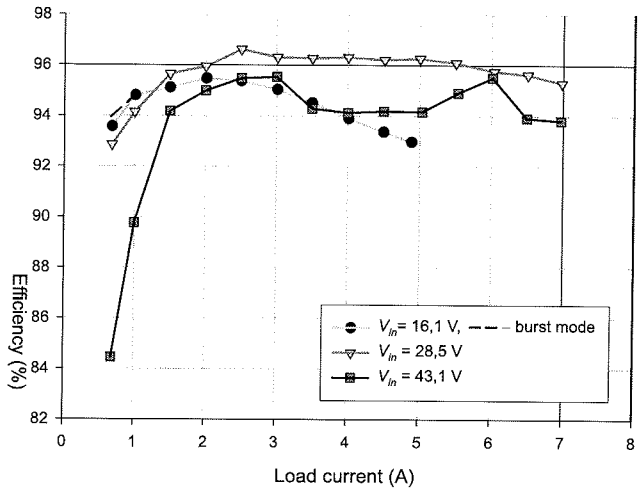

Fig. 7: Conversion efficiency at V_{load} *= 24 V.*

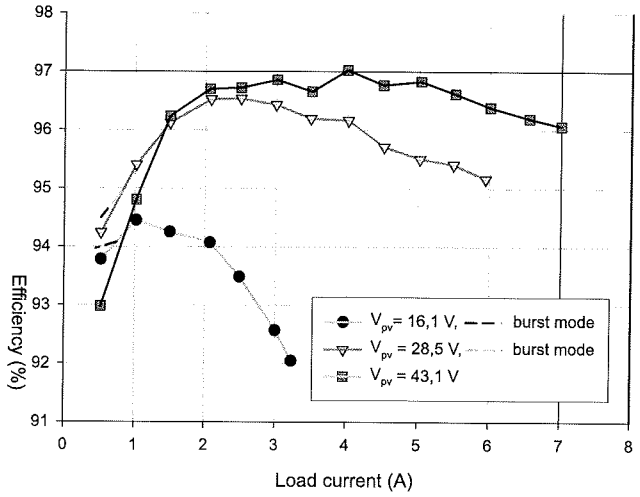

Fig. 8: Conversion efficiency at V_{load} *= 36 V.*

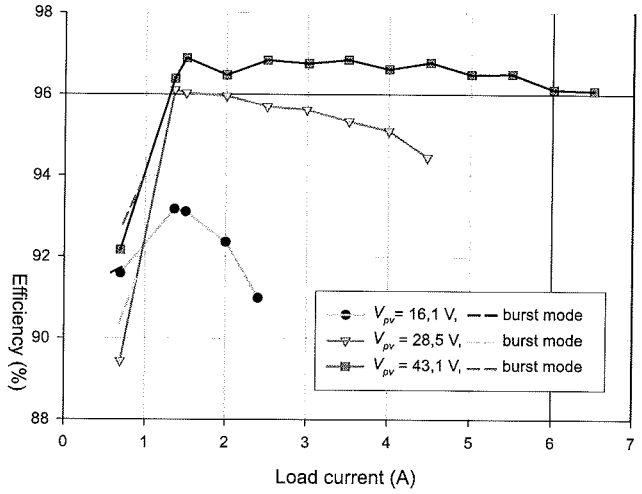

Fig. 9: Conversion efficiency at V_{load} *= 48 V.*

A comparison of forced continuous switching mode and burst switching mode operation was made to determine higher efficiency conversion at higher load currents. Regulator introduces higher level of feedback hysteresis in burst mode and produces output signals to the MOSFETs Q3 and Q4 that turns them on for several cycles, followed by a variable "sleep" interval depending upon the load current. In boost operation at higher load currents burst mode is more appropriate and results in improved efficiency by few percents.

The major sources of power loss in the converter are the switching losses of the MOSFETs, the inductor, the DC-DC low voltage converter and the I^2R losses on current-sensing resistors and power traces on circuit board. It is difficult to further improve the efficiency over the whole interval of operation. Selected intervals of operation with component specific values should be chosen to further optimize the efficiency.

3. Implemented MPPT algorithms

Indirect MPPT algorithms, such as look-up table based, fuzzy logic and neural network MPPT algorithms were not implemented in platform mainly because they depend on previous PV characterization and self teaching process /8/, /9/. Among direct seeking algorithms, *input* and *output Hill-Climbing* (*H-C*), *Perturbe and Observe* (*P&O*), *Incremental Conductance* (*IncCond*) and *Derivative dP/dt* have been implemented in the platform. Let us shortly review their principles and properties.

H-C algorithms have been investigated by several authors /2/, /3/, /10/, where MPP is tracked by changing the duty-cycle ratio of a DC-DC converter. Power is determined in each cycle by measuring current and/or voltage at the input or output side of the converter. If the power has increased after duty-cycle ratio change, the algorithm will continue in the same direction in the next cycle, otherwise the direction of duty-cycle ratio will be reversed. Both power and direction of duty-cycle ratio change have to be stored for each iteration. *H-C input* algorithm maximizes output power by sensing at the input side (PV generator), while *H-C output* maximizes power measured on the load.

Next type of algorithm is *Perturbe and Observe* (*P&O*) /2/, /3/, /11/. The *P&O* algorithms are widely used because of their simple structure. They operate by periodically perturbing (i.e. incrementing or decrementing) the PV generator terminal voltage and comparing the output power with that of the previous perturbation cycle. If the power is increasing, the perturbation will continue in the same direction in the next cycle, otherwise the perturbation direction will be reversed. In every perturbation PV generator reference voltage (V_{ref}) is calculated. This means the PV generator terminal voltage is regulated in every perturbation cycle by separate voltage regulating loop. Therefore when the MPP is reached, the *P&O* algorithm will oscillate around it.

An example of applied *P&O* algorithm for increased irradiance from 500 W/m^2 to 800 W/m^2 is presented in Fig. 9

at constant ambient temperature (T_{air}), 100 Hz regulating frequency of perturbation and 50 mV discrete step of V_{ref}. Initially the algorithm stabilized the maximum power point tracker at the maximum power for 500 W/m^2 irradiance. New level of irradiance (800 W/m^2) was applied step-wise and presents the most dynamic outdoor scenario. After increased irradiance the algorithm is changing V_{ref} towards the new maximum power point voltage. The jitter in the tracking path is a consequence of discrete reference voltage step. In this experiment the algorithm needed 1,2 s to reach the new maximum power point. The stabilization would be faster if the discrete step of V_{ref} was increased, however the fluctuation around the reached P_{MPP} would be greater. In reality such rapid changes of irradiance are generally not expected therefore a faster tracking is not required. Results from different scenarios demonstrate that the algorithm with given parameters is capable of tracking irradiance changes up to 250 W/m2 per second.

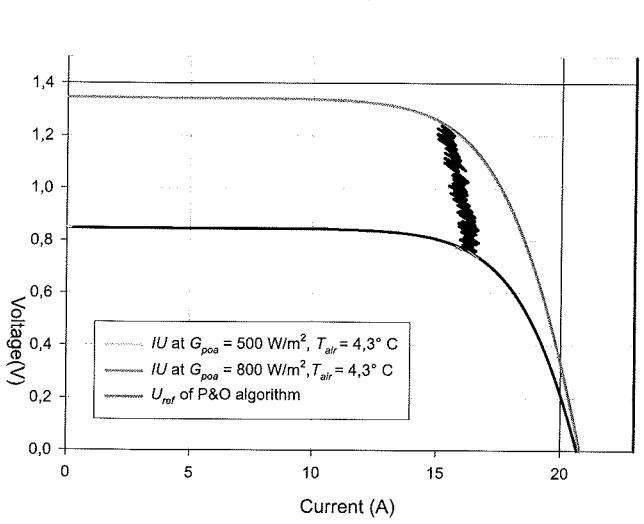

Fig. 10: Maximum power point tracking of P&O *algorithm.*

IncCond algorithm that measures and compares incremental and instantaneous conductance for rapidly changing ambient conditions was implemented in /2/, /3/, /12/ to increase tracking speed and lower the oscillations at steady conditions. Condition of maximum power $dP_{PV}/dV_{PV} = 0$ in (1) leads to (2), where the left side of the equation represents instantaneous conductance I_{PV}/V_{PV}, while its right side represents incremental conductance, determined by "I_{PV} and "V_{PV} as difference between values of the current and present cycle.

$$\frac{dP_{PV}}{dV_{PV}} = I_{PV}\frac{dV_{PV}}{dV_{PV}} + V_{PV}\frac{dI_{PV}}{dV_{PV}} = I_{PV} + V_{PV}\frac{dI_{PV}}{dV_{PV}} = 0 \qquad (1)$$

$$\frac{I_{PV}}{V_{PV}} = -\frac{dI_{PV}}{dV_{PV}} \approx -\frac{\Delta I_{PV}}{\Delta V_{PV}} \qquad (2)$$

The *IncCond* algorithm predicts in what direction the reference voltage should change to match the change of ambient conditions. If dP_{PV}/dV_{PV} is less than zero the PV generator is operating at voltage higher than voltage in P_{MPP} (V_{MPP}) (see Fig. 2), otherwise it operates at voltage lower than V_{MPP}. Like in the *P&O* algorithms, a separate voltage high-speed regulating loop must be applied to regulate PV generator output voltage $V_{PV} \approx V_{ref}$.

The last algorithm that we have implemented is *derivative dP/dt* algorithm /13/. When PV generator operates at the MPP, the equations (3) and (4) must be fulfilled. MPP is reached by forcing its derivative *dP/dt* to zero under the power feedback control.

$$\frac{dP_{PV}}{dt} = \frac{d(I_{PV}V_{PV})}{dt} = V_{PV}\frac{dI_{PV}}{dt} + I_{PV}\frac{dV_{PV}}{dt} = 0 \qquad (3)$$

$$VdI = -IdV \Rightarrow V\Delta I = -I\Delta V \qquad (4)$$

If $-I\Delta V$ is less than $V\Delta I$, PV generator operates in voltage source mode ($V>V_{MPP}$, see Fig. 1) and the PV generator voltage must decrease, otherwise it operates in current source mode ($V<V_{MPP}$) and the generator voltage must increase to reach MPP. A separate voltage regulating loop is used to control PV generator output voltage.

The platform allows a user to implement and evaluate additional direct algorithms.

4. Conclusions

A maximum power point tracking platform has been successfully developed. Its wide input voltage and current range enable connection of majority of PV modules available on the market. The platform's conversion efficiencies are above 96% for broad range of output voltages and loads. The developed platform opens a route to implement and examine several direct MPPT algorithms along with sensitivity study of their parameters according to the given PV module, load characteristics and nature of changing of ambient conditions. Since PV generators are still the most expensive part of the PV systems, this could path the way to further maximize their conversion efficiency.

5. References:

/1/ A.I. Pressman, Switching Power Supply Design, 2nd ed., New York: McGraw-Hill, 1998, pp. 32-35.

/2/ T. Esram, P.L. Chapman, Comparison of Photovoltaic Array Maximum Power Point Tracking Techniques, IEEE Transactions on Energy Conversion, Vol. 22, pp. 439-449, (2007),.

/3/ V. Salas, E. Olías, A. Barrado, A. Lázaro, Review of the Maximum Power Point Tracking Algorithms for Stand-alone Photovoltaics Systems, Solar Energy Materials & Solar Cells Vol. 90, pp. 1555-1578, (2006).

/4/ Web site for ATMEGA168 microcontroller, datasheet <http://www.atmel.com/dyn/resources/prod_documents/doc2545.pdf>, accessed on 05/08/2008.

/5/ Web site for LTC3780 DC-DC buck/boost converter regulator, datasheet <http://www.linear.com/pc/downloadDocument.do?navId=H0,C1,C1003,C1042,C1116,P10090,D7197>, accessed on 01/09/2008.

/6/ Web site for LTC4444 high voltage gate driver, datasheet <http://www.linear.com/pc/downloadDocument.do?navId=H0,C1,C1003,C1142,C1041,P39339,D25652>, accessed on 11/09/2008.

/7/ Web site for LTC6101 high side, high voltage current sens amplifier, datasheet <http://www.linear.com/pc/downloadDocument.do?navId=H0,C1,C1154,C1009,C1077,P10220,D7277>, accessed on 02/09/2008.

/8/ N. Mutoh, T. Matuo, K. Okada, M. Sakai, Prediction-data-based maximum-power-point-tracking method for photovoltaic power generation systems, Proc. 33rd Annu. IEEE Power Electron. Spec. Conf., pp. 1489-1494, (2002).

/9/ I.H. Altas, A.M. Sharaf, A novel maximum power fuzzy logic controller for photovoltaic solar energy systems, Renewable Energy, Vol. 33, p.p. 388-399, (2008).

/10/ N. Dasgupta, A. Pandey, A.K. Murkerjee, Voltage-sensing-based Photovoltaic MPPT with Improved Tracking and Drift Avoidance Capabilities, Solar Energy Materials & Solar Cells, Vol. 92, pp. 1552-1558, (2008).

/11/ D. Shmilovitz, Photovoltaic Maximum Power Tracking Employing Load Parameters, IEEE Proc. ISIE, Dubrovnik, Croatia, (2005), pp. 1037-1042.

/12/ K. H. Husein, I. Muta, T. Hoshino, M. Osakada, Maximum power tracking: an algorithm for rapidly changing atmospheric conditions, IEE Proc. Gener. Transm. Distrib, Vol. 142pp. 59-64, (1995).

/13/ C. Kunlun, Z. Zhengming, Y. Liqiang, Implementation of Standalone Photovoltaic Pumping System with Maximum Power Point Tracking, Electrical Machines and Systems, ICEMS Proc., Vol. 1, pp. 612-615, (2001).

Tine Andrejašič, univ. dipl. ing. el.
Dr. Marko Jankovec, univ. dipl. ing. el.
Prof. Dr. Marko Topič, univ. dipl. ing. el.

University of Ljubljana,
Faculty of Electrical Engineering,
Laboratory of Photovoltaics and Optoelectronics,
Tržaška cesta 25, SI-1000 Ljubljana, Slovenia

E-mail: tine.andrejasic@fe.uni-lj.si

Prispelo (Arrived): 10.03.2009 *Sprejeto (Accepted): 09.09.2009*

A NOVEL APPROACH TO ANALYSIS OF NONLINEAR CIRCUITS EXCITED BY MODULATED SIGNALS

Amir Vaezi, Abdolali Abdipour, Abbas Mohammadi

Microwave/mm-Wave & Wireless Communication Research Lab,
Radio Communication Centre of Excellence, dElectrical Engineering Department,
Amirkabir University of Technology, Tehran, Iran

Key words: ET-HB, nonlinear circuits, modulated signals

Abstract: In this paper, a new formulation to Envelope Transient Harmonic Balance (ET-HB) method is proposed that is appropriate to analysis nonlinear active microwave circuits. This formulation uses an ET-HB with small value of time step during the transient time and a classic HB method after the transient. This highly reduces the time consuming classic ET-HB computation time. As an example, we applied this method to analyze a power amplifier where it is driven by QPSK and 16-QAM modulated signals. The spectral growth, error vector magnitude symbol error rate degradation, and constellation performance reduction due to nonlinearity of the power amplifier are studied using the proposed technique. The obtained results show that the proposed technique can be efficiently used to analyze and simulation of the nonlinear microwave circuits when they are used in modern wireless standards.

Nov pristop k analizi nelinearnih vezij vzbujanih z moduliranimi signali

Kjučne besede: ET-HB, nelinearna vezja, modulirani signali

Izvleček: V članku je predstavljen nov pristop k metodi ET-HB, ki je primerna za analizo nelinearnih aktivnih mikrovalovnih vezij. Ta metoda uporablja majhne vrednosti časovnega koraka med prehodnim pojavom, kar močno zmanjša čas potreben za izračune. Kot primer smo to metodo uporabili za analizo močnostnega ojačevalnika vzbujanega z QPSK in 16-QAM modulirnimi signali. Dobljeni rezultati pričajo, da predlagano metodo lahko uspešno uporabimo za analizo in simulacijo nelinearnih mikrovalovnih vezij.

1. Introduction

To achieve high bandwidth (BW) efficiency, new standards such as WiMAX and WCDMA use complex modulation schemes such as a quadrature phase-shift keying (QPSK) and quadrature amplitude modulation QAM /1,2/. Nowadays, engineers seek for simulation methods and test procedures closer to the system's final operation regime. Actually, telecommunications signals are usually composed of the carrier modulated by information signals (i.e., signals that are necessarily aperiodic in time), and presenting band-limited continuous spectra /3/. Due to analyze circuits exited by these digital modulated signals, accurate and reliable CAD tools and numerical algorithms are one of the main challenging aspects of modern communication systems. A number of methods exist for numerical analysis of such systems. As discussed in /4/, Since the excitation is a multi-rate signal with widely separated rates, the time domain - the most effective method for transient response - has difficulty. Because, simulating the slowest signal component period, time-steps need to be smaller than the period of the fastest so leads to a large number of time point and increases simulation time, enormously. On the other hand, Harmonic Balance (HB), an efficient method to analyze the microwave circuits, is only applicable to periodic (or quasi-periodic) systems. Therefore, mixed mode techniques are seemed to be efficient. In fact, in these methods like Envelope Transient HB (ET-HB) or Circuit Envelope, the high frequency dynamic is treated by microwave steady state simulator like HB and the low frequency dynamic with time domain (TDI). In the literature several formulations were presented /5-16/.

In this paper, a novel closed formulation of Envelope Transient HB appropriate for analysis of nonlinear active microwave circuits and systems is proposed. This formulation form enables using adaptive time scales, resulting in saving in simulation time. Then, as an example of application, a linear power amplifier in WiMAX technology frequency band is presented, and then the simulation results using this method are compared with other methods. Finally, using the proposed CAD, we considered the effect of the nonlinearity of the power amplifier when driven with 16-QAM and QPSK modulated signals on the system performance.

2. Theoretical formulation

Modulated signal in which the information signal is typically aperiodic and has a spectral content of much lower frequency than the periodic carrier, is a practical example of multi-rate signals /4/. When the circuit is faced to this type of signals, it will be possible to use mixed mode simulation techniques, handling the solution dependence of some of its time and variables in time-domain, and the course of the solution to other time variable in frequency domain.

If we consider a modulated carrier driving signal, exciting signal $v_s(t)$ in the circuit may be written as equation (1):

$$v_s(t) = v_m(t)(e^{-j2\pi f_c t} + e^{j2\pi f_c t}) \quad (1)$$

Where f_c is carrier frequency and $v_m(t)$ represents the envelope (modulating) signal. Considering a multi-time representation for $v_s(t)$, constructed as follows, for the slow varying parts of the expression for $v_s(t)$, t is replaced by t_s, and for the fast varying parts, t_c. the resulting function of two variables is denoted by $v_s(t_s, t_c)$.

$$\hat{v}_s(t_s, t_c) = v_m(t_s)(e^{-j2\pi f_c t_c} + e^{j2\pi f_c t_c}) \quad (2)$$

Given an active nonlinear circuit under modulated excitation including linear and nonlinear elements, it can be subdivided into two, nonlinear and linear part /4,5/. The multi rate representation of differential equation of the circuit leads to a new version of HB equation, a multi partial differential equation as follows:

$$\boldsymbol{f}_{NL}(\boldsymbol{v}(t_s,t_c)) = \boldsymbol{i}_L(t_s,t_c) + \frac{\partial \boldsymbol{q}_{nl}(\boldsymbol{v}(t_s,t_c))}{\partial t_c} + \frac{\partial \boldsymbol{q}_{nl}(\boldsymbol{v}(t_s,t_c))}{\partial t_s} + \boldsymbol{i}_{nl}(\boldsymbol{v}(t_s,t_c)) + \boldsymbol{i}_S(t_s,t_c) = \boldsymbol{0} \quad (3)$$

Where, $\boldsymbol{v}$ *is* the vector of port voltages; $\boldsymbol{i}_S$ the vector of source contributions at ports; $\boldsymbol{i}_L(t_s, t_c)$ the vector of linear part current and $\boldsymbol{i}_{nl}$, $\boldsymbol{q}_{nl}$ define the contributions of nonlinear reactive and conductive elements, respectively.

Since eq.(3) is periodic respect to the t_c, applying Fourier series, it is reduced to:

$$\mathbf{F}_{NL}(\mathbf{V}(t_s)) = \mathbf{I}_L(t_s) + j\boldsymbol{\Omega}\mathbf{Q}_{nl}(\mathbf{V}(t_s)) + \frac{\partial \mathbf{Q}_{nl}(\mathbf{V}(t_s))}{\partial t_s} + \mathbf{I}_{nl}(\mathbf{V}(t_s)) + \mathbf{I}_S(t_s) = \mathbf{0} \quad (4)$$

Where, its components are vectors of time-varying Fourier series coefficients, $V(t_s)$ is the vector of unknowns where

$$v(t_s, t_c) = \sum_{k=-K}^{k=K} V_k(t_s) \cdot e^{jk\omega_0 t_c}$$

$$V_k(t_s) = \frac{1}{2\pi} \int_{-\frac{BW}{2}}^{\frac{BW}{2}} V_k(\omega_s) \cdot e^{j\omega_s t} d\omega_s$$

So, $V_k(t_S)$ is time variant complex envelope of the *k'th* harmonic of carrier frequency ω_c, BW is the largest bandwidth of the carrier frequency envelopes. So, in the standard form of piecewise HB circuit with N nonlinear elements (figure 2) the time varying vectors in Eq (4) presented as: $V(t_s) = [V_1(t_s) \; K \; V_n(t_s) \; V_N(t_s)]^T$ and $V_n(t_s) = [V_{n0}(t_s) \; K \; V_{nK}(t_s) \ldots V_{nK}(t_s)]^T$. And Ω is a diagonal matrix of harmonics of carrier frequency. As follows:

$$\boldsymbol{\Omega} = \begin{bmatrix} \boldsymbol{\omega}_n & \boldsymbol{O} & \Lambda & \boldsymbol{O} \\ \boldsymbol{O} & \boldsymbol{\omega}_n & \boldsymbol{O} & \boldsymbol{M} \\ \boldsymbol{M} & \boldsymbol{O} & \boldsymbol{O} & \boldsymbol{O} \\ \boldsymbol{O} & \Lambda & \boldsymbol{O} & \boldsymbol{\omega}_n \end{bmatrix}, \quad \boldsymbol{\omega}_n = \begin{bmatrix} 0 & 0 & \Lambda & 0 \\ 0 & \omega_c & 0 & \mathrm{M} \\ \mathrm{M} & 0 & 0 & 0 \\ 0 & \Lambda & 0 & K\omega_c \end{bmatrix}$$

and $\boldsymbol{O} = \boldsymbol{O}_{(K+1)\times(K+1)}$ is a zero matrix.

In piecewise harmonic balance I_L should be evaluated. Since linear part matrix, Y_L is only realized in frequency domain, so $I_L(\omega_s, \omega_c) = Y_L(\omega_s, \omega_c)V(\omega_s, \omega_c)$. In which ω_S is related to t_s . $t_s \Leftrightarrow \omega_s$.

It can be proven that by restricting the envelope dynamics to be slow compared with the carrier, $I_L(t_s, \omega_c)$ is calculated as follows (it is truncated to the order of R_T): /5/

$$I_{Lk}(t_s) = \sum_{R=0}^{R_T} \left[\frac{1}{n! j^R} \frac{d^R Y_L(\omega)}{d\omega^R}\bigg|_{\omega=k\omega_c} \frac{\partial^R V_k(t_s)}{\partial t_s^R} \right] \quad (5)$$

An appropriate discretization for t_S, leads to the complete set of (2K+1) differential equation, converted into a conventional HB equation for each time sample. Using backward difference (Euler rule),

$$\frac{\partial \boldsymbol{Q}_{nl}(\boldsymbol{V}(t_s))}{\partial t_s}\bigg|_{t_s=t_{si}} = \frac{\boldsymbol{Q}_{nl}(\boldsymbol{V}(t_{si})) - \boldsymbol{Q}_{nl}(\boldsymbol{V}(t_{s\,i-1}))}{\Delta t_s} \quad (6)$$

$$\frac{\partial^R \boldsymbol{V}_k(t_s)}{\partial t_s^R}\bigg|_{t_s=t_{si}} = \frac{1}{(\Delta t_s)^R} \sum_{r=0}^{R} \left[(-1)^r \binom{R}{R-r} \boldsymbol{V}(t_{s\,i-r}) \right] \quad (7)$$

And also applying this rule to eq (4). We have:

$$\boldsymbol{F}_{NL}(\boldsymbol{V}(t_{si})) = \sum_{R=0}^{R_T} \left\{ \frac{1}{n! j^R} \frac{d^R \boldsymbol{Y}_L(\omega)}{d\boldsymbol{\omega}^R}\bigg|_{\omega=\omega_k} \frac{1}{(\Delta t_s)^R} \sum_{r=0}^{R} \left[(-1)^r \binom{R}{R-r} \boldsymbol{V}(t_{s\,i-r}) \right] \right\} + j\boldsymbol{\Omega}\boldsymbol{Q}_{nl}(\boldsymbol{V}(t_{si})) + \frac{\boldsymbol{Q}_{nl}(\boldsymbol{V}(t_{si})) - \boldsymbol{Q}_{nl}(\boldsymbol{V}(t_{s\,i-1}))}{\Delta t_s} + \boldsymbol{I}_{nl}(\boldsymbol{V}(t_{si})) + \boldsymbol{I}_S(t_{si}) = \boldsymbol{0} \quad (8)$$

Where $\boldsymbol{\omega}_k = [0 \; \Lambda \; K\omega_c]^T$.

$$\boldsymbol{F}_{NL}(\boldsymbol{V}(t_{si})) = \boldsymbol{Y}_L^{ET} \boldsymbol{V}(t_{si}) + j\boldsymbol{\Omega}^{ET}\boldsymbol{Q}_{nl}(\boldsymbol{V}(t_{si})) + \boldsymbol{I}_{nl}(\boldsymbol{V}(t_{si})) + \boldsymbol{I}_S(t_{si}) + \boldsymbol{I}_{i-1} = \boldsymbol{0} \quad (9-a)$$

$$\boldsymbol{Y}_L^{ET} = \sum_{R=0}^{R_T} \left\{ \frac{1}{n! j^R} \frac{d^R \boldsymbol{Y}_L(\omega)}{d\boldsymbol{\omega}^R}\bigg|_{\omega=\omega_k} \frac{1}{(\Delta t_s)^R} \right\}$$

$$\boldsymbol{\Omega}^{ET} = \boldsymbol{\Omega} + \frac{\boldsymbol{1}}{\Delta t_s}$$

$$\boldsymbol{I}_{i-1} = \sum_{R=0}^{R_T} \left\{ \frac{1}{n! j^R} \frac{d^R \boldsymbol{Y}_L(\omega)}{d\boldsymbol{\omega}^R}\bigg|_{\omega=\omega_k} \frac{1}{(\Delta t_s)^R} \left(\sum_{r=1}^{R} \left[(-1)^r \binom{R}{R-r} \boldsymbol{V}(t_{s\,i-r}) \right] \right) \right\} + \frac{-\boldsymbol{Q}_{nl}(\boldsymbol{V}(t_{s\,i-1}))}{\Delta t_s} \quad (9)$$

Where, $\boldsymbol{1}$ is a unit matrix. As we can see in eq (9-a), this equation is similar to $\boldsymbol{F(V)}$, ordinary HB equation. There are some differences in $\boldsymbol{Y}_L^{ET}$, $\boldsymbol{I}_{i-1}$ and $\boldsymbol{\Omega}^{ET}$ described. As we can see in Eq.(9), $\boldsymbol{I}_{i-1}$ must be calculated from previous time steps. So, solving this equation for each time step,

leads to the varying envelope of desirable voltage at harmonics of carrier frequency.

Assuming Eq (5) with order of R_T, Enables analysis of nonlinear circuits excited by arbitrary bandwidth. So the simulation leads to more accurate results.

2.1. Small Band Modulating Signals

The case of most practical interest to microwave and wireless systems is the one in which the modulating signals are very slowly varying signals, $BW << f_c$, the calculation converges for $R_T \geq 1$. Thus, by assuming $R_T=1$, calculation for each time step only requires knowing at one previous time step results. So Y_L^{ET} and I_{i-1} in Eq.(9) can be reduced to:

$$Y_L^{ET} = Y_L + \frac{1}{j\Delta t_s}\frac{dY(\omega)}{d\omega}\bigg|_{\omega=\omega_k}$$

$$I_{i-1} = \frac{1}{j}\frac{dY(\omega)}{d\omega}\bigg|_{\omega=\omega_k}\frac{-V(t_{s\,i-1})}{\Delta t_s} + \frac{-Q_{nl}(V(t_{s\,i-1}))}{\Delta t_s} \quad (10)$$

2.2. Adaptive Time Scales

Let consider eq (8) for example with $R_T=1$, where $Q_{nl}(V(t_{si})) = Q_{nl}(V(t_{s\,i-1}))$, with this assumption, the Eq (8) converts to a common Harmonic Balance equation. In this case we don't need to solve the equation for *i+1* step if $I_S(t_{si}) = I_S(t_{s\,i+1})$ (results in $V(t_{si}) = V(t_{s\,i-1})$). This means that we can assume Δt_s small enough to fallow the input transient effects precisely and after ending transient effects, we can use a HB instead of many ET-HB routines. Therefore using this technique, if we choose adaptive time steps, Δt_s^j, also, it will offer some improvement in efficiency and time-saving, to follow the input transient effects and also evaluate the steady state response of microwave circuits containing waveforms with sharp edge and spikes in which; For spikes and sharp edges of waveform we choose Δt_s very small and for smooth parts of signal larger amounts of Δt_s is chosen. Using this method, results in a good saving in simulation time (it will be explained in the next part). The improvement in efficiency may be observed in some circuits more clear than others e.g. PLLs transient responses can be efficiently observed using this technique.

3. Simulation and Results

In this section as an example of application, a one-stage class A power amplifier with 17 dB of gain and output power of 18 dBm suitable for use in Fixed WiMAX technology based on IEEE 802.16 d standard is studied. It is designed to work with 200MHz bandwidth centered at frequency of 3.5 GHz. The amplifier includes input and output Microstrip matching networks and the necessary DC bias circuitry. The Pseudomorahic InGaAs/ AlGaAS/GaAs HEMT /17/ is used to realized power amplifier. According to reduction of harmonic distortion on output power, it is biased in class A so V_d =6 V and V_g =0 V is chosen (Standard schematic of the power amplifiers). Matching networks are designed and optimized to obtain maximum output power and minimum possible harmonic distortion. So, simulating circuit under one-sinusoidal tone excitation using HB, results in 1-dB compression point of P_{1dB}= 18.7 with an associated Gain of 17 dB and PAE of nearly 20%. This is illustrated in figure 2.

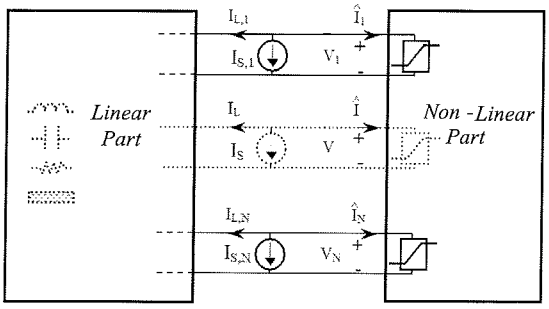

Fig. 2. Deviding a nonlinear circuit by a linear and nonlinear part.

As the second step, the designed power amplifier should be exited by a modulated signal. due to confirm the formulation and CAD presented, first, it is applied to the circuit derived with a RF pulse source (modulated source), creates a pulse modulated RF carrier with frequency of f_c (with rise-time, fall-time and width of constant portion of pulse of 0.25, 0.25 and 3 n sec, respectively). Accordingly, the absolute value of output voltage evaluated with proposed CAD is confirmed with Time-Domain simulation. It is shown in figure 3. ET-HB in comparison to time domain techniques proposes a more fast simulation. In addition, using adaptive time steps, Δt_s^j, for spikes and sharp edges of waveform we chose Δt_s very small and for smooth parts of signal, larger amounts of Δt_s is chosen. Consequently, in this case, led to more time saving about 68 percent.

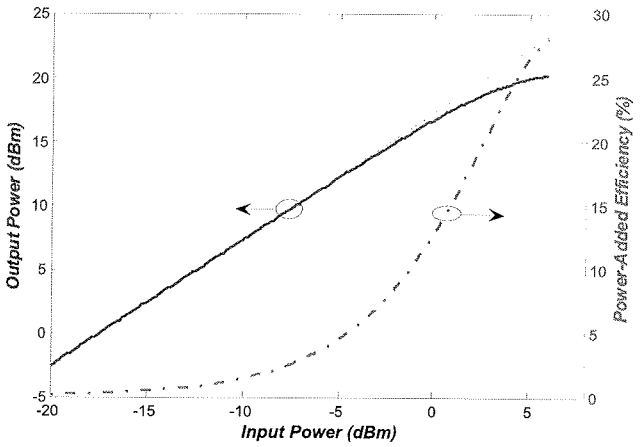

Fig. 3. Output power and Power added Efficiency of the amplifier versus input signal level.

Now, we can consider analysis of designed amplifier with modulated excitation using proposed CAD formulation. Since, One of the important digital modulation schemes, allowed in IEEE 802.16 standard (*WirelessMAN-SCa*), is

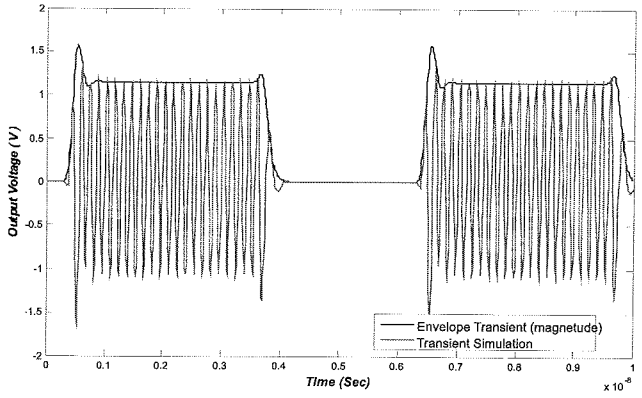

Fig. 4. Proposed CAD results comply with Time domain simulation.

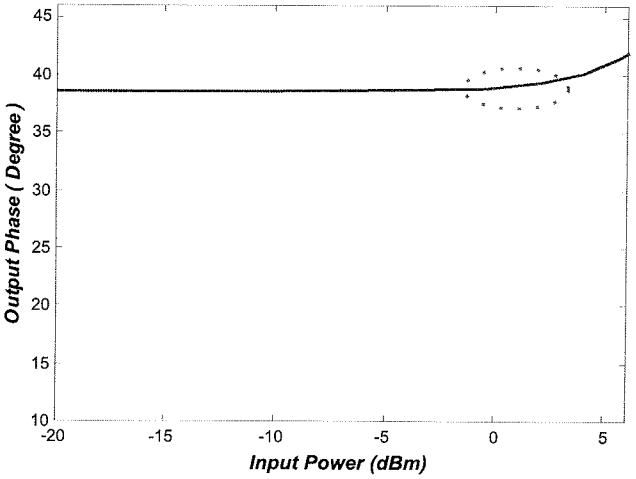

Fig. 5. Plot of simulation excess phase-shift versus input drive level, for illustrating AM-PM characterization.

16-QAM, so, we have considered an input excitation of a modulated signal at 3.5 GHz. Modulating signal, a 16-QAM symbol stream, is responsible for the envelope of the RF carrier. Applying proposed CAD, we can consider the adverse effect of nonlinearity of the power amplifier on modulated signal and then, on output demodulated signal. The input signal was first set at a power that was low-enough to prevent strong nonlinearity (maximum of input power was much set lower than $P_{1\ dB}$). Regarding the constellation diagram of the output voltage signal, we can understand that a phase shift of about 40 degrees with comparison of constellation diagram of input is apparent. This phase variation may be related to the AM-PM conversion. As it is depicted in figure 5, the calculating AM-PM conversion confirms this subject. The constellation diagram of the input and output envelope at P_{1dB} is shown in figure 6-a. Figure 6-c presents the input and output time domain envelope signal. Spectrum of the output signal for 16-QAM is shown in figure 6-d. Note that the phase shift is compensated and amounts are normalized (with small signal gain) in all presented constellation diagrams.

(a)

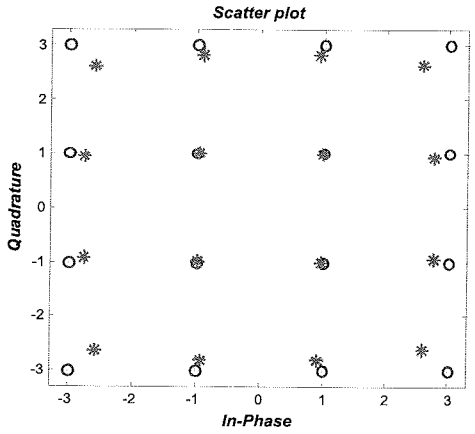

(b)

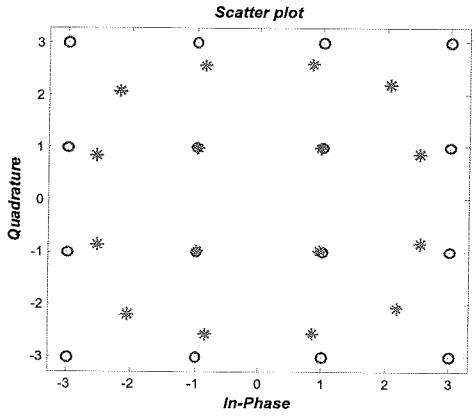

(c)

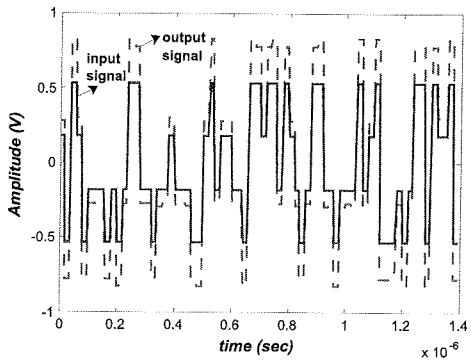

(d)

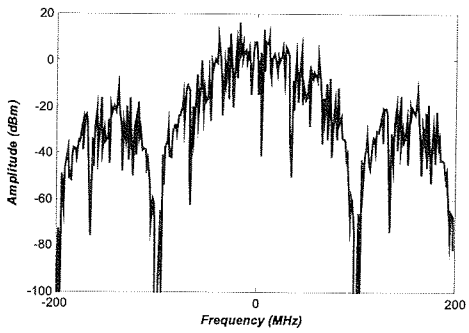

Fig. 6. (a) Constellation diagram @ P_{1dB} (circles: input diagram; stars: output diagram), (b) Constellation diagram @ P_{1dB} +3 (circles: input diagram; stars: output diagram), (c) time-domain envelope (solid line: input signal; dotted line: output signal scaled with 2.5) and (d) spectrum of the output signal for 16-QAM.

Increasing the input power up to P_{1dB} or more causes more distortion especially in gain. So, the constellation changes. Figure 6-b shows constellation of output voltage with input power of (P_{1dB}+3) dBm. By focusing more on this figure, as we expected, we realized that the symbols with larger magnitude due to lower gain have larger variance in respect to its relative position. Therefore, increasing the input power changes the arrangement of symbols in constellation diagram.

The Error Vector Magnitude (EVM) defines the average constellation error with respect to the farmost constellation point power, and defined by following equation /18/:

$$EVM = \sqrt{\frac{\frac{1}{N}\sum_{1}^{N}(\Delta I^2 - \Delta Q^2)}{S_{\max}^2}} \qquad (11)$$

Where, N is the number of symbols in the measurement period and S_{max} the maximum constellation amplitude.

EVM diagram for 16-QAM modulation schemes versus various input power is shown in figure 7. Enlarging the input power leads to stronger nonlinearity and consequently, the EVM increases.

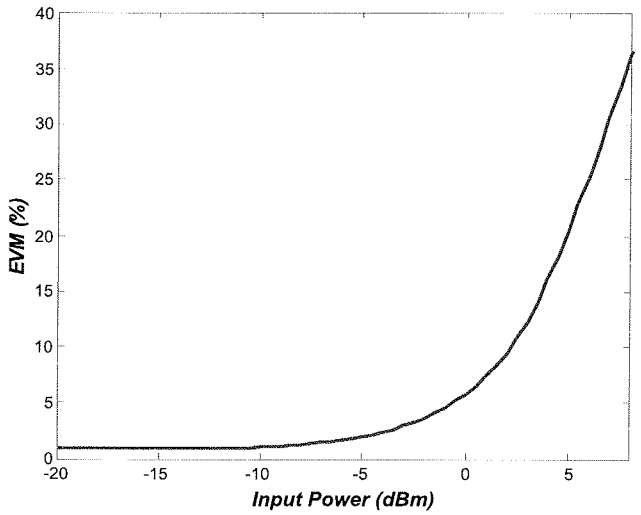

Fig. 7. Error Vector Magnitude versus input power

Also, this nonlinearity phenomenon causes a more symbol error rate (SER) in communication system. In the figure 8 we have shown the effect of nonlinearity of this power amplifier on SER of a 16-QAM signal through a noisy Gaussian channel. As it is illustrated, enlarging the input power results in worse Symbol Error Rates. Let consider QPSK, another modulation mode supported in IEEE 802.16 standard (WirelessMAN-SCa), for input excitation signal. PSK is a digital modulation where the carrier phase is keyed by the digital modulation signal. So, a finite number of phases are used. Therefore in the case of PSK, amplitude distortion (AM-AM) could not chiefly cause any defect. The main distortion could affect on system performance. Thus, have a flat AM-PM conversion characteristic,

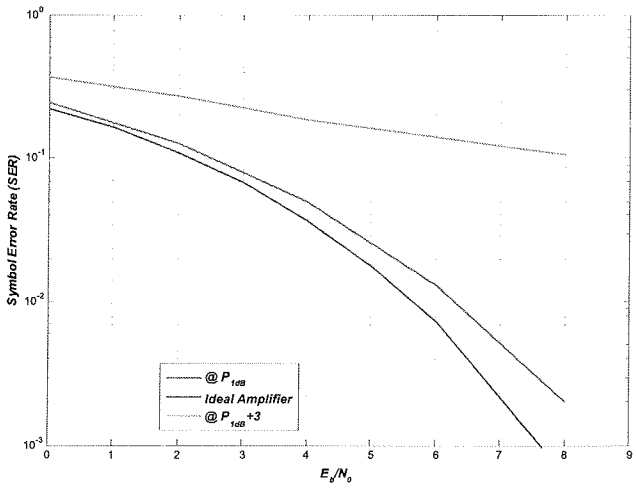

Fig. 8. SER through the Gaussian channel for 3 excitation power for 16-QAM

results in lower errors at the output of demodulator. The constellation diagram of the input and output envelope with QPSK modulation at P_{1dB} is shown in figure 9-a. Figure 9-b presents the input and output time domain envelope signal. Spectrum of the output signal for QPSK is shown in figure 9-c.

4. Conclusion

A new formulation of Envelope Transient HB appropriate for transient and steady state analysis of nonlinear active microwave circuits was presented. This novel approach enables using adaptive time scales resulting in fast simulation of microwave circuits. The performance of this method was investigated by applying on a microwave circuit. As an application of this method, a power amplifier in WiMAX frequency band excited by 16-QAM and QPSK modulated signal was considered. And the effect of nonlinearity on the output and system performance was discussed. As a result, we showed that QPSK is more resistant to the amplifier nonlinearity than QAM. It was shown that, enlarging the input power for 16-QAM results in worse Symbol Error Rate and Error vector magnitude.

5. Acknowledgement

This work is supported in part by Iran Telecommunication Research Center (ITRC)

References

/1/ A. B. Carlson, "*Communication Systems*", 4th Ed, McGraw-Hill, 2002.

/2/ J. G. Proakis, M. Salehi, "*Digital Communications*", 5. th. Edition, McGraw-Hill, 2008

/3/ Kenington, P., *"High-Linearity RF Amplifier Design"*, Norwood, MA: Artech House, 2000.

/4/ J. Roychowdhury, *"Effcient Methods for Simulating Highly Nonlinear Multi-Rate Circuits"* IEEE Trans. Circuits Syst. I, Fundam. Theory Appl., 2001.

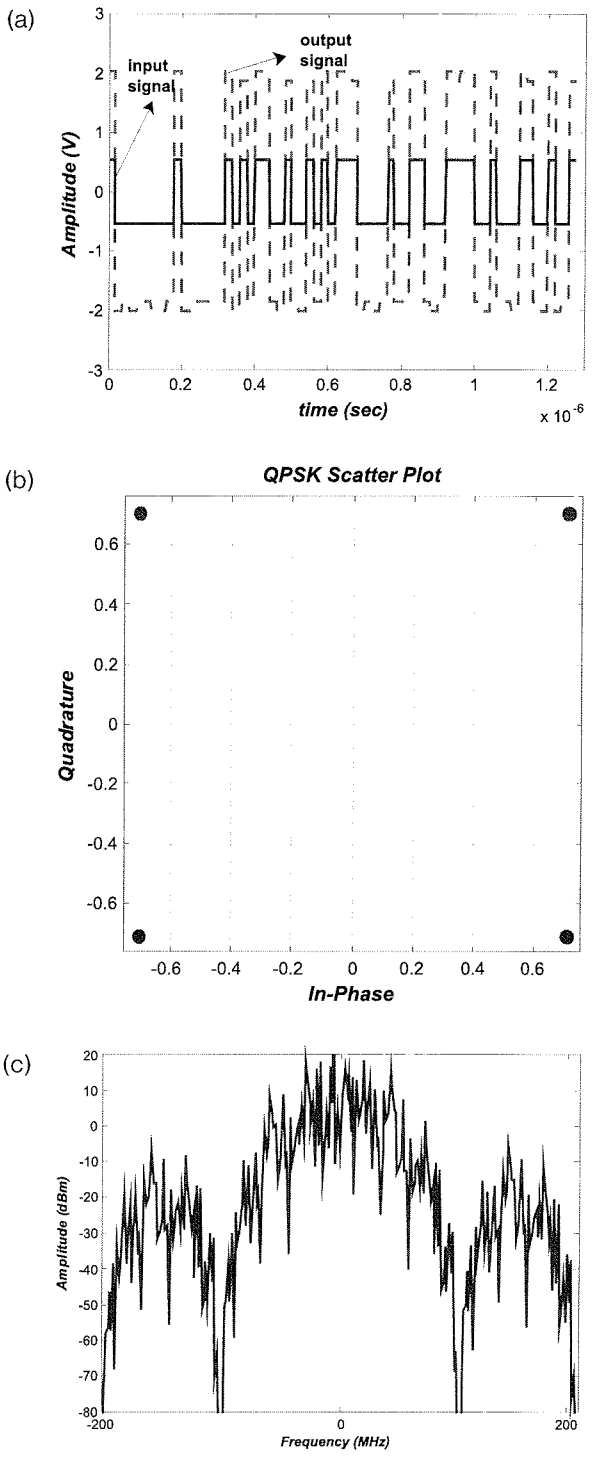

Fig. 9. (a) Constellation diagram @ P_{1dB} (circles: input diagram; stars: output diagram), (b) time-domain envelope (solid line: input signal; dotted line: output signal) and (c) output and input signals and spectrum of the output signal for QPSK.

/5/ J.C. Pedro and N.B. Carvalho, ***"Intermodulation distortion in microwave and wireless circuits"***, Artech House, Norwood, MA 2003.

/6/ Kundert, K.S.; Sorkin, G.B.; Sangiovanni-Vincentelli,A, ***"Applying harmonic balance to almost-periodic circuits"*** Microwave Theory and Techniques, IEEE Transactions on Volume 36, Issue 2, Feb 1988 Page(s):366 - 378

/7/ E. Ngoya and R. Larchevčque, ***"Envelope transient analysis: a new method for the transient and steady-state analysis of microwave communications circuits and systems,"*** in IEEE MTT-S Int. Microw. Symp. Dig., San Francisco, CA, Jun. 1996, pp. 1365-1368.

/8/ S. Sancho, A. Suarez, and J. Chuan, ***"General envelope-transient formulation of phase-locked loops using three time scales,"*** IEEE Trans. Microw. Theory Tech., vol. 52, no. 4, pp. 1310-1320, Apr. 2004.

/9/ H. Vahdati, A. **Abdipour**, ***"Nonlinear stability analysis of microwave oscillators using circuit envelope technique"***, will be appeared in journal of Transaction, on IEICE, vol E92-e, No.2 Feb**2009**,

/10/ Carvalho, N.B.; Pedro, J.C.; Jang, W.; Steer, M.B. ***,"Nonlinear RF circuits and systems simulation when driven by several modulated signals"*** Microwave Theory and Techniques, IEEE Transactions on Volume 54, Issue 2, Feb. 2006 Page(s): 572 - 579

/11/ V. Rizzoli, A. Neri, and F. Mastri, *"A modulation-oriented piecewise harmonic-balance technique suitable for transient analysis and digitally modulated signals,"* in Proc. 26th Eur. Microw. Conf., Prague, Czech Republic, Sep. 1996, pp. 546-550.

/12/ J. C. Pedro and N. B. Carvalho, *"Simulation of RF circuits driven by modulated signals without bandwidth constraints,"* in IEEE MTT-S Int.Microw. Symp. Dig., Seattle, WA, Jun. 2002, pp. 2173-2176.

/13/ M. Condon and E. Dautbegovic, *"Anovel envelope simulation technique for high-frequency nonlinear circutis,"* in Proc. 33rd Eur. Microw. Conf., Munich, Germany, Oct. 2003, pp. 619-622.

/14/ D. Sharrit, "Method for Simulating a Circuit," U.S. Patent 5 588 142, May 12, 1995.

/15/ N. B. Carvalho, J. C. Pedro, W. Jang, and M. B. Steer, "Nonlinear simulation of mixers for assessing system-level performance," Int. J. RF Microw. Computer-Aided Eng.

/16/ V. Rizzoli, A. Neri, F. Mastri, and A. Lipparini, "Modulation-oriented harmonic balance based on Krylov-subspace methods," in IEEE MTT-S Int. Microw. Symp. Dig., Jun. 1999, pp. 771-774.

/17/ Siddiqui, M.K.; Sharma, A.K.; Callejo, L.G.; Lai, R.,***"A high-power and high-efficiency monolithic power amplifier at 28GHz for LMDS applications"*** Microwave Theory and Techniques, IEEE Transactions on Volume 46, Issue 12, Dec 1998 Page(s):2226 - 2232

/18/ IEEE Std 802.16™-2004 (Revision of IEEE Std 802.16-2001, IEEE Standard for Local and metropolitan area networks, Part 16: Air Interface for Fixed Broadband Wireless Access Systems, Approved 24 June 2004.

Amir Vaezi, Abdolali Abdipour, Abbas Mohammadi

Microwave/mm-Wave & Wireless Communication Research Lab, Radio Communication Centre of Excellence, dElectrical Engineering Department, Amirkabir University of Technology, 424 Hafez. Ave, Tehran, Iran

Prispelo (Arrived): 17.03.2009 *Sprejeto (Accepted): 09.09.2009*

MODELIRANJE BRALNE GLAVE OPTIČNEGA ENKODERJA IN MERITEV ULTRA MAJHNIH KOTOV

Tomaž Dogša, Matej Šalamon, Bojan Jarc, Mitja Solar

Fakulteta za elektrotehniko, računalništvo in informatiko, Maribor, Slovenia

Kjučne besede: optični enkoder, makromodeliranje,simulacija vezij, SPICE, merjenje ultra majhnega kota.

Izvleček: Optične enkoderje uporabljamo za precizno merjenje pomika oziroma kota. V prispevku je opisan SPICE makromodel bralne glave optičnega enkoderja oziroma sin/cos senzorja. Modelirana je oblika signala (amplituda, fazni kot, popačenje, enosmerni premik) in poljubna dinamika premikanja (hitrost, pospešek) glave. Z dodatnim elektronskim interpolatorjem lahko še povečamo točnost merjenja. Ker motnje (npr. fazni zamik, neenakost amplitud), ki nastanejo pri branju, zelo vplivajo na interpolacijo, je dodano posebno vezje za korekcijo vhodnega signala (signal conditioning module). Ena izmed nalog tega vezja je korekcija faze, ki odstopa od 90°. Za preverjanje učinkovitosti načrtovanja fazne korekcije, potrebujemo zelo natančno meritev faze, ki se izvaja na nivoju SPICE simulatorja. Izbrali smo meritev faze, ki temelji na meritvi prehoda obeh signalov skozi 0 V in poznavanju hitrosti. S to metodo lahko zasledujemo tudi časovno odvisnost faznega kota. Izvedena je analiza napake, ki nastane pri merjenju kota za neidealne signale, katerim se spreminja amplituda, frekvenca in enosmerni premik.

Optical Encoder Scanning Head Modelling and Ultra Small Phase Shift Measurement

Key words: optical encoders, macromodelling, circuit simulation, SPICE, ultra small phase shift measurement.

Abstract: Optical encoders are used for high accuracy position measurement. Our first aim was to find a SPICE model of the optical encoder scanning head. In this paper macromodelling of the optical encoder scanning head (sin/cos sensor) is presented. The shape of the output signal (amplitude, phase shift, distortion) and movement of the head (velocity, acceleration) are modelled by behavioural models. The dynamic of the movement is defined by simple table. The resulting frequency of sin/cos signal is a piecewise-linear function with soft corners.

The measurement precision is improved with additional electronic interpolator. Since the distortion of sin/cos signal affects the interpolation, the signal conditioning module is inserted between the interpolator and the scanning head. One of the goals of the signal conditioning module is the elimination of the phase shift that differs from the 90°. For the verification of the design effectiveness the precision phase shift measurement method on the SPICE level is needed. The Lissajous figures that are often used to measure phase shift were not appropriate for this case. Our second goal was to measure the time-dependent ultra small phase shift in the circuit where the amplitude, frequency and DC offset were also varying with the time. The measurement algorithm should be implemented with the SPICE scripting language. Since the frequency (velocity of scanning head) was known we chose the measurement that is based on the detection of zero voltage crossing of the sin and cos signals. The analysis of the error estimation of this measurement method for the signals that vary from their nominal values is also presented. The accuracy of the measurement depends on the time interval error, stability of the frequency and DC offset.

1. Uvod

Senzor sin/cos predstavlja enega izmed ključnih gradnikov linearnih in rotacijskih enkoderjev, ki jih uporabljamo za precizno merjenje pomika oziroma kota (slika 1). Letev in ustrezni senzor sta lahko magnetna ali optična. Princip merjenja pomikov je inkrementalni in temelji na štetju rastrskih razdelkov na referenčni letvi oziroma mrežici. Z dodatnim interpolatorjem lahko ločljivost še dodatno povečamo.

Na izhodu idealnega sin/cos senzorja je idealen sinusni in kosinusni signal z amplitudama 1. Dejanski izhodni signali so samo približno harmonični. Zaradi neenake občutljivosti fotodiod so izhodni signali (±SIN, ±COS) različnih amplitud, enosmerno premaknjeni in imajo dodatni fazni premik. To povzroča pogrešek pri merjenju pomikov manjših od periode mrežice. Z različnimi spremembami v optičnem delu lahko zmanjšamo harmonična popačenja /5/. V /4/ so dosegli zmanjšanje amplitude tretjega harmonika iz 4,35 % na 1,45 % in amplitude petega harmonika iz 0,44 % na 0,17 %. V /2/ so s pomočjo Vernierjevega principa zmanjšali THD (skupno harmonsko popačenje) na -60dB. Struktura in princip delovanja optičnega sin/cos senzorja je na kratko opisan v drugem poglavju. Opis SPICE modela bralne glave je v tretjem poglavju. Modelirana je oblika signala (amplituda, fazni kot, popačenje) in dinamika premikanja (hitrost, pospešek) glave. Vsi ti parametri so časovno odvisni in tvorijo scenarij uporabe bralne glave.

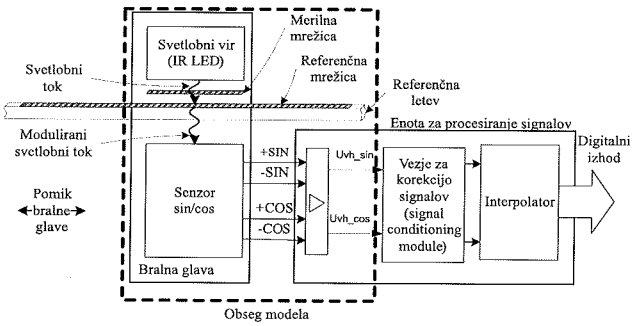

Slika1: Blokovna shema optičnega linearnega enkoderja in območje modeliranja

Fig. 1: Configuration of linear optical encoder. Dashed line marks the modelled area.

Ker na točnost zelo vpliva tudi kvaliteta signala, ki prihaja iz bralne glave (U_{vh_sin}, U_{vh_cos}), je med bralno glavo in enkoderjem vstavljeno vezje za korekcijo signalov (signal conditioning module). Njegova naloga je uskladiti amplitudo, zmanjšati harmonična popačenja in enosmerno premaknitev ter ustrezno korigirati fazni premik. Ker se razvoj tega vezja začne na nivoju simulatorja, je potrebno modelirati bralno glavo. Za preverjanje učinkovitosti raznih variant vezja za fazno korekcijo potrebujemo pri simulaciji tudi zelo natančno in relativno hitro meritev zelo majhnih faznih odstopanj. V laboratoriju takšno meritev običajno izvedemo s pomočjo Lissajoujevih krivulj. Ker so te krivulje večlične parametrične funkcije in fazna premaknitev ni konstantna, je pri simulaciji zelo težko na ta način natančno izmeriti trenutni fazni kot. V prispevku se bomo zato osredotočili na meritev faze, ki temelji na meritvi prehoda obeh signalov skozi 0V. V četrtem delu je teoretična obravnava merjenja ultra majhnih kotov in vpliv amplitude, pospeška ter enosmernega premika na natančnost. Pravilnost izpeljav je bila preverjena s simulacijo. Podobna analiza je v /1/, ki pa se nanaša le na arkustangens algoritem.

2. Struktura in delovanje senzorja sin/cos

Slika 1 prikazuje strukturo klasičnega linearnega optičnega enkoderja s presevanjem mrežic. Sestavljata ga optična glava z virom svetlobe (dioda IR LED) in optičnim senzorjem, ter enota za procesiranje signalov z vezjem za korekcijo signalov in interpolatorjem.

Referenčna in merilna mrežica sta ključna gradnika optičnega enkoderja. Sestavljeni sta iz paralelnih za svetlobo slabo oz. neprepustnih linij, ločenih s transparentnimi področji enake širine. Za natančno delovanja enkoderja je potrebno zagotoviti strogo periodičnost mrežic. Razen referenčne mrežice se na referenčni letvi nahaja še indeksna sled, ki v različnih izvedbah omogoča grobo a hitro določitev velikosti pomika v relativnem smislu ali določitev trenutnega položaja bralne glave v absolutnem smislu. Za obravnavo optičnega enkoderja v tem prispevku indeksni signal ni pomemben, zato na sliki ni prikazan.

Optični sin/cos senzor sestavljajo fotodiode, ki zaznavajo svetlobo. Ta preseva, se odbija ali pa uklanja na mrežicah. Pri klasičnih enkoderjih z dvema mrežicama se svetlobni tok, ki preseva mrežici, spreminja približno sinusno zaradi interference področij mrežic, ki svetlobe ne prepuščajo (slika 2). Interferenca nastopi pri prekrivanju dveh vzporednih mrežic z malenkost različno periodo ali dveh mrežic z enako periodo, vendar med sabo nagnjenih za majhen kot. Pojav se kaže kot Moirov vzorec /3/, /4/ (slika 2).

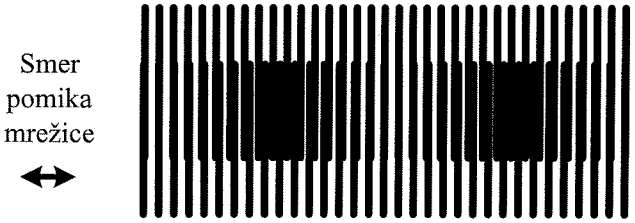

Slika2: Moirov vzorec, kot posledica prekrivanja dveh mrežic z malenkost različno periodo.
Fig. 2: Moiré fringe generated by superimposed gratings, with slightly different periods.

S premikom mrežice za pol periode so področja, kjer sta bili mrežici v fazi, sedaj v protifazi in obratno. Svetlobni tok, ki ga izmerimo ob vzdolžnem premikanju mrežice, se spreminja približno sinusno. Pomik mrežice za eno periodo povzroči spremembo svetlobnega toka prav tako za eno periodo. Razen dolžine lahko določimo tudi smer pomika, če imamo vzdolž mrežic nameščeni vsaj dve fotodiodi, ki zaznavata fazno premaknjena svetlobna tokova. Vendar so zaradi kompenzacije vpliva zunanje svetlobe teoretičen minimum vsaj štiri fotodiode, ki zaznavajo fazno premaknjene svetlobne tokove s premaknitvami $n \times 90°$, $n = 0, 1, \ldots 3$. Ustrezne fazne premaknitve svetlobnega toka zagotovimo z več-fazno premaknjenimi merilnimi mrežicami /4/. Z diferenco dveh proti-faznih signalov iz fotodiod (0° in 180° ter 90° in 270°) izločimo vpliv zunanje svetlobe, ki se odraža kot enosmerna premaknitev signala fotodiode. Tako dobimo dva, med sabo za 90° premaknjena harmonična signala (sinus in kosinus), ki omogočata detekcijo velikosti in smeri pomika.

Do sedaj obravnavana zgradba optičnega enkoderja je v rabi za periode mrežice nekje do 20 μm. Z zmanjševanjem velikosti periode mrežice v velikostni razred valovne dolžine svetlobe, ki jo izseva dioda IR, uklon svetlobe na mrežici ni več zanemarljiv. Enkoderji s periodo mrežice manjšo od 8 μm uporabljajo reflektivno referenčno mrežico, ki za razliko od transmisijske svetlobo odbija.

V novejših enkoderjih je uporabljena integrirana izvedba optičnega dela enkoderja (slika 3 a), ki vsebuje diodo LED in dve merilni mrežici z optičnimi detektorji (fotodiode na mrežici so trakaste oblike). Sistem deluje z reflektivno referenčno mrežico.

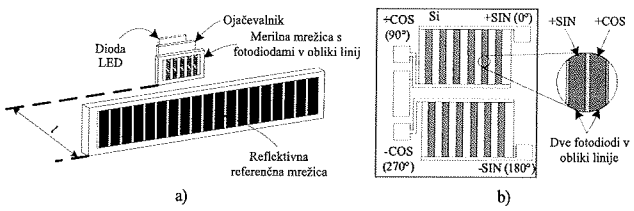

Slika 3: Integrirana izvedba optičnega dela enkoderja /5/, /6/. a) princip, b) izvedba.
Fig. 3: Integrated version of optical encoder /5/, /6/. a) principle, b) implementation.

Merilna mrežica je napravljena s fotolitografijo. Na posameznem območju merilne mrežice (slika 3 b, zgornja oz. spodnja polovica) sta realizirani dve fotodiodi (slika 3 b, povečan izsek), ki zaznavata 90° premaknjena svetlobna tokova. Z dvema mrežicama s fazno premaknitvijo 180° (slika 3 b) dobimo štiri ustrezno fazno premaknjene signale za izločitev vpliva zunanje svetlobe. Svetloba diode

LED, ki leži na spodnji plasti, sveti skozi reže med trakovi merilne mrežice. Ker so fotodiode na rezini blizu skupaj, so razlike v njihovih svetlobnih občutljivostih in jakostih okoliške svetlobe majhne. Električni odziv je posledica povprečnega svetlobnega toka, ki ga zaznavajo posamezne fotodiode. S tem je zmanjšan vpliv motenj, kot so to npr. poškodbe ali umazanija na referenčni mrežici.

Zaradi namestitve fotodiod na samo merilno mrežico in njihove izvedbe v obliki linij se optični del integriranega enkoderja obnaša kot sistem s tremi mrežicami /4/ nameščenimi ena za drugo na oddaljenosti *l*. Pri tem se reže srednje mrežice oziroma reflektivne linije referenčne mrežice na sliki 3 a) obnašajo kot zaslonke, ki projicirajo vzorec merilne mrežice na fotodiode. Na fotodiodah dobimo več projekcij referenčne mrežice, ki med sabo interferirajo. Razen boljšega kontrasta pri malih periodah mrežice, imajo enkoderji s sliko mrežice tudi dvakrat večjo ločljivost od klasičnih enkoderjev z dvema mrežicama (enkoderji s senco mrežice). Ob premiku integriranega senzorja za razdaljo *d* se slika mrežice premakne v nasprotno smer za razdaljo *d*. Relativno se torej med merilno mrežico in sliko mrežice razdalja spremeni za 2*d*. Če torej senzor premaknemo za periodo mrežice *p* se bo svetlobni tok spremenil za dve periodi oz. je ločljivost integriranega enkoderja dvakrat večja, kot jo določa perioda mrežice *p*.

3. Model sin/cos senzorja

Pri modeliranju sin/cos senzorja smo se osredotočili predvsem na funkcionalnost, ki naj omogoča enostavno simulacijo statičnih in dinamičnih lastnosti. Modelirano področje senzorja je na sliki 1 označeno s črtkano črto. Idealna pretvorba premika *x* v električni signal je odvisna od položaja, oziroma hitrosti *v* in periode *p*:

$$U_{vh\_\cos}(t) = \cos[2\pi x(t)/p] \quad (1)$$

$$U_{vh\_\sin}(t) = \sin[2\pi x(t)/p] \quad (2)$$

$$x(t) = \int_0^t v(t)dt \quad (3)$$

Ker nas pri simulaciji zanima dogajanje v električnem prostoru, bomo v nadaljevanju namesto hitrosti vpeljali frekvenco.

$$f = v/p \quad (4)$$

Če še upoštevamo popačenja lahko signala, ki sta na vhodu vezja za korekcijo signalov, opišemo z :

$$U_{vh\_\cos}(t) = A_c \cos(2\pi ft + \Delta\varphi) + \\ + A_{ck} \cos(k2\pi ft + \Delta\varphi) + U_c \quad (5)$$

$$U_{vh\_\sin}(t) = A_s \sin(2\pi ft) + A_{sk} \sin(k2\pi ft) + U_s \quad (6)$$

$\Delta\varphi$ je fazna motnja (odstopanje faze glede na idealen sinus in kosinus), *f* je frekvenca, U_c, U_s je enosmerni premik kosinusnega oziroma sinusnega signala, A_c, A_s je amplituda osnovne harmonske komponente signala in A_k, je amplituda k-te harmonske komponente. Razen amplitud višje harmon-skih komponent, so vsi parametri časovno spremenljivi. V idealnih razmerah je $A_c=A_s=1$, $A_k=U_s=U_c=0$ in $\Delta\varphi=0$.

Premikanje glave se odvija po določenem scenariju, ki je sestavljen iz segmentov s konstantnimi hitrostmi in segmentov pospeševanja ter pojemanja. Ker ostri prehodi med segmenti povzročajo konvergenčne probleme, morajo biti prehodi med segmenti zvezni oziroma zaobljeni (glej zgled na sliki 4). Večina sodobnih simulatorjev SPICE pozna vedenjske modele, katerih obnašanje definiramo z matematičnim izrazom, ki je omejen na eno vrstico. S pomočjo takšnih modelov in integratorja smo tvorili makromodel sin/cos senzorja. Časovno odvisnost posameznega parametra smo modelirali z napetostnim virom v obliki tabelaričnega modela. Le-ta je najprimernejši za modeliranje poljubnih scenarijev, saj z lomnimi točkami enostavno definiramo željen potek (glej zgled na sliki 4).

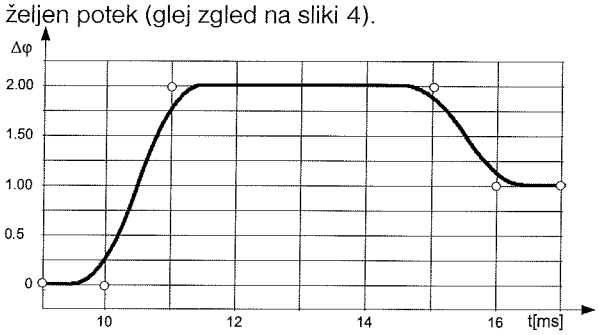

Slika 4: Z lomnimi točkami definiramo časovni potek spreminjanja kota. Na podoben način opisujemo tudi hitrost. S polno črto je označeno dejansko spreminjanje kota.

Fig. 4: Time-dependent phase shift is defined by specifying the points. In a similar way the velocity is defined. The resulting phase shift is marked by the full line.

4. Meritev faznega premika

Pred interpolator vstavljeno vezje za korekcijo (signal conditioning module) skuša popraviti vsa odstopanja od idealne oblike signala. Eno izmed odstopanj je dodatni fazni premik $\Delta\varphi$. Za preverjanje učinkovitosti fazne korekcije potrebujemo pri simulaciji zelo natančno in relativno hitro meritev fazne razlike obeh signalov, katerih frekvenca *f(t)*, fazni kot $\Delta\varphi(t)$, amplituda *Ac* in enosmerni premik *Uc* se lahko tudi spreminjajo. V bistvu je potrebno določiti časovno spremenljiv zelo majhen kot $\Delta\varphi(t)$ v izrazu:

$$u_c(t) = A_c \cos(2\pi f(t)t + \Delta\varphi(t)) + U_c \quad (7)$$

Ker je pri simulaciji hitrost oziroma frekvenca znana, je zelo primerna meritev faznega premika, ki temelji na meritvi prehoda obeh signalov skozi 0 V (glej sliko 5), oziroma z meritvijo časovnega intervala $\Delta T'$. Na to meritev ne vpliva vrednost amplitude. Če je $\Delta T/4 <> \Delta T'$, potem je med signalo-

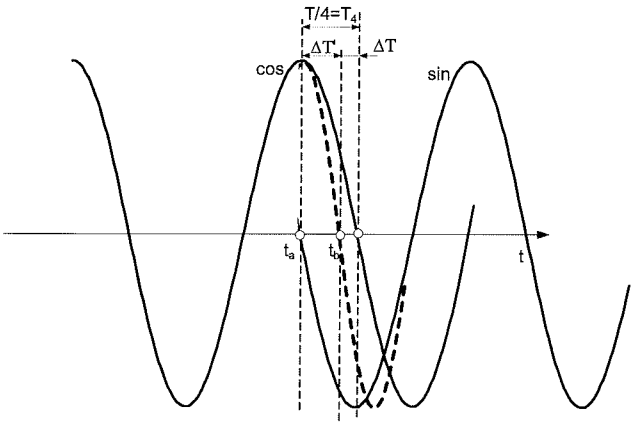

Slika 5: Meritev faznega premika. ΔT je lahko posledica spremembe faze ali frekvence ali hkrati faze in frekvence.

Fig. 5: Phase shift measurement. ΔT could be the result of the phase shift or the frequency change or both.

ma sin in cos dodatna fazna zakasnitev ali pa se je v četrtini periode spremenila frekvenca oziroma hitrost. Če je frekvenca konstantna, zakasnitev izračunamo s pomočjo izraza:

$$\Delta T[s] = \Delta T' - \frac{T}{4} \tag{8}$$

oziroma

$$\Delta\varphi[^\circ] = 90^\circ - \Delta T' \cdot f \cdot 360^\circ \tag{9}$$

To pomeni, da če želimo izmeriti kot 0,1° s točnostjo ±10%, je potrebno v intervalu dolgem 250μs zaznati spremembo 0,278μs z enako točnostjo.

Ker želimo zaznati zelo majhna odstopanja faznega premika, mora biti izpisni korak ustrezno kratek (npr. za frekvenco 1kHz približno 0,02μs). Pri 40ms dolgi simulaciji dobimo 2×10^6 točk. Če se frekvenca spreminja, določimo korak glede na najvišjo frekvenco. Fazni kot (9) izračunamo peš ali pa s pomočjo skripta, ki ga izvaja grafični postprocesor.

4.1. Analiza pogreška

$$\Delta\varphi[^\circ] = 90^\circ - \Delta T' \cdot f \cdot 360^\circ \pm \Delta\varphi_e \tag{10}$$

$$\Delta\varphi_e = \Delta\varphi_m + \Delta\varphi_{nf} + \Delta\varphi_{nu} \tag{11}$$

Skupni pogrešek faznega premika $\Delta\varphi_e$ je vsota treh pogreškov: $\Delta\varphi_m$ nastane pri meritvi časovnega intervala ΔT, $\Delta\varphi_{nf}$ je posledica nestabilne frekvence in $\Delta\varphi_{nu}$, ki nastane zaradi enosmernega premika. Ker je $\Delta\varphi_m$ odvisen le od simulacijskega koraka in relativne konvergenčne napake[1], bosta v nadaljevanju obravnavana le $\Delta\varphi_{nf}$ in $\Delta\varphi_n$.

4.2. Vpliv stabilnosti hitrosti oziroma frekvence

Ker na vrednost izmerjene faze vpliva tudi enosmerni premik in sprememba frekvence, bomo skušali oceniti, kolikšen je vpliv spremembe frekvence. Prehod skozi nič se bo zgodil v t =ΔT' oziroma, ko bo argument kosinusne funkcije (7) zavzel vrednost π/2 (glej sliko 5). Če predpostavimo, da ni dodatnega faznega zamika in da frekvenca f linearno narašča s hitrostjo k_f od vrednosti f_0, je $f(t) = k_f t + f_0$, in za argument dobimo kvadratno enačbo

$$2\pi\left(k_f t + f_0\right)\cdot t = \pi/2 \tag{12}$$

katere rešitev je:

$$\Delta T'[s] = \frac{-f_0 + f_0\sqrt{1+\frac{k_f}{f_0^2}}}{2k_f} \tag{13}$$

Ta zakasnitev predstavlja navidezni kot oziroma pogrešek pri meritvi faznega premika, ki nastane zaradi spremembe hitrosti oziroma frekvence. Teoretični izračun in simulacija kažeta, da je ΔT' v prvi periodi največji nato pa se počasi krajša. Pri pogoju $f_0^2 >> k_f$ lahko zgornji izraz poenostavimo, če izraz pod korenom razvijemo v Taylorjevo vrsto in upoštevamo prve tri člene:

$$\Delta T' = \frac{-f_0 + f_0\left(1+\frac{1}{2}\frac{k_f}{f_0^2}-\frac{1}{8}\frac{k_f^2}{f_0^4}\right)}{2k_f} \tag{14}$$

$$\Delta T' = \frac{1}{4f_0} - \frac{1}{16}\frac{k_f}{f_0^3}$$

Z upoštevanjem enačbe (8) zgornji izraz preuredimo v:

$$\Delta T = \frac{1}{16}\frac{k_f}{f_0^3} \tag{15}$$

Ko časovni interval izrazimo s kotom, dobimo prirastek navideznega kota v intervalu T/4:

$$\Delta\varphi_{nf} \approx \frac{360k_f}{16f_o^2} \tag{16}$$

Če dobljeni izraz delimo s T/4, dobimo približno odvisnost navideznega kota od frekvence in pospeška:

$$\Delta\varphi_{nf}(t) \approx \frac{90k_f}{f_o}t \tag{17}$$

Na sliki 6 je prikazana primerjava med teoretičnim izračunom (17) in simulacijo. Ker nismo upoštevali, da se ΔT' krajša, se razlika pojavi čez nekaj period. Zato enačba (17) predstavlja najbolj neugoden primer naraščanja navideznega kota, ki nastane pri linearnem naraščanju oziroma padanju frekvence. Npr.: za signal s frekvenco 1kHz in dopustnim pogreškom 0,1° je lahko v intervalu 50ms sprememba frekvence največ 22Hz.

1 *V simulatorju SPICE je to parameter RELTOL.*

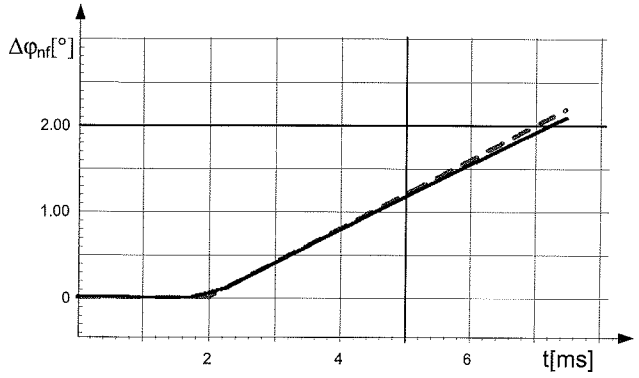

Slika 6: Potek navideznega kota (pogreška) $\Delta\varphi_{nf}(t)$ za primer, ko frekvenca 1kHz po času 2ms začne naraščati s hitrostjo 4,4Hz/ms. (Črtkano je teoretični izračun, polna črta je simulacija.)

Fig. 6: The virtual phase shift (measurement error) $\Delta\varphi_{nf}(t)$ for the case when the starting 1kHz frequency after 2ms begins to raise with the gradient 4,4Hz/ms. (The theoretical analysis is denoted by the full line, and the implemented approximation corresponds to the dashed line).

4.3. Vpliv enosmerne napetosti

Zaradi premaknitve signala navzgor se čas prehoda skozi 0V za ΔT podaljša.

$$0 = A_c \cos(2\pi ft) + U_c \tag{18}$$

$$\cos(2\pi ft) = \cos(2\pi fT/4 + 2\pi f\Delta T) \tag{19}$$

Kosinusno funkcijo razvijemo v Taylorjevo vrsto in upoštevamo prva člena:

$$\cos(2\pi fT/4 + 2\pi f\Delta T) \approx \cos(2\pi fT/4) + \\ + 2\pi f\Delta T \sin(2\pi fT/4) = 2\pi f\Delta T$$

Iz enačbe (18) lahko sedaj izrazimo navidezni kot, ki nastane zaradi majhnega enosmernega premika kosinusnega signala:

$$\Delta\varphi_{nu} = 180\frac{U_c}{\pi A_c} \tag{20}$$

Podoben izraz dobimo za sinusni signal. Najbolj neugoden primer nastopi, ko sta oba signala premaknjena v isto smer:

$$\Delta\varphi_{nu} = \frac{180}{\pi}\left(\left|\frac{U_c}{A_c}\right| + \left|\frac{U_s}{A_s}\right|\right) \tag{21}$$

Npr.: za signal s frekvenco 1kHz in dopustnim navideznim kotom oziroma pogreškom 0,1° je lahko enosmerni premik obeh signalov največ 872μV. Pri amplitudi 1V je to 872ppm.

4.4. Primerjava obeh merilnih metod

Za ilustracijo smo izvedli meritev faznega kota, ki smo ga spreminjali po scenariju iz slike 4. Amplituda obeh signalov je bila 1V. Ker sta bila frekvenca oziroma hitrost konstantni in ni bilo enosmernega premika, je nastopal samo $\Delta\varphi_m$, ki nastane pri meritvi časovnega intervala ΔT. Slika 7 kaže, da lahko s pomočjo Lissajoujevih krivulj le ocenimo območje, znotraj katerega se je spreminjal kot. Kljub temu da je bila amplituda konstantna, je praktično nemogoče določiti časovno odvisnost kota. Predlagana meritev faze, ki temelji na meritvi prehoda obeh signalov skozi 0 V, skorajda ne odstopa od dejanskih vrednosti (slika 8).

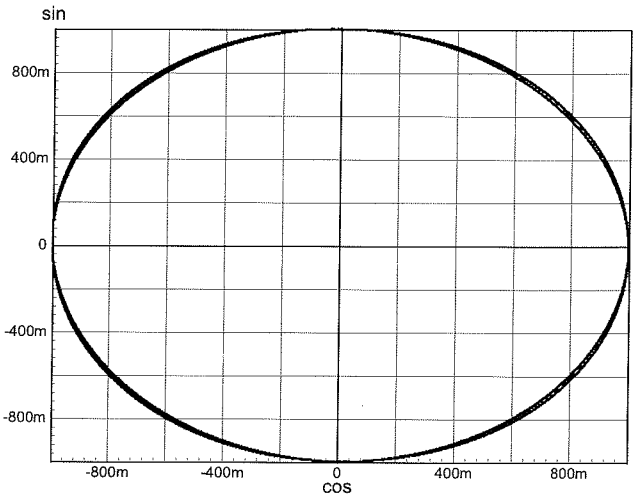

Slika 7: Meritev kota iz slike 4 s pomočjo Lissajoujevih krivulj.

Fig. 7: Phase measurement by using Lissajous figures. Phase shift is changing according to Fig. 4.

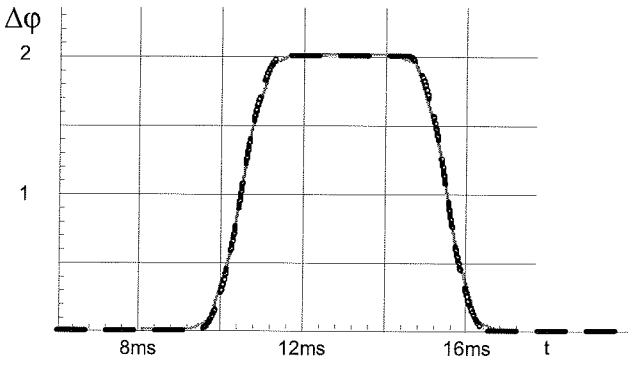

Slika 8: Simulacija predlagane meritve faznega kota. Dejanski potek (slika 4) je označen s črtkano, izmerjen pa s polno črto.

Fig. 8: The simulation of the proposed phase shift measurement. The actual phase shift (see Fig. 4) is presented by the dashed line and the measured phase shift is denoted by the full line.

5. Zaključek

Z obstoječimi vedenjskimi modeli lahko enostavno modeliramo bralno glavo, ki daje dva sinusna in kosinusna sig-

nala. Razne scenarije uporabe in časovno odvisnost parametrov opišemo kot funkcijo z linearnimi segmenti in mehkimi prehodi. Za meritev časovne odvisnosti ultra majhnih kotov smo izbrali metodo, ki temelji na meritvi prehodov skozi 0 V. Na točnost meritve vplivajo: pogrešek meritve časovnega intervala, stabilnost frekvence in enosmerni premik. Izpeljani so analitični izrazi, ki omogočajo oceno natančnosti meritve. Če izraze obrnemo, lahko izračunamo potrebno frekvenčno stabilnost in največji dopusten enosmerni premik.

6. Literatura

/1/ L. M. Sanchez-Brea, T. Morlanes: *"Metrological errors in optical encoders"*, Measurement science & technology, ISSN 0957-0233, vol. 19, štev. 11, 2008.

/2/ J. Rozman, A. Pleteršek: "Optical encoder system with THD below -60dB! ", Informacije MIDEM, vol 39, štev. 1, 2009.

/3/ D. Shetty, R. A. Kolk: *"Mechatronics System Design,"* PWS Pub., Boston, 1997.

/4/ Hyung Suck Cho: *"Opto-Mechatronic Systems Handbook, Techniques and Applications,"* Boca Raton, CRC Press, cop. 2003.

/5/ K. Hane, T. Endo, Y. Ito, M. Sasaki: *"A compact optical encoder with micromachined photodetector,"* J. Opt. A: Pure Appl. Opt., 3, 191-195, 2001.

/6/ Hane, K., Endo, T., Ishimori, M., Ito, Y., and Sasaki, M.,: *"Integration of grating-image-type encoder using Si micromachining,"* Sensors Actuators *A*, 97-98, 139-146, 2002.

Tomaž Dogša, Matej Šalamon, Bojan Jarc, Mitja Solar
Fakulteta za elektrotehniko, računalništvo in informatiko,
Univerza v Mariboru, Smetanova 17, Maribor
Tel. (+386 (0)2 220 7231, E-mail: tdogsa@uni-mb.si

Prispelo (Arrived): 01.06.2009 *Sprejeto (Accepted): 09.09.2009*

UDK621.3:(53+54+621+66), ISSN0352-9045 Informacije MIDEM 39(2009)3, Ljubljana

DECISION SUPPORT SYSTEM TO SUPPORT THE SOLVING OF CLASSIFICATION PROBLEMS IN TELECOMMUNICATIONS

Rok Rupnik

University of Ljubljana, Faculty of Computer and Information Science, Ljubljana, Slovenija

Key words: data mining; decision support; decision support system; knowledge discovery; classification; telecommunications.

Abstract: Traditional techniques of data analysis do not enable the solution of all kind of problems and for that reason they have become insufficient. This caused a new interdisciplinary field of data mining to arise, encompassing both classical statistical, and modern machine learning techniques to support the data analysis and knowledge discovery from data. Data mining methods are powerful in dealing with large quantities of data, but on the other hand they are difficult to master by business users to facilitate decision support. In this paper we introduce our approach to integration of decision support system with data mining method called classification. We discuss the role of data mining to facilitate decision support, the use of classification method in decision support system, discuss applied approaches and introduce a data mining decision support system called DMDSS (Data Mining Decision Support System). We also present some obtained results and plans for future development.

Sistem za podporo odločanju za reševanje klasifikacijskih problemov na področju telekomunikacij

Kjučne besede: odkrivanje zakonitosti v podatkih; podpor odločanju; sistem za podporo odločanju; odkrivanje znanja; klasifikacija; telekomunikacije.

Izvleček: Tradicionalne tehnike za analizo podatkov ne omogočajo reševanja vseh vrst problemov. Nekatere vrzeli na tem področju zapolnjuje multidisciplinarno področje odkrivanja zakonitosti v podatkih, ki omogoča analizo podatkov na podlagi klasičnih statističnih tehnikah in tehnikah strojnega učenja. Metode odkrivanja zakonitosti v podatkih so učinkovite tudi na večjih količinah podatkov, vendar so praviloma prezahtevne, da bi jih poslovni uporabniki sami obvladovali za potrebe podpore odločanju. V okviru članka je predstavljen naš pristop uporabe metode klasifikacije za potrebe podpore odločanju. V uvodu je predstavljena vloga odkrivanja zakonitosti v podatkih za potrebe podpore odločanju s poudarkom na uporabi metode klasifikacije. V nadaljevanju pa je predstavljen DMDSS (Data Mining Decision Support System), sistem za podpor odločanju, ki temelji na uporabi metode klasifikacije. V zaključku so predstavljeni rezultati uporabe sistema DMDSS ter plani za njegov nadaljnji razvoj.

1. Introduction

Companies use several types of decision support systems to facilitate decision making. Traditionally, OLAP tools are used for an advanced data analysis and decision support in the business area. OLAP tools follow what is in essence a deductive approach (JSR-73 Expert Group, 2004). The drawback of this approach is that it depends on coincidence or even luck of choosing the right dimensions at drilling-down to acquire the most valuable information, trends and patterns. It lacks algorithmic approach and depends on the analysts' insight, coincidence or even luck for acquiring the most valuable information, trends and patterns from data. And finally, even for the best analyst there is a limitation to a number of attributes he can simultaneously consider in order to acquire accurate and valuable information, trends and patterns (Goebel and Gruenwald, 1999). It seems that with the increase in data volume, traditional data analysis has become insufficient, and new methods for data analysis are needed.

To satisfy this need, a new interdisciplinary field of data mining appeared. Data mining encompasses statistical, pattern recognition, and machine learning tools to support the discovery of patterns, trends and rules that lie within data given (Heinrichs and Lim, 2003). Performing analysis through data mining follows an inductive approach of analyzing data where machine learning algorithms are applied to extract non-obvious knowledge from data (JSR-73 Expert Group, 2004). Data mining reduces or even eliminates the above mentioned drawback. As opposed to classical data analysis techniques, data mining strategies often take a slightly different view, i.e. the nature of the data itself could dictate the problem definition and lead to discovery of previously unknown but interesting patterns. Data mining methods also extend the possibilities of discovering information, trends and patterns by using richer model representations (e.g. decision rules, decision trees, ...) than the usual statistical methods, and are therefore well-suited for making the results more comprehensible to the non-technically oriented business users. OLAP tools mostly enable the answers to the questions like: "What has been going on?" On the other hand, data mining enables the answers to different kind of questions, e.g.: "What are characteristics of our best customers?" Indeed, the use of data mining advances the whole field of data analysis including its role in the decision-making process to a higher level (Nemati and Barko, 2002).

Data mining can be used through two approaches. The first approach is called *data mining software tool approach*. In this approach data mining is used through ad hoc data mining projects by the use of data mining software tools (Goebel and Gruenwald, 1999; Kohavi and

Sahami, 2000; Holsheimer, 1999). Data mining software tools require a significant expertise in data mining methods, databases and statistics. They are rather complex, because they offer a variety of methods and parameters that the user must understand in order to use them effectively (Kohavi and Sahami, 2000). Data mining software tool approach has a disadvantage in a number of various experts needed to collaborate in a project, the complexity of software tools and in transferability of results and models (Srivastava et al., 2000; Hirji, 2001). The disadvantages mentioned call for different approach, which in this paper we call *data mining application system approach*. Data mining application systems approach signifies the possibility to develop decision support systems which use data mining methods and do not demand expertise in data mining for business users. It is an approach which focuses on business users and other decision makers, enabling them to view data mining models which are presented in a user-understandable manner through a user friendly and intuitive GUI using standard and graphical presentation techniques (Aggarwal, 2002). Through the use of data mining application systems approach, data mining becomes better integrated in business environments and their decision processes (Goebel and Gruenwald, 1999; Holsheimer, 1999; Kohavi and Sahami, 2000; Bayardo and Gehrke, 2001). We hope to demonstrate the latter by introducing the DMDSS (Data Mining Decision Support System), which we developed.

The paper is structured as follows. In the second section we are making a brief introduction of data mining and decision support systems. In the third section we are introducing the motivation for the use of data mining to facilitate decision support. We are presenting two approaches of the use of data mining and data mining standards. In the fourth section we are going to introduce DMDSS, decision support system based on data mining method called classification which we developed for telecommunication service provider. We are presenting the process model for the use of DMDSS and the platform of DMDSS. We are also introducing the functionalities of DMDSS for classification data mining method supported by DMDSS. In fifth section we are representing the results and the experiences of the use of DMDSS after five months of production. We are also representing the brief list of enhancements planed for new version of DMDSS. And finally, we are introducing summary and concluding remarks.

2. Decision support systems and data mining: a brief introduction

Decision support systems (DSS) are defined as interactive application systems which are intended to help decision makers utilize data and models in order to identify problems, solve problems and make decisions. They incorporate both data and models and they are designed to assist decision makers in decision making processes. They provide support for decision making, they do not replace it (Steblovnik et.al., 2005). The mission of decision support systems is to improve effectiveness, rather than the efficiency of decisions (Mladenić et al., 2003b). A decision support system can take many different forms and in general we can say that every decision support system is developed for a specific objective and bases on a particular decision process and set of methods, techniques and approaches. The DSS can be developed for the purpose of simulation (Chen, 2004; Kuan, 2004), analysis (Bohanec, 2001; Heinrichs and Lim, 2003; Ward, 2000), forecasting (Zhong et al., 2005; Patelis et al. 2005) and optimization (Heinrichs and Lim, 2003). The design of DSS is very dependant on decision-making process and decision problems which the DSS is going to support (Heinrichs and Lim, 2003). In the context of our paper especially important are repetitive decision problems, which must be supported daily in a non ad-hoc manner.

The objective of data mining is to discover relationships, patterns and knowledge hidden in data (Sherry and Xiaoui, 2005; Kukar, 2006). Data mining is the process of analyzing data in order to discover implicit, but potentially useful information and uncover previously unknown patterns and relationships hidden in data. Data mining is an interdisciplinary field which encompasses statistical, pattern recognition, and machine learning tools to support the analysis of data and discovery of principles that lie within the data. The data mining learning problems that we consider can be roughly categorized as either *supervised* or *unsupervised* (Witten and Frank, 2000). In supervised learning, the goal is to predict the value of an outcome based on a number of input measures. In unsupervised learning, there is no outcome measure, and the goal is to describe associations and patterns among a set of input measures.

3. Integrating data mining and decision support

Companies use several types of decision support systems to facilitate decision support. For the purposes of analysis and decision support in the business area traditionally OLAP based decision support systems are used. OLAP systems represent a tool enabling decision support on a tactical level. They enable drill-down concept, i.e. digging through a data warehouse from several viewpoints to acquire the information the decision maker is interested in (Bose and Sugumaran, 1999). OLAP systems support analysis processes and decision processes, where the analysts are supposed to look for information, trends and patterns. They do it by viewing OLAP forms swapping dimensions and drilling-down through them (Goebel and Gruenwald, 1999). Performing analysis through OLAP follows a deductive approach of analyzing data (JSR-73 Expert Group, 2004). The disadvantage of such an approach is that it depends on coincidence or even luck of choosing the right dimensions at drilling-down to acquire the most valuable information, trends and patterns. We could say that OLAP systems provide analytical tools enabling user-

led analysis of the data, where the user has to start the right query in order to get the appropriate answer (Mladenić et al., 2003a). Such an approach enables mostly the answers to the questions like: "What has been going on?" What about the answers to the questions like: "What are characteristics of our best customers?" Those answers can not be provided by OLAP systems, but can be provided by the use of data mining, which follows an inductive approach of analyzing data (JSR-73 Expert Group, 2004; Kukar, 2003).

When discussing the relation between data mining and OLAP it is not the question of which one of them is better or worse. Data mining enables the answers to different questions than OLAP, i.e. it enables the solution of different problems and to acquire different information. Decision processes in general, depending on problem, need both, OLAP and data mining, to get the appropriate level of support of decision processes (Forgionne and Rubenstein-Montano, 1999).

Several authors discuss the use of data mining to facilitate decision support and they all confirm the value of it. Chen and Liu (2004) argue that the use of data mining helps institutions make critical decisions faster and with a greater degree of confidence. They believe that the use of data mining lowers the uncertainty in decision process. Nemati and Barko (2002) state that the use of data mining offers companies an indispensable decision-enhancing process to exploit new opportunities by transforming data into valuable knowledge and a potential competitive advantage. Authors also introduce their survey which indicates that the use of data mining can improve the quality and accuracy of decisions. Lee and Park (2003) state that the knowledge gained from data sources by the use of data mining methods can be crucial for the decision making processes. Mladenic et al. claim that the integration of data mining and decision support can lead to the improved performance of decision support systems and can enable the tackling of new types of problems that have not been addressed before. They also argue that the integration of data mining and decision support can significantly improve current approaches and create new approaches to problem solving, by enabling the fusion of knowledge from experts and knowledge extracted from data (Mladenić et. al., 2003c). Chen and Liu (2005) state that data mining is a very useful technology which opens new opportunities for data analysis. Tseng and Lin (2007) have used data mining for efficient discovery of temporal movement patterns or objects in sensor networks.

3.1. Data mining software tool approach

Data mining can be used through two different approaches. The first approach is called *data mining software tool approach* where the use of data mining is typically initiated through ad hoc data mining projects (Goebel and Gruenwald, 1999; Kohavi and Sahami, 2000; Holsheimer, 1999; Radivojevic et. al., 2003). Ad hoc data mining projects are initiated by a particular objective on a chosen area which represents a basis for the defining of the domain. They are performed using data mining software tools which require a significant expertise in data mining methods, databases and/or statistics (Kohavi and Sahami, 2000). They usually operate separately from the data source, requiring a significant amount of additional time spent with data export from various sources, data import, pre-processing, post-processing and data transformation (Holsheimer, 1999; Goebel and Gruenwald, 1999). The result of a project is usually a report explaining the models acquired during the project using various data mining methods. Data mining software tool approach has a disadvantage in a number of various experts needed to collaborate in a project and in transferability of results and models (Srivastava et al., 2000; Hirji, 2001). The latter indicates that results and models acquired by the project can be used for reporting, but cannot be directly utilized in other application systems. Data mining software tool approach represents the first generation of data mining (Holsheimer, 1999).

3.2. Data mining application system approach

The data mining software tool approach has revealed some disadvantages. The most important of them is the fact that due to the complexity of data mining software tools, they can not be directly used by business users. Data mining models are produced for business users. For that reason we need applications which will enable them to view and exploit data mining models effectively to facilitate decision support (Kohavi and Sahami, 2000; Goebel and Gruenwald, 1999). This implies to the new approach of the use of data mining which we call *data mining application system approach*. It is an approach which focuses on business users and other decision makers, enabling them to view and exploit data mining models. Models are presented in a user-understandable manner through a user friendly and intuitive GUI using standard and graphical presentation techniques (Aggarwal, 2002). Decision makers can focus on specific business problems covered by areas of analysis with the possibility of repeated analysis in periodic time intervals or at particular milestones. Through the use of data mining application systems approach, data mining becomes better integrated in business environments and their decision processes (Goebel and Gruenwald, 1999; Holsheimer, 1999; Kohavi and Sahami, 2000; Bayardo and Gehrke, 2001).

Data mining standards undoubtedly represent an important issue for data mining application systems approach (Holsheimer, 1999). Employing common standards simplifies the development of data mining application systems and business application systems utilizing data mining models. A considerable effort in the area of data mining standards has already been done within the data mining community. Established and emerging data mining standards address several aspects of data mining where application interface (API) is probably one of the most important of them (Grossman, 2003). The standardized data

mining API represents the key issue for data mining application systems approach. Its main advantage in the possibility to leverage data mining functionality using standard API shared by all application systems within information system. JDM (Java Data Mining) is a Java based API specification which has reached final release status in 2004 (JSR-73 Expert Group, 2004). Another important standard for the area of data mining is PMML. PMML is an XML-based standard and language which in theory provides a way for applications to define statistical and data mining models and to share models between PMML compliant applications (Grossman, 2003). In practice, this is limited to sharing the models between different systems that use the same platform (e.g., ODM). All models in DMDSS are stored in the PMML format.

4. Data mining based decision support system to facilitate classification problems

We have developed a data mining based decision support system for a telecommunication service provider. In the following part of the paper it will be called simply a company. We first did a survey about CRM implementation. One of the aims of the survey was to explore and demonstrate various approaches and methods for the area of analytical CRM. The important statement of the survey was that company intolerably needs data mining for performing analysis in the area of analytical CRM. It was stated that the application system approach is more suitable for the introduction of data mining. The main reason for choosing the application system approach was the fact that the area of analytical CRM in the company represents a rather dynamic environment with continual need for repeated analyses. Right after the survey, the development project for decision support system was initiated. The decision support system is called DMDSS and will be introduced in the following part of the paper.

4.1. Related Work

Some decision support systems that use data mining have already been developed and introduced in the literature. Lee and Park (2003) presented *Customized Sampling Decision Support System* (CSDSS) which uses data mining. CSDSS is a web-based system that enables the user to select a process sampling method that is most suitable according to his needs at purchasing semiconductor products. The system enables the autonomous generation of available customized sampling methods and provides the performance information for those methods. CSDSS uses clustering data mining method within the generation of sampling methods. The system is not designed to support other domains; it only supports the domain mentioned.

Bose and Sugumaran (1999) introduced *Intelligent Data Miner* (IDM) decision support system. IDM is a Web-based application system intended to provide organization-wide decision support capability for business users. Besides data mining it also supports some other function categories to enable decision support: data inquiry and multidimensional analysis through enabling OLAP views on multidimensional data. In the data mining part of IDM it supports the creation of models, manipulation of models and presentation of models in various presentation techniques of, among others, the following data mining methods: association rules, clustering and classifiers (classification). The system also performs data cleansing and data preparation and provides necessary parameters for data mining algorithms. Interesting characteristic of IDM is that it makes a connection to external data mining software tool which performs data mining model creation. The system enables predefined and ad-hoc data mining model creation. The authors state that the disadvantage of IDM is the fact that non-technical users (business users) need to have a fair amount of understanding of data mining and that the use of data mining and the creation of data mining models still needs to be clearly directed by the user, especially with ad-hoc model creation.

Polese et. al. (2002) introduced decision support system based on data mining. The system was designed to support tactical decisions of a basketball coach during a basketball match through suggesting tactical solutions based on the data of the past games. The decision support system only supports association rules data mining method and uses association rule algorithm called *Apriori* algorithm combined with *Decision query* algorithm. The decision support system enables the coach to submit data about his tactical strategies and data about the game and the rival team. After that the system provides the coach with opinion about the chosen strategies and with suggestions. The system is not designed to support other domains; it only supports the basketball domain.

Heindrichs and Lim (2003) have done research on the impact of the use of web-based data mining tools and business models on strategic performance capabilities. His paper reveals web-based data mining tools to be a synonym for data mining application system. The author states that the main disadvantage of data mining software tool approach is the fact that it provides results on a request basis on static and potentially outdated data. He emphasizes the importance of the data mining application system approach, because it provides ease-of-use and results on real-time data. The author also discusses the importance of data mining application systems through arguing that sustaining a competitive advantage in the companies demands a combination of the following three prerequisites: skilled and capable people, organizational culture focused on learning, and the use of leading-edge information technology tools for effective knowledge management. Data mining application systems with no doubt contribute to the latter. In the paper the author also introduces the empirical test which proves positive effect on dependent variable "Strategic performance capabilities" by independent variables "Web-based data mining tools" and "Business models".

Sasa et.al. (2008) presented interesting results in the area of improving and automating decision making through ontologies. Their research did not base on data mining, but the results are important in context of improving and facilitating decision making by business users.

4.2. The Process Model TO SUPPORT decision Making

To determine the process model for DMDSS was one of the key issues within the design of DMDSS. We needed the model which would be appropriate to enable decision support for the purposes of analytical CRM in the company. The process model shows how decision processes are supported by the decision support system. The design of process model was based on CRISP-DM (CRoss-Industry Standard Process for Data Mining) process model. CRISP-DM is a data mining process model which was developed by the industry leaders and the collaboration of experienced data mining users and data mining software tool providers (Shearer, 2000; Clifton and Thuraisingham, 2001; Grossman, 2003). There are some other data mining process models found in the literature. They use slightly different terminology, but they are semantically equivalent to CRISP-DM (Goebel and Gruenwald, 1999; Li et al., 2002). The analysis of data mining process models confirmed CRISP-DM as the most appropriate process model for DMDSS. CRISP-DM process model breaks down the data mining activities into the following six phases which all include a variety of tasks (Shearer, 2000; Clifton and Thuraisingham, 2001): business understanding, data understanding, data preparation, modelling, evaluation and deployment.

CRISP-DM process model was adapted to the needs of DMDSS as a two stage model: the *preparation stage* and the *production stage* (Figure 1). The division into two stages is based on the following two demands, which are the consequence of data mining application system approach used. First, DMDSS should enable repeated creation of data mining models based on up-to-date data set for every area of analysis. Second, business users should only use it within the deployment phase with only basic level of understanding of data mining concepts.

The preparation stage represents the process model for the use of DMDSS for the purposes of preparation of the area of analysis for the production use. During the preparation stage the CRISP-DM phases are performed in multiple iterations with the emphasize on the first five phases: from business understanding to evaluation. The aim of executing multiple iterations of all CRISP-DM phases for every area of analysis is to achieve step-by-step improvements in all of the phases. In the business understanding phase the slight redefinitions of the objectives can be made, if necessary, according to the results of other phases, especially the results of evaluation phase. In the data preparation phase the improvements in the procedures which execute the recreation of data set can be achieved. Data set must be recreated automatically every night based on

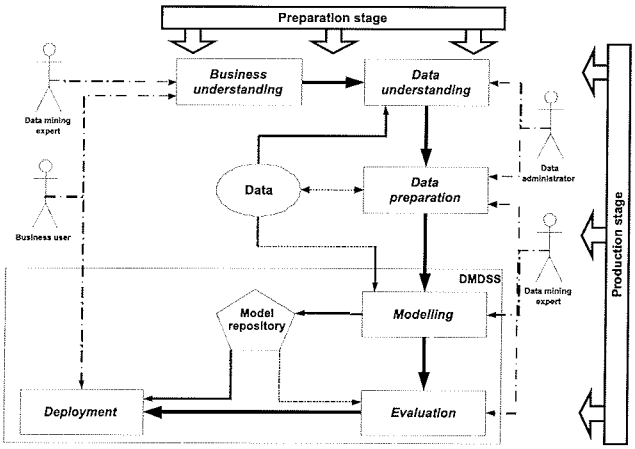

Fig. 1: The process model of DMDSS

the current state of data warehouse and transactional databases. The problems detected in the data preparation phase can also demand changes in the data understanding phase. In the data preparation phase the attribute names of data sources are transformed to aliases which are user-friendly and enable the user to easily understand the meaning of the attribute. In cases when the attribute has the limited set of discrete codes, the codes are decoded to values which are more appropriate to the user than the codes.

In the modelling phase and evaluation phase the model is created and evaluated for several times with the aim to do the fine-tuning of data mining algorithms through finding the proper values of the parameters for the algorithms. It is essential to do enough iterations in order to monitor the level of changes in data sets and data mining models acquired. Through multiple iterations the stability of data preparation phase is reached and optimal values of parameter values for data mining algorithms are identified. According to the results gained in the evaluation phase through multiple iterations, the preparation stage can either reject the area of analysis due to the insufficient quality of models; either approves it with or without minor redefinitions of objectives in the business understanding phase and consequently the changes in other phases. The mission of the preparation stage is to confirm the fulfilling of the objectives of area of analysis for decision support and to assure the stability of data preparation.

The production stage represents the production use of DMDSS for an area of analysis. In the production stage the emphasis is on the phases of modelling, evaluation and deployment, what does not mean that other phases are not encompassed in the production stage. Data preparation, for example, is executed automatically based on procedures developed in the preparation stage. The modelling and evaluation are performed by data mining expert, while the deployment phase is performed by business users. Figure 1 introduces the schema of the process model of DMDSS showing a preparation stage and production stage in a joint view. The schema reflects the phases of

both stages of the process model. Beside that schema also shows the roles of data administrator, data mining expert and business user and the phases where they take part in: either actively as the executor of the phase, either only collaborating. The schema also reveals that DMDSS only supports the phases of modelling, evaluation and deployment. The functionalities of DMDSS will be introduced later on in this section.

4.3. The Platform

DMDSS uses Oracle database and was developed on J2EE platform through several iterations (Bajec et.al., 2007). The selection of Oracle was the consequence of the fact that Oracle introduced ODM (Oracle Data Mining) option. ODM has two important components. The first component is a data mining engine (DME), which provides the infrastructure that offers a set of data mining services. The second component is Java-based data mining application interface (ODM API), which enables access to services provided by DME (JSR-73 Expert Group, 2004). Another factor that influenced the platform selection was the fact that practically all of the data needed for initial set of areas of analysis was available in Oracle databases in the company. Before finally accepting Oracle and ODM, an evaluation sub-project was initiated. The aim of the project was to evaluate ODM, i.e. to verify the quality of its algorithms and results. It was the first version of ODM and evaluation was simply necessary to reduce the risk of using an immature product. The evaluation gave positive results.

4.4. The functionalities of dmdss to support the solving of classification problems

The design of functional demands for DMDSS and the design of data mining process model were done simultaneously. Both activities are very interrelated, because the process model implies the functionality of a decision support system to a great extent. The functionalities of DMDSS will be introduced based on the production stage of the process model proposed and the functionalities offered by forms to a user. DMDSS supports two roles: *data mining expert* and *business user*. Each of the roles has the access to the forms and their functionalities according to the production stage of the process model (Figure 1).

DMDSS enables the data mining expert to create classification models by using model creation form (Figure 2). When creating the model he inputs a unique model name and a purpose of model creation. Beside that there are four algorithm parameters to be set before the model creation. The user can choose the value for each parameter from the set of discrete values which was defined as appropriate in the preparation stage of process model for a particular area of analysis. At the bottom of the form there are recommended values for parameters to acquire a model with fewer or more rules: recommended settings for fewer rules in a model, and settings for more rules in a model.

The examples of forms in the figures shown in the following part of the section are for the area of analysis called "Customers classification". Model testing is performed automatically as the last step of the model creation.

Within the evaluation phase data mining expert can view and evaluate the model using data mining expert model viewing form. This form is very similar to the form for model viewing which is used by business user in the deployment phase and will be introduced later on. While evaluating, the data mining expert can input comments for the model. The role of comments is to help the business users to understand and interpret the models better. In case of classification model evaluating signifies the evaluation of the quality of the model. Model evaluation is performed based on results of the model testing step within the model creation.

As the final step of evaluation phase data mining expert can change the published status of a model to a value *true* if the relative model quality reaches a certain level, and if the model is different from the previously created model of particular area of analysis. It is the duty of data mining expert to evaluate the practical quality of the model, both qualitative and quantitative, and the level of difference of newly created model in relation to previously created model and decide about it. Business users have access only the models with published status set to *true*.

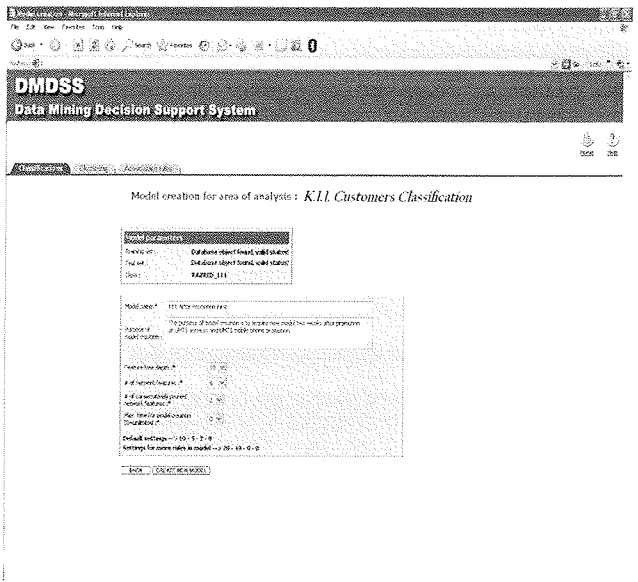

Fig. 2: A model creation form for data mining expert

Within the deployment phase business users have access to the form for model viewing for a business user (Figure 3). There are two visualization techniques available to support model viewing. The first technique is a table where classification rules are presented in IF-THEN form. The second technique is decision trees, where classification rules are converted into decision trees showing equivalent information as classification rules. The decision trees

technique is a graphical technique, which enables visual presentation of rules and for that reason it is very appropriate for business users. It is appropriate for business users because it enables them obtain information in an easier way and it can be especially useful in case when model has a lot of rules (over 10, for example). The form shows general information about the model: model name, date of model creation, number of rules, number of comments and number of classification classes. The form enables the filtering of classification rules according to the class. The user can choose either to view the rules for all classes, either only the rules for a chosen class. The form also shows the last comment of a model written by the data mining expert and enables the user to view all other comments through the opening of the form for comments.

In order to present the information about the quality of the model the form also presents testing parameters relative model quality and classification accuracy. For a business user the parameter relative model quality is presented in qualitative form. It is more appropriate than the quantitative form, because this way business user doesn't have to remember exact values. For example: *middle* is when the value is greater than 0 and smaller than 0.5, that is, the relative improvement of model quality is between 0% and 50% with respect to the prediction of the most frequent class (*mode*).

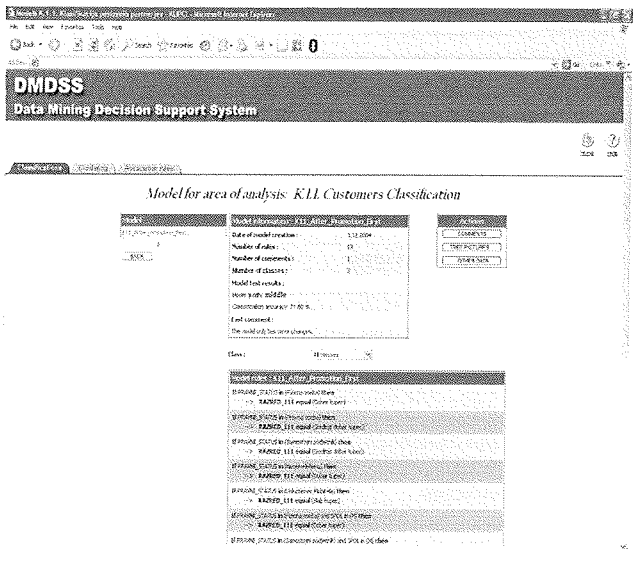

Fig. 3: A model viewing form for business users

The example of the area of analysis which uses classification method in DMDSS is called *Customers classification*. For the purpose of area of analysis customers are ranked into three categories, i.e. classes: a good customer, a normal customer and a bad customer. The aim of the area of analysis is to acquire the model for each customer category. The model acquired enables business users to monitor characteristics of a particular customer category and plan better customer category focused marketing campaigns for acquiring new customers. DMDSS supports additional areas of analysis for the purposes of mobile phone sales analysis, other areas of customer analysis and vendor analysis.

4.5. Example of the Scenario of Use

The area of analysis called *Loyalty model* enables the company to acquire the classification model for customers which are possible defectors, i.e. customers who potentially could switch to another telecommunication service provider. This area of analysis is very important for the company due to intense campaigns for acquiring new customers launched by the competition. Data mining expert creates the new model every day in order to detect changes as soon as possible. If the new model is different comparing to previous one, the data mining expert changes the published status to the value *true*. Analyst in marketing department first checks the new model to evaluate changes. After that the model is applied on the whole set of existing customers. Every customer who is according to the model acquired a possible defector and who hasn't been sent a special offer (a new mobile phone for a very low price) in the last 30 days, gets a special offer to increase the loyalty of the customer and to lower the possibility for him to switch to another company. The results of this area of analysis will be introduced later on in the paper.

4.6. Semantic contribution OF the use of dmdss

While designing and developing DMDSS and monitoring its use by the business users we have been considering and exploring the semantic contribution of the use of a data mining application system like DMDSS in a decision process and performing any kind of business analysis. For that reason one of our goals of the project was also to illustrate the semantic contribution of the use of DMDSS in decision processes. We decided to use the concept of data-model for that purpose.

A data-model is a concept which can be, among other things, used for describing a particular domain on a conceptual level (Bajec and Krisper, 2004). A meta-model shows domain concepts and relations between them. In this case the meta-model describes a decision process on the conceptual level with emphasis on demonstrating the contribution and the role of the use of DMDSS as data mining application system (Figure 4). UML class diagrams were used as technique for the meta-model. Decision support concepts are represented as classes and relations between them are represented as associations and aggregations. Concepts and relations, which in our opinion represent a contribution of the use of DMDSS in the decision process, are represented in a dotted line style.

The meta-model shows various concepts that influence the decision process and represent a basis for a decision. Information technology engineers often believe that decisions mostly depend on data from OLAP systems and other in-

formation acquired from information systems. It is true that they represent a very important basis for the decision, although in more than a few cases decisions mostly depend on factors like intuition and experience (Furlan and Bajec, 2008).

Knowledge is in our opinion probably the most important basis for the decision, because it enables the correct interpretation of data, i.e. acquiring of information. The contribution of the use of DMDSS and models and rules it creates is in contribution to the accumulation of the knowledge acquired by models and their rules. A detailed description of decision process and creation of a detailed meta-model is beyond the scope of the paper.

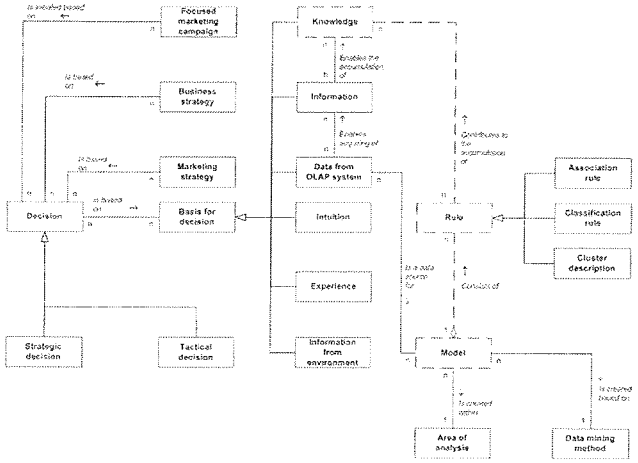

Fig. 4: A meta-model presenting the semantic contribution of the use of DMDSS

5. The experience of use

DMDSS has now been in production use in the company for five months. Before the start of production first the tutorial for data mining for business users was organised. The aim of tutorial was to educate business users with the basic concepts of data mining with the emphasis on teach then how to interpret data mining models correctly. After the tutorial the training was organised where business users learned how to use and truly exploit DMDSS to facilitate decision support through the use of data mining. For one employee from the company, who was planed to take over the role of data mining expert, there was no special training organised. He was a member of the development team and he all time actively collaborated in the preparation stage for every area of analysis.

Business users use DMDSS at their daily work. They use patterns and rules identified in models as the new knowledge, which they use for analysis and decision process at their work. It is becoming apparent that they are getting used to DMDSS. According to their words they have already become aware of the advantages of continual use of data mining for analysis purposes to facilitate decision support. The most important achievement after five months of use is the fact that business users have really started to understand the potentials of data mining. Suddenly they have got many new ideas for new areas of analysis, because they have started to realize how to define areas of analysis to acquire valuable results. The list of new areas of analysis is regularly updated, and after the first year of production it will be discussed and evaluated. Selected areas of analysis will then be implemented and introduced to DMDSS according to the process model introduced in the paper, which also determines the methodology of introducing new areas of analysis to DMDSS.

The use of DMDSS to facilitate decision support has already shown some measurable and non-measurable results:

- Based on the before mentioned area of analysis called *Loyalty model* the company's managers have defined a strategy for continual focused campaigns to increase the loyalty of possible defectors. The first three-month campaign has already been launched and two months after the campaign there were 9% less defectors according to two months before the campaign. Business results from previous years do not show any significant seasonal changes between the two compared time frames. The achievement was gained despite of intensive campaigns launched by the competition.
- The area of analysis called *Customer classification* enables the possibility to acquire the classification model for good, normal and bad customers. The company's managers are defining a strategy for treating new customers based on that model, because it enables the forecasting of customer category for a new customer. Especially important for the company are of course customers who are potentially good. Beside that they are defining a strategy for continual focused marketing campaigns for acquiring good customers.
- The area of analysis called *Customers and mobile phone categories* enables the company to acquire the classification model for customers and three mobile phones categories they are purchasing: high-price, mid-price and low-price mobile phones. For each mobile phone category the model describes the properties of the customers who purchased mobile phones of that category. The company's managers are defining a strategy for continual focused campaigns based on the model to increase the sales of mobile phones. The start of implementation of the strategy is planned in two or three months.

It is important to stress that the strategies mentioned are being defined based on the fact that DMDSS enables the daily creation of models and consequently repeated campaigns with the frequency which is determined by decision maker. It in general mainly depends on the policy covering the area of analysis and also on the frequency of changes in data mining models within the area of analysis.

5.1. The plan for future development

There are some new functionalities planned besides introducing new areas of analysis. The experience of the use of DMDSS has revealed that business users need the possibility to make their own archive of classification rules. They also need to have an option to make their own comments to archived rules in order to record the ideas gained by viewing and analysing the rules. We also plan to enhance DMDSS with other data mining methods.

6. Summary and conclusion

DMDSS is decision support system which supports decision processes through classification method. It is a passive DSS, because it supports decision processes through new knowledge acquired without producing explicit decision suggestions or solutions. The mission of DMDSS is to offer an easy-to-use tool which enables business users to exploit classification data mining models with only a basic level of understanding of the classification concepts, which enables them to interpret the models correctly. The process model of DMDSS defines the roles of business user and data mining expert, where phases that demand expertise in data mining are performed by data mining expert and are hidden from business user. Business users only exploit data mining models, which are created by data mining expert. The experience shows that through such a process model we have achieved a rather high level of integration of data mining into daily decision processes through DMDSS. DMDSS was developed for a telecommunications service provider, but its process model and architecture enable its use in any business environment.

Comparing DMDSS to decision support systems introduced in the related work section, we would like to put out the following remarks. First, DMDSS uses data mining services of data mining engine in Oracle database. It does not use external data mining software like IDM, it also does not contain self programmed data mining algorithms like CSDSS (Lee and Park, 2003) and system introduced by Polese et al. (2002). The solution and platform used by DMDSS enables the deployment of data mining models to other J2EE based application systems, what we plan to utilize in the future for the purposes of prediction. The dilemma between data mining software tools and database built-in data mining engines is justified, because data mining software tools have reached a very high level of maturity. But, on the other hand we intensively follow the development of the platform of choice, Oracle Data Mining and accompanying tools, which have already gained a certain level of maturity.

Second, DMDSS only enables predefined areas of analysis like system introduced by Polese et al. (2002) and CSDSS (Lee and Park, 2003) do, whereas IDM enables also ad-hoc data mining analysis. The architecture and the design of DMDSS enable to include any area of analysis as long as data set is available in Oracle database. We believe that in order decision support system to be more appropriate for business users, it should not enable ad-hoc data mining model creation. The process of creation of ad-hoc models should be controlled rigorously in this case and this demands a rather high level of knowledge of data mining. We see that the problem of predefined and ad-hoc areas of analysis is interrelated to the problem the knowledge of data mining and the division of user's roles. We hold the opinion that the users of data mining based decision support system should be divided into two groups: data mining experts who create and evaluate models and business users who exploit models to support decision processes. We believe that with the concepts of predefined areas of analysis and the use of two user roles mentioned, we managed to make DMDSS a useful tool. It is accepted by business users as a tool which enables decision support through data mining models with only a basic level of knowledge of data mining, which is needed to interpret the models.

Although DMDSS is a rather new application system, there exists a plan for further development of DMDSS. On one hand, there is a list of new areas of analysis being built up by business users, on the other hand there are also enhancements planned in the area of functionalities of DMDSS. We intend to provide our users with more data mining methods when they become available. We believe that both satisfying the user requirements as well as providing them with a choice of new data mining methods will contribute to better results of the use of DMDSS to facilitate decision support.

7. References

Aggarwal, C.C. (2002) 'Towards-Effective and Interpretable Data Mining by Visual Interaction', *SIGKDD Explorations*, Vol. 3, No. 2, pp. 11-22.

Agrawal, R. and Srikant, R. (1994) 'Fast Algorithms for Mining Association Rules in Large Databases', *Proceedings of the 20th International Conference on Very Large Data Bases VLDB'94*, pp. 487-499.

Bajec, M., Vavpotic, D. and Krisper, M. (2007) 'Practice-Driven Approach for Creating Project Specific Software Development Methods', *Information and Software Technology,* Vol. 49, No. 4, pp. 345-365.

Bajec, M. and Krisper, M. (2004) 'A Methodology and Tool Support for Managing Business Rules in Organizations', *Information Systems,* Vol. 30, No. 6, pp. 423-443.

Bayardo, R. and Gehrke, J.E. (2001) 'Report on the Workshop on Research Issues in Data Mining and Knowledge Discovery Workshop (DMKD 2001)', *SIGKDD Explorations,* Vol. 3, No. 1, pp. 43-44.

Bohanec, M. (2001) 'What is Decision Support?', *Proceedings Information Society IS-2001: Data Mining and Decision Support in Action!*, pp. 86-89.

Bose, R. and Sugumaran, V. (1999) 'Application of Intelligent Agent Technology for Managerial Data Analysis and Mining', *The DATABASE for Advances in Information Systems*, Vol. 30, No. 1, pp. 77-94.

Chen, K.C. (2004) 'Decision Support System for Tourism Development: System Dynamic Approach' *Journal of Computer Information Systems*, Vol. 45, No. 1, pp. 104-112.

Chen, S.Y. and Liu, X. (2004) 'The Contribution of Data Mining to Information Science', *Journal of Information Science*, Vol. 30, No. 6, pp. 550-558.

Chen, S.Y. and Liu, X. (2005) 'Data Mining From 1994 to 2004: an Application Oriented Review', *International Journal of Business Intelligence and Data Mining*, Vol. 1, No. 1, pp. 4-21.

Clifton, C. and Thuraisingham. M. (2001) 'Emerging Standards for Data Mining', *Computer Standards & Interfaces*, Vol. 23, No. 3, pp. 187-193.

Forgionne, G.A. and Rudenstein-Montano, B. (1999) 'Post Data Mining Analysis for Decision Support Through Econometrics', *Information, Knowledge, Systems Management*, Vol. 1, No. 2, pp. 145-157.

Furlan, S. and Bajec, M. (2008) 'Holistic Approach to Fraud Management in Health Insurance', *Journal Of Information and Organizational Sciences*, Vol. 32, No. 2, pp. 99-114.

Goebel, M. and Gruenwald, L. (1999) 'A Survey of Data Mining Knowledge Discovery Software Tools', *SIGKDD Explorations*, Vol. 1, No. 1, pp. 20-33.

Grossman, R. (2003) 'KDD-2003 Workshop on Data Mining Standards, Services and Platforms (DM-SSP 03)', *SIGKDD Explorations*, Vol. 5, No. 2, pp. 197.

Heinrichs, J.H. and Lim, J.S. (2003) 'Integrating Web-based Data Mining Tools with Business Models for Knowledge Management', *Decision Support Systems*, Vol. 35, No. 1, pp. 103-112.

Hirji, K.K. (2001) 'Exploring Data Mining Implementation', *Communications of ACM*, Vol. 44, No. 7, pp. 87-93.

Holsheimer, M. (1999) 'Data Mining by Business Users: Integrating Data Mining in Business Process', *Proceedings of International Conference on Knowledge Discovery and Data Mining KDD-99*, pp. 266-291.

JSR-73 Expert Group (2004) 'Java™ Specification Request 73: Java™ Data Mining (JDM)', Java Community Process.

Kohavi, R. and Sahami, M. (2000) 'KDD-99 Panel Report: Data Mining into Vertical Solutions', *SIGKDD Explorations*, Vol. 1, No. 2, pp. 55-58.

Kuan, C.C. (2004) 'Decision Support System for Tourism Development: System Dynamics Approach', *Journal of Computer Information Systems*, Vol. 45, No. 1, pp. 104-112.

Lee, H.L. and Park, C. (2003) 'Agent and Data Mining Based Decision Support System and its Adaptation to a New Customer Centric Electronic Commerce', *Expert Systems with Applications*, Vol. 25, No. 4, pp. 619-635.

Li, T., Li, Q., Zhu., S. and Ogihara, M. (2002) 'A Survey on Wavelet Applications in Data Mining', *SIGKDD Explorations*, Vol. 4, No. 2, pp. 49-68.

Kukar, M. (2003) 'Transductive reliability estimation for medical diagnosis', *Artificial Intelligence in Medicine,* Vol. 29, pp. 81-106.

Kukar, M. (2006) 'Quality assessment of individual classifications in machine learning and data mining', *Knowledge and Information Systems,* Vol. 9, No. 3, pp. 364-384.

Mladenić, D., Lavrač, N., Bohanec, M. and Moyle, S. (2003) *'Data Mining and Decision Support: Integration and collaboration (Chapter 1: Data Mining: Authors; Lavrac, N. and Grobelnik, M.)'*, Kluwer Academic Publishers, Dordrecht, The Nederlands.

Mladenić, D., Lavrač, N., Bohanec, M. and Moyle, S. (2003) *'Data Mining and Decision Support: Integration and collaboration (Chapter 3: Decision Support, Author: Bohanec, M.)'*, Kluwer Academic Publishers, Dordrecht, The Nederlands.

Mladenić, D., Lavrač, N., Bohanec, M. and Moyle, S. (2003) *'Data Mining and Decision Support: Integration and collaboration (Chapter 4: Integration of Data Mining and Decision Support, Authors: Lavrac, N. and Bohanec, M.)'*, Kluwer Academic Publishers, Dordrecht, The Nederlands.

Nemati, H. and Barko, C.D. (2002) 'Enhancing Enterprise Decisions Through Organizational Data Mining', *Journal of Computer Information Systems*, Vol. 42, No. 4, pp. 21-28.

Patelis, A., Metaxiotis, K., Nikolopoulos, K. and Assimakopoulos, V. (2003) 'ForTV: Decision Support System for Forecasting Television Viewership', *Journal of Computer Information Systems,* Vol. 46, No. 1, pp. 25-34.

Polese, G., Troiano, M. and Tortora, G. (2002) 'A data Mining Based System Supporting Tactical Decisions', *Proceedings of the 14th international conference on Software engineering and knowledge engineering*, pp. 681-684.

Radivojevic, Z., Cvetanovic, M., Milutinovic, V. and Sievert, J. (2003) 'Data Mining: A Brief Overview and Recent IPSI Research', *Annals of Mathematics, Computing & Teleinformatics,* Vol. 1, No. 1, pp. 84-90.

Sasa, A., Juric, M.B. and Krisper, M. (2008) 'Service-Oriented Framework for Human Task Support and Automation', *IEEE Transactions on Industrial Informatics*, Vol. 4, No. 4, pp. 292-302.

Shearer, C. (2000) 'The CRISP-DM Model: The New Blueprint for Data Mining', *Journal of Data Warehousing*, Vol. 5, No. 4, pp. 13-22.

Srivastava, J., Cooley, R., Deshpande, M., and Tan, P.N. (2000) 'Web Usage Mining: Discovery and Applications of Usage Patterns from Web Data', *SIGKDD Explorations*, Vol. 1, No. 2, pp. 12-23.

Steblovnik, K., Tasič, J., and Zazula D. (2005) 'Intelligent Home Assistant', *Informacije MIDEM*, Vol. 35, No. 4, pp. 240-252.

Tseng, V.S. and Lin, K.W. (2007) 'Energy Efficient Strategies for Object Tracking in Sensor Networks: A Data Mining Approach', *Journal of Systems and Software*, Vol. 80, No. 10, pp. 1678-1698.

Ward, S.G. (2000) 'Decision Support for What-If Analysis and the Confirmation Bias', *Journal of Computer Information Systems*, Vol. 40, No. 4, pp. 84-92.

Witten, I.H. and Frank, E. (2000) *Data Mining*, Morgan-Kaufmann, New York.

Zhong, M., Klein, G., Pick, R.A. and Jiang, J.J. (2005) 'Vector Error-Correction Models in a Consumer Packaged Goods Category Forecasting Decision Support System', *Journal of Computer Information Systems*, Vol. 46, No. 1, pp. 25-34

dr. Rok Rupnik
University of Ljubljana, Faculty of Computer and Information Science
Tržaška 25, 1000 Ljubljana, Slovenija
Email: rok.rupnik@fri.uni-lj.si
Fax: +386-1-300-7879
Tel: +386-1-4768-814

Prispelo (Arrived): 18.03.2009 *Sprejeto (Accepted): 09.09.2009*

COMPUTATION OF ELECTRIC CHARGE ON POWER TRANSMISSION LINES

Aleš Berkopec

Fakulteta za elektrotehniko, Ljubljana, Slovenia

Key words: quasi-static charge computations, power transmission lines

Abstract: A system of parallel lines above a conducting or insulating plane serves as a model of a transmission line system. We present a few computational steps and results that address the question of the synchronicity of electric potential and charge on a given wire of the power line system. The differences in phase angles of the oscillating charge and the associated potential depend on the geometry of the system. For a benchmark and three additional cases the charges on the wires were computed using the described procedure. They are presented in the results section.

Izračun električnega naboja na močnostnih prenosnih linijah

Kjučne besede: kvazistatični izračuni električnega naboja, daljnovodni sistemi

Izvleček: Dvodimenzionalni sistem vzporednih vrvi končnih polmerov, ki se razpenjajo nad prevodno ali včasih neprevodno ravnino, služi kot osnovni model pri obravnavi sistemov daljnovodnih napetostnih vodov.

V članku pokažemo, da naboj danega vodnika in njegov potencial v splošnem ne nihata sofazno. Razlika med faznima kotoma potenciala in njemu pripadajočega naboja je odvisna od geometrije sistema. Predlagamo ustrezno pot do iskanih nabojev. Le-ti so osnova za izračun ostalih električnih količin, predvsem električne poljske jakosti v okolici sistema, in prikažemo nekaj rezultatov za izbrane postavitve daljnovodnih vrvi.

1 Introduction

The most basic among the models of power transmission line systems is two-dimensional. It consists of conducting parallel straight lines with known phase angles and r.m.s. values of electric potentials. The diameters of the lines are small compared to the distances between wires. The task is to determine linear charge densities on the lines from the given electric potentials of the lines.

There are more realistic models of power transmission lines, for instance, the diameter of the conductors may not be small compared to the distances between the lines, or the gravity and string forces may be included, which distort the straight lines into the chain curves. Further more, some computer programs consider the electrical properties and geometry of the pylons and even terrain.

For all the cases mentioned the computational algorithm is basically the same, although the matrix coefficients may be a way more difficult to compute and the size of the matrix tends to grow considerably /1/.

2 Methods

The notation used in this article for a-priori known quantities is:

r_i: position of the i-th wire, (x_i, y_i),

V_i: electrical potential of the i-th wire,

ϑ_i: phase angle of the electrical potential V_i, and for a-priori unknowns:

q_k: linear charge density of the k-th wire,

φ_k: phase angle of the linear charge density q_k.

The potential of the i-th wire has a form $V_i \cdot \cos(\omega t+\vartheta_i)$, where $\omega = 2\pi\nu$ and ν is the frequency.

The frequency ν = 50 Hz justifies a quasi-static approach for power transmission lines, so at any given time the potential of i-th wire may be written as a superposition of the charge on all wires /5/:

$$V_i \cdot \cos(\omega t+\vartheta_i) = \frac{q_i \cdot \cos(\omega t+\varphi_i)}{2\pi\varepsilon_0} \ln\frac{1}{r_{i0}} + \sum_{k\neq i} \frac{q_k \cdot \cos(\omega t+\varphi_k)}{2\pi\varepsilon_0} \ln\frac{1}{|r_i - r_k|}. \quad (1)$$

The introduction of parameter P_{ik} defined as

$$P_{ik} = \begin{cases} \frac{1}{2\pi\varepsilon_0} \ln\frac{1}{r_{i0}} & ; \ i = k \\ \frac{1}{2\pi\varepsilon_0} \ln\frac{1}{|r_i - r_k|} & ; \ i \neq k \end{cases}$$

gives a shorter form of equation (1):

$$V_i \cdot \cos(\omega t+\vartheta_i) = \sum_k P_{ik} \cdot q_k \cdot \cos(\omega t+\varphi_k). \quad (2)$$

The identity $\cos(\alpha + \beta) = \cos\alpha\cos\beta - \sin\alpha\sin\beta$ and equation (2) lead to two separate parts of the system of equations, the first oscillating as $\cos(\omega t)$,the second as $\sin(\omega t)$:

$$V_i \cdot \cos\vartheta_i = \sum_k P_{ik} \cdot q_k \cdot \cos\varphi_k \quad (3)$$

$$V_i \cdot \sin\vartheta_i = \sum_k P_{ik} \cdot q_k \cdot \sin\varphi_k \quad (4)$$

Any attempt to solve equations (3) and (4) directly for unknown q_k and ρ_k is bound to fail for almost any set of input parameters r_i, V_i, and ϑ_i. However, with the introduction of new variables, as shown in the following paragraph, the

system of equations can be linearized, its matrix becomes diagonally dominant, and therefore suitable for further numerical manipulation.

The system of equations (3) and (4) can be linearized by introducing variables

$a_k = q_k \cdot \cos\varphi_k$

$b_k = q_k \cdot \sin\varphi_k$

$V_{c;i} = V_i \cdot \cos\vartheta_i$

$V_{s;i} = V_i \cdot \sin\vartheta_i$,

and takes the form of two separate sets of linear equations:

$$V_c = P \cdot a \quad (5)$$

$$V_s = P \cdot b, \quad (6)$$

where a = (a_1, a_2,...), b = (b_1, b_2,...), and

$$P = \begin{pmatrix} P_{11} & P_{12} & \dots \\ P_{21} & P_{22} & \dots \\ \vdots & \vdots & \ddots \end{pmatrix}.$$

Since $r_{i0} \ll |r_i - r_k|$ for each i and k it follows that **P** is diagonally dominant.

After solving (5) and (6) one can obtain the unknown linear charge densities q_k and phase angles φ_k as:

$$q_k = \sqrt{a_k^2 + b_k^2}$$

$$\varphi_k = \arctan \frac{b_k}{a_k}.$$

3 Results

This section presents computational outcomes – the linear charge densities and their phase angles – for three different systems of power transmission lines. All cases deal with 400 kV systems, with wires of 1 centimeter in diameter, but differ in some other aspects. The zeroth example serves as a benchmark. It is followed by the first case, which is a realistic example of the 400 kV system. The second example and the third example are a bit exotic: the second only because of the geometry chosen, while the third deals also with the number of the wires and their potentials that can hardly be found in practice.

In a view of the conductivity of the ground both extreme possibilities were taken into account. When the ground is considered to be a perfect insulator the computations are performed as explained in the previous section, and their results in the examples section may be found under $q_{min}/(2\pi\varepsilon_0)$ and φ_{min}. With the ground as a perfect conductor the solution is obtained by applying the method of images, and the results for each wire in these cases may be found in $q_{max}/(2\pi\varepsilon_0)$ and φ_{max} columns. No additional unknowns are introduced in the case of a perfectly conducting ground, since the image charge of q_k-th linear charge density at time t has a value $q_k \cdot \cos(\omega t + \varphi_k + \pi)$.

Each of the following examples has three parts: input data, two-dimensional (x, y) sketch of the wires with the ground, and the resulting q_k and φ_k for all the wires in cases of insulating and conducting grounds.

3.1 Example 0

Table 1

input data				
i	x [m]	y [m]	V_{max} [V]	θ [°]
0	0.0	10.0	100000.0	0.0

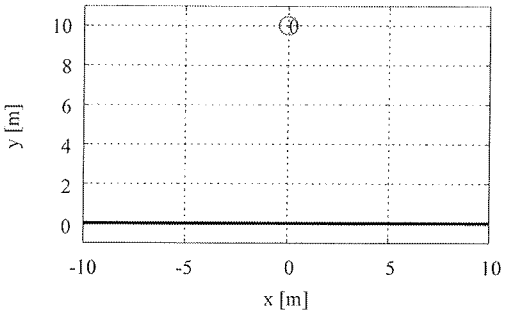

Table 2

output data				
i	$\frac{q_{min}}{2\pi\varepsilon_0}$ [V]	φ_{min} [°]	$\frac{q_{max}}{2\pi\varepsilon_0}$ [V]	φ_{max} [°]
0	18873.9	0.0	12056.8	0.0

Consider a wire with potential $V = V_0 \cdot \cos(\omega t)$, where V_0 = 100 kV. We can obtain an analytical result for the charge on the wire if it is suspended above a conducting plane by the method of images

$$V_0 \cdot \cos(\omega t) = \frac{q_0 \cdot \cos(\omega t + \varphi_0)}{2\pi\varepsilon_0} \ln \frac{2h}{r_0}, \quad (7)$$

where r_0 is the radius of the wire, and h is the ele-vation of the wire above the ground. The solution of (7) gives φ_0 = 0, where for given r_0 = 5 mm and h = 10 m we get: $\frac{q_0}{2\pi\varepsilon_0} = V_0/\ln\frac{2h}{r_0} \approx 12.057\text{kV}$.

The results of the computational algorithm below give the same result for $q_{max}/(2\pi\varepsilon_0)$. The charge of the wire above a conducting ground matches the analytical result, but the result for an insulating ground should be ignored, since a single infinite conducting line does not have a uniquely defined electric potential. The numerical value q_{min} in the output data equals $\frac{1}{2\pi\varepsilon_0}\ln(1/r_0)$ and cannot be connected to the electric potential of the wire.

3.2 Example 1

Six parallel wires serve as a first model for a double 400 kV power transmission line system.

Table 3

input data				
i	x [m]	y [m]	V_{max} [V]	θ [°]
0	-1.0	6.0	230940.0	0.0
1	0.0	6.0	230940.0	-120.0
2	1.0	6.0	230940.0	120.0
3	-1.0	10.0	230940.0	120.0
4	0.0	10.0	230940.0	-120.0
5	1.0	10.0	230940.0	0.0

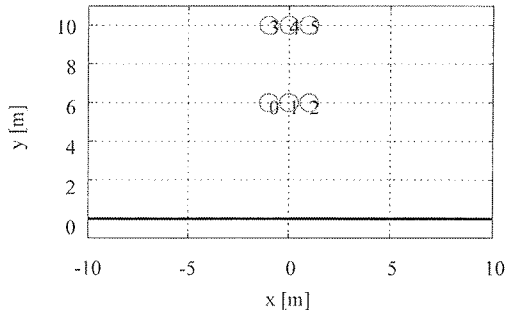

Table 4

output data				
i	$\frac{q_{min}}{2\pi\varepsilon^0}$ *[V]*	φ_{min} *[°]*	$\frac{q_{max}}{2\pi\varepsilon^0}$ *[V]*	φ_{max} *[°]*
0	*57059.9*	*23.4*	*41393.0*	*4.7*
1	*25853.9*	*-120.0*	*44887.5*	*-120.0*
2	*57059.9*	*96.6*	*41393.0*	*115.3*
3	*57059.9*	*96.6*	*41291.5*	*115.4*
4	*25853.9*	*-120.0*	*44983.3*	*-120.0*
5	*57059.9*	*23.4*	*41291.5*	*4.6*

The maximum value of the electric potential of the wires is $V_{max} = 400000/\sqrt{3} \approx 230.94$kV, conside-ring the electric potential of the conducting ground is zero.

The results show that the phase angles of the middle wires $i = 1$ and $i = 4$ are the same for the input potentials and for the resulting charges, but differ for other wires, as one would expect considering the geometrical symmetries of the system. For any taken wire the difference between the phase angle of the electric potential and the phase angle of the line charge does not exceed 5°.

3.3 Example 2

In the next example we consider six scattered parallel wires of the 400 kV power line system. The geometry we choose introduces no symmetries, and the results show none. Nevertheless, the differences between the phase angles of the potential and charge again do not exceed 5.

Table 5

input data				
i	*x* [m]	*y* [m]	V_{max} [V]	θ [°]
0	-3.0	5.0	230940.0	0.0
1	0.0	4.0	230940.0	-120.0
2	4.0	6.0	230940.0	120.0
3	-1.0	8.0	230940.0	120.0
4	0.0	11.0	230940.0	-120.0
5	2.0	10.0	230940.0	0.0

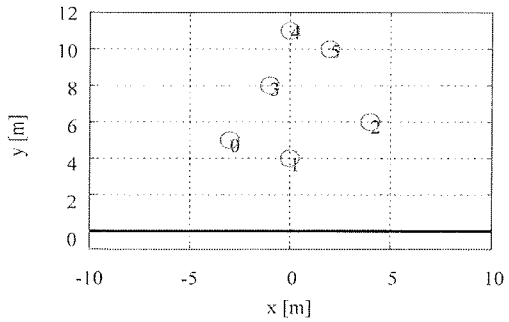

Table 6

output data				
i	$\frac{q_{min}}{2\pi\varepsilon^0}$ *[V]*	φ_{min} [°]	$\frac{q_{max}}{2\pi\varepsilon^0}$ *[V]*	φ_{max} [°]
0	34911.5	2.6	35897.4	0.7
1	36301.6	-121.2	37000.7	-119.7
2	34183.5	119.9	33535.9	120.1
3	38125.3	120.4	37194.1	120.1
4	37119.6	-123.9	37348.7	-122.4
5	37314.3	2.2	37808.8	1.3

3.4 Example 3

As the last one, we present a highly exotic example in the theory and practice of 400 kV power transmission line systems. It consists of nine wires with some unusual phase angles of electric potential, and therefore represents an electrically non-symmetric case. There is no apparent geometrical symmetry, either.

Table 7

input data				
i	*x* [m]	*y* [m]	V_{max} [V]	θ [°]
0	-3.0	5.0	230940.0	0.0
1	0.0	4.0	230940.0	-120.0
2	4.0	6.0	230940.0	120.0
3	-1.0	8.0	230940.0	120.0
4	0.0	11.0	230940.0	-120.0
5	2.0	10.0	230940.0	0.0
6	6.0	2.0	230940.0	50.0
7	7.0	6.0	230940.0	170.0
8	8.0	9.0	230940.0	-80.0

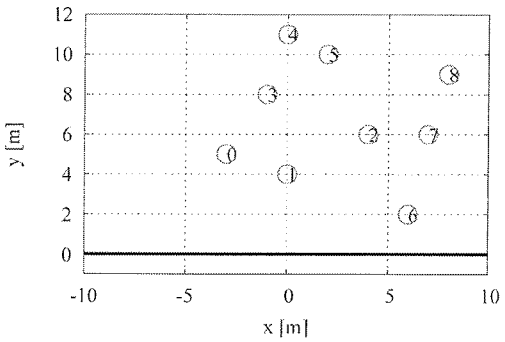

Table 8

output data				
i	$\frac{q_{min}}{2\pi\varepsilon^0}$ *[V]*	φ_{min} [°]	$\frac{q_{max}}{2\pi\varepsilon^0}$ *[V]*	φ_{max} [°]
0	34207.6	3.7	36038.4	1.1
1	36981.1	-122.2	36893.5	-119.5
2	34012.1	117.3	33301.3	115.8
3	39140.8	119.9	37643.3	119.1
4	35552.5	-125.8	35909.1	-123.0
5	37776.4	6.0	38716.0	4.5
6	33940.1	46.8	36733.5	45.8
7	34302.0	169.8	33058.4	170.0
8	32441.4	-75.5	33802.6	-73.9

As shown before, for a given wire the phase angles of the potential and the charge do not differ significantly. In this particular case the differences are larger than in the previous examples, but still below 10°. Given a set of values of potential phase angles and a set of phase angles of line charges, the matching pairs can be found only by checking input and output tables even for this geometry. Howev-

er, one can easily imagine an example where this is not so, no matter how more exotic it might be.

4 Discussion

The importance of the electric charge computation for quasi-static low-frequency sources, like power transmission lines, is vast. Since the charge is the source of the electric field, its distribution only enables us to find the appropriate values of the surrounding field. Traditionally, the electric field values were used for the estimation of the loses due to corona discharges, while today with the increasing interest in possible health issues associated with the non-thermal effects of electromagnetic radiation they play a role in the design of power line grids /3, 2, 4/.

As shown in the article, the charge is not oscillating synchronously with the electric potential in general, so its computation is a task on its own. The system of equations is non-linear, but can be linearized, or it better should be, in order to avoid computational problems. Even the simplest of models, the model of infinite straight lines presented here, gives us the elliptically polarized results for the electric field strength vector. This we intend to discuss in our future work.

References

/1/ Zakariya Al-Hamouz. Finite element computation of corona around monopolar transmission lines. Electric Power Systems Research, 48(1):57 - 63, 1998.

/2/ B. S. Ashok Kumar, William A. Klos, and Eric R. Taylor. Influence of low-frequency electromagnetic fields on living organisms. Electric Power Systems Research, 30(3):229 - 234, 1994.

/3/ J.C. Matthews and D.L. Henshaw. Measurements of atmospheric potential gradient fluctuations caused by corona ions near high voltage power lines. Journal of Electrostatics, In Press, Corrected Proof:-, 2009.

/4/ R. Mongelluzo, A. Piccolo, and F. Rossi. Modeling environmental effects of EHV and UHV transmission lines. Electric Power Systems Research, 4(3):235 - 245, 1981.

/5/ Anton R. Sinigoj. Osnove elektromagnetike (in Slovene). Fakulteta za elektrotehniko, Ljubljana, aSlovenija, 1996.

dr. Aleš Berkopec
Fakulteta za elektrotehniko, Tržaška 25,
1000 Ljubljana, Slovenija
ales.berkopec@fe.uni-lj.si

Prispelo (Arrived): 06.05.2009 *Sprejeto (Accepted): 09.09.2009*

Informacije MIDEM
Strokovna revija za mikroelektroniko, elektronske sestavine dele in materiale

NAVODILA AVTORJEM

Informacije MIDEM je znanstveno-strokovno-društvena publikacija Strokovnega društva za mikroelektroniko, elektronske sestavne dele in materiale - MIDEM. Revija objavlja prispevke s področja mikroelektronike, elektronskih sestavnih delov in materialov. Ob oddaji člankov morajo avtorji predlagati uredništvu razvrstitev dela v skladu s tipologijo za vodenje bibliografij v okviru sistema COBISS.
Znanstveni in strokovni prispevki bodo recenzirani.

Znanstveno-strokovni prispevki morajo biti pripravljeni na naslednji način:

1. Naslov dela, imena in priimki avtorjev brez titul, imena institucij in firm
2. Ključne besede in povzetek (največ 250 besed).
3. Naslov dela v angleščini.
4. Ključne besede v angleščini (Key words) in podaljšani povzetek (Extended Abstract) v angleščini, če je članek napisan v slovenščini
5. Uvod, glavni del, zaključek, zahvale, dodatki in literatura v skladu z IMRAD shemo (Introduction, Methods, Results And Discsussion).
6. Polna imena in priimki avtorjev s titulami, naslovi institucij in firm, v katerih so zaposleni ter tel./Fax/Email podatki.
7. Prispevki naj bodo oblikovani enostransko na A4 straneh v enem stolpcu z dvojnim razmikom, velikost črk namanj 12pt. Priporočena dolžina članka je 12-15 strani brez slik.

Ostali prispevki, kot so poljudni cčlanki, aplikacijski članki, novice iz stroke, vesti iz delovnih organizacij, inštitutov in fakultet, obvestila o akcijah društva MIDEM in njegovih članov ter drugi prispevki so dobrodošli.

Ostala splošna navodila

1. V članku je potrebno uporabljati SI sistem enot oz. v oklepaju navesti alternativne enote.
2. Risbe je potrebno izdelati ali iztiskati na belem papirju. Širina risb naj bo do 7.5 oz.15 cm. Vsaka risba, tabela ali fotografija naj ima številko in podnapis, ki označuje njeno vsebino. Risb, tabel in fotografij ni potrebno lepiti med tekst, ampak jih je potrebno ločeno priložiti članku. V tekstu je treba označiti mesto, kjer jih je potrebno vstaviti.
3. Delo je lahko napisano in bo objavljeno v slovenščini ali v angleščini.
4. Uredniški odbor ne bo sprejel strokovnih prispevkov, ki ne bodo poslani v dveh izvodih skupaj z elektronsko verzijo prispevka na disketi ali zgoščenki v formatih ASCII ali Word for Windows. Grafične datoteke naj bodo priložene ločeno in so lahko v formatu TIFF, EPS, JPEG, VMF ali GIF.
5. Avtorji so v celoti odgovorni za vsebino objavljenega sestavka.

Rokopisov ne vračamo. Rokopise pošljite na spodnji naslov.

Uredništvo Informacije MIDEM
MIDEM pri MIKROIKS
Stegne 11, 1521 Ljubljana, Slovenia
Email: Iztok.Sorli@guest.arnes.si
tel. (01) 5133 768, fax. (01) 5133 771

Informacije MIDEM
Journal of Microelectronics, Electronic Components and Materials

INSTRUCTIONS FOR AUTHORS

Informacije MIDEM is a scientific-professional-social publication of Professional Society for Microelectronics, Electronic Components and Materials - MIDEM. In the Journal, scientific and professional contributions are published covering the field of microelectronics, electronic components and materials.
Authors should suggest to the Editorial board the classification of their contribution such as : original scientific paper, review scientific paper, professional paper...
Scientific and professional papers are subject to review.

Each scientific contribution should include the following:

1. Title of the paper, authors' names, name of the institution/company.
2. Key Words (5-10 words) and Abstract (200-250 words), stating how the work advances state of the art in the field.
3. Introduction, main text, conclusion, acknowledgements, appendix and references following the IMRAD scheme (Introduction, Methods, Results And Discsussion).
4. Full authors' names, titles and complete company/institution address, including Tel./Fax/Email.
5. Manuscripts should be typed double-spaced on one side of A4 page format in font size 12pt. Recommended length of manuscript (figures not included) is 12-15 pages
6. Slovene authors writing in English language must submit title, key words and abstract also in Slovene language.
7. Authors writing in Slovene language must submit title, key words and extended abstract (500-700 words) also in English language.

Other types of contributions such as popular papers, application papers, scientific news, news from companies, institutes and universities, reports on actions of MIDEM Society and its members as well as other relevant contributions, of appropriate length , are also welcome.

General informations

1. Authors should use SI units and provide alternative units in parentheses wherever necessary.
2. Illustrations should be in black on white paper. Their width should be up to 7.5 or 15 cm. Each illustration, table or photograph should be numbered and with legend added. Illustrations, tables and photographs must not be included in the text but added separately. However, their position in the text should be clearly marked.
3. Contributions may be written and will be published in Slovene or English language.
4. Authors must send two hard copies of the complete contributon, together with all files on diskette or CD, in ASCII or Word for Windows format. Graphic files must be added separately and may be in TIFF, EPS, JPEG, VMF or GIF format.
5. Authors are fully responsible for the content of the paper.

Contributions are to be sent to the address below.

Uredništvo Informacije MIDEM
MIDEM pri MIKROIKS
Stegne 11, 1521 Ljubljana, Slovenia
Email: Iztok.Sorli@guest.arnes.si
tel.+386 1 5133 768, fax.+386 1 5133 771

MIDEM
DRUŠTVO-SOCIETY
Slovenia Chapter

M I D E M

Strokovno društvo za mikroelektroniko,
elektronske sestavne dele in materiale
MIDEM pri MIKROIKS
Stegne 11, 1521 Ljubljana
SLOVENIJA

TEL.: +386 (0)1 5133 768
FAX: +386 (0)1 5133 771
Email / WWW
iztok.sorli@guest.arnes.si
http://paris.fe.uni-lj.si/midem/

MIDEM SOCIETY REGISTRATION FORM

1. First Name ..... Last Name .....

   Adress .....

   City .....

   Country ..... Postal Code .....

2. Date of Birth .....

3. Education (please, circle whichever appropriate)

   PhD MSc BSc High School Student

3. Profession (please, circle whichever appropriate)

   Electronics Physics Chemistry Metallurgy Material Sc.

4. Company .....

   Adress .....

   City .....

   Country ..... Postal Code .....

   Tel.: ..... FAX: .....

   Email .....

5. Your Primary Job Function

   Fabrication Engineering Facilities QA/QC
   Management Purchasing Consulting Other

6. Please, send mail to a) Company adress b) Home Adress

7. I wil regularly pay MIDEM membership fee, 25,00 EUR/year

MIDEM member recive Journal "Informacije MIDEM" for free !!!

Signature ..... Date .....

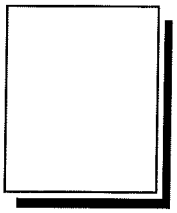

MIDEM at MIKROIKS
Stegne 11

1521 Ljubljana
Slovenija